
GEOPHYSICAL SIGNATURES OF WESTERN AUSTRALIAN MINERAL DEPOSITS: AN OVERVIEW

Michael C. Dentith¹, Kim F. Frankcombe² & Allan Trench³

1. Department of Geology and Geophysics, The University of Western Australia, Nedlands, W.A. 6009

2. Kambalda Nickel Mines/St Ives Gold Mines, Western Mining Corporation Ltd, Kambalda, W.A. 6442

3. Normandy Exploration Ltd, 8 Kings Park Road, West Perth, W.A. 6005

ABSTRACT

Geophysical exploration in Western Australia is hindered by a mantle of conductive and magnetic weathered rocks that covers much of the State. This has required the adaptation of most geophysical methods for successful application in Western Australian conditions, and has led to the development and widespread use of, for instance, high-resolution aeromagnetics and time-domain electromagnetic methods. However, these difficulties have not prevented geophysics from being an integral part of exploration for base metal, diamond, gold, iron ore, manganese, nickel and uranium deposits in Western Australia.

Mississippi Valley-type base-metal deposits are difficult geophysical targets and direct detection of the ore is not usually possible. However, gravity and magnetic data can be used to locate basement highs associated with such deposits and, on a semi-regional scale, induced polarisation surveys have been used to locate marcasite halos associated with the orebodies. Volcanic-hosted massive sulphide base-metal deposits have variable geophysical responses. Physical property contrasts with their host are highly variable and thus methods such as magnetics, induced polarisation and electromagnetics may fail to generate recognisable responses. Mise-a-la-masse surveys have proved highly successful for mapping such mineralisation on a prospect scale, once it has been intersected by drilling. The only example of a sedimentary exhalative deposit in the State for which data are available has distinct gravity, magnetic and time-domain electromagnetic anomalies.

Diamonds in Western Australia mainly occur in lamproite pipes. These pipes have variable magnetisations but can usually be detected using high-resolution aeromagnetic surveys. The pipes can also be conductive and mapped using electromagnetic techniques if the host rocks are suitably resistive.

The major geophysical method utilised in gold exploration is high-resolution aeromagnetics which is used to map favourable structures and rock types. Electrical and electromagnetic methods can also be used where gold is associated with sulphides.

Geophysics has been comparatively little used in exploration for iron ore. Exploration for supergene-enriched deposits mainly uses aeromagnetics, to map favourable structures and to detect magnetite destruction and replacement associated with mineralisation, and gamma-ray logging for stratigraphic correlation purposes.

The major technique used in manganese exploration is the gravity method, taking advantage of the positive density contrast between ore and host rocks.

The mineral sands industry uses aeromagnetic data to map placer deposits containing ilmenite, but the relatively low cost of drilling limits the use of geophysical exploration methods.

Nickel sulphide mineralisation can be directly detected using induced polarisation and electromagnetic techniques. Gravity and magnetic surveys are also used, but mainly in a mapping role.

Carbonatitic intrusions associated with rare-earth-element mineralisation give rise to large magnetic anomalies. Radiometric and gravity anomalies can also occur.

Uranium mineralisation has been directly detected using radiometric data, but some deposits are concealed below cover. Magnetic, electromagnetic, electrical and gravity surveys can be used to locate the rocks and structures which host mineralisation.

KEY WORDS: Archaean lode gold, calcrete-related uranium, diamondiferous lamproite pipes, downhole logging, electromagnetics, gabbro-associated nickel, gravity, heavy mineral sand placers, induced polarisation, intrusive dunite-associated nickel, lateritic bauxite, magnetic induced polarisation, magnetics, magnetometric resistivity, mise-a-la-masse, Mississippi Valley-type lead-zinc deposits, placer gold, Proterozoic sediment-hosted lode gold, radiometrics, rare earth elements associated with carbonatitic intrusions, regolith, remote sensing, SEDEX deposits, supergene gold, regolith, resistivity, seismic reflection, seismic refraction, supergene-enriched iron ore, supergene manganese, volcanogenic massive-sulphide deposits, uranium in channel sandstones, volcanic peridotite-associated nickel

INTRODUCTION

Due to the vast size of Western Australia, and the general lack of outcrop, geophysics plays a major

role in mineral exploration. The entire State has been covered by regional gravity and magnetic data collected by AGSO. The magnetic data (see cover) were mainly collected at a flight height of 150 m and line

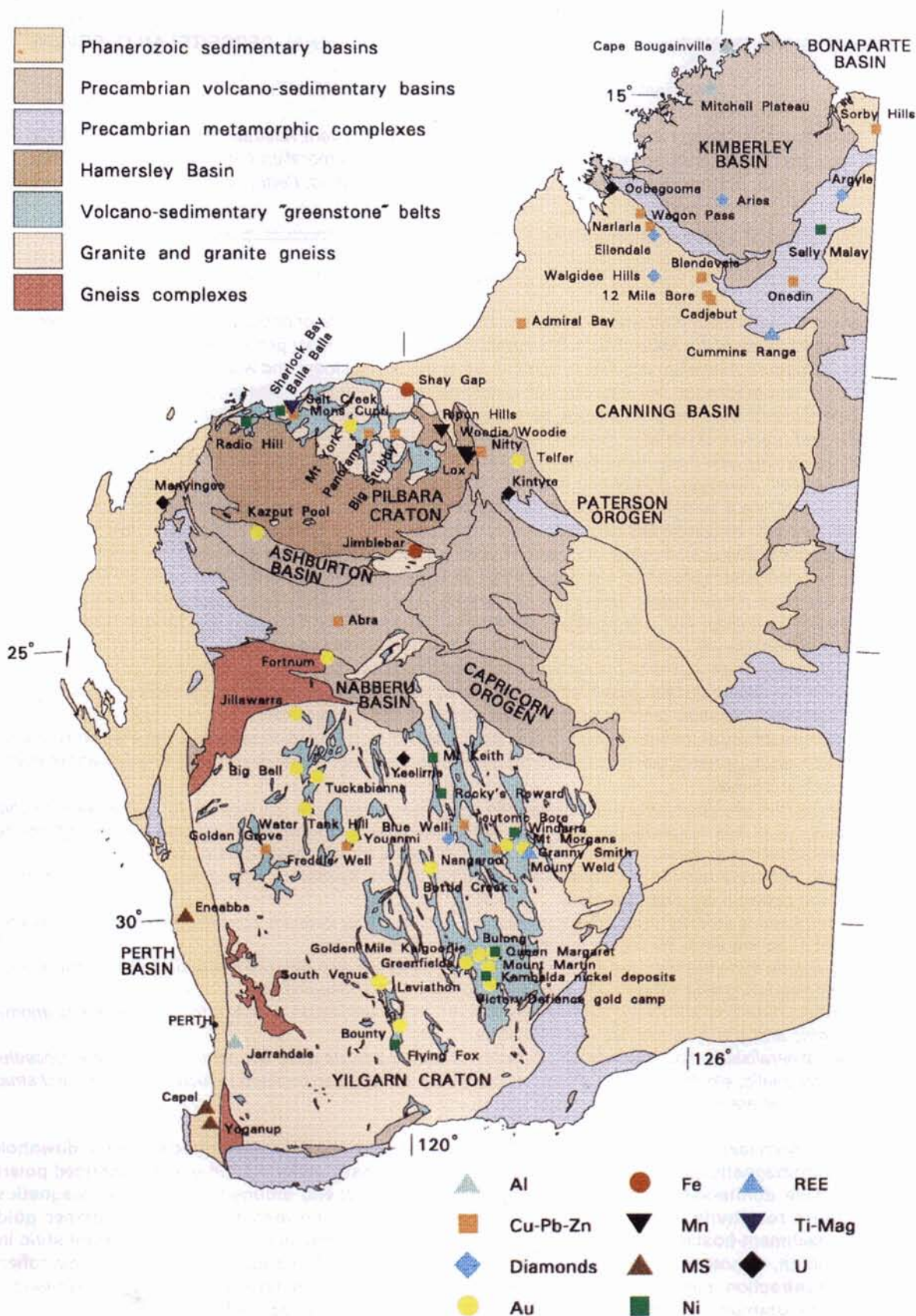


FIGURE 1 Location map showing the mineral deposits mentioned in the text and the major tectonic elements of Western Australia. Geology adapted from Myers & Hocking (1988).

spacing of 1600 m, although line spacings as low as 400 m and flight heights between 300 m and 60 m have also been used. Radiometric data were acquired in many areas during the acquisition of the aeromagnetic data. Gravity data were collected at a spacing of 11 km with levels determined using barometers. These regional geophysical datasets define the main geological elements of the State very well. However, they are not of sufficient detail to be useful in mineral exploration beyond the level of, for example, defining the extent of greenstone belts or mapping major lineaments. Prospect-scale structures controlling mineralisation, and the mineralisation itself, cannot usually be located using these data.

This paper reviews, by commodity and deposit style, the geophysical signatures of mineral deposits in Western Australia. The paper is primarily documentary with discussion limited to brief summaries at the end of each commodity section. Where possible, at least one case-study of each type of mineralisation is presented to supplement the case-study papers in the main body of the book. Particular emphasis is placed on deposits and mineralisation styles not described later in the volume. Unless otherwise stated, the interpretations are those of the original authors.

With the exception of aluminium, geophysics is an integral part of exploration for all the main commodities found in Western Australia. These include world-class deposits of diamonds, gold, iron and nickel plus significant base metal, mineral sand and uranium mineralisation. For a more detailed description of the geology and mineralisation of Western Australia the reader is referred to the review by Groves *et al.* (this volume). Figure 1 is a map showing the locations of the mineral deposits mentioned in this paper, along with the main tectonic elements comprising Western Australia.

An important aspect of the geology of Western Australia, from a geophysical perspective, is the mantle of weathered material that covers most of the State. The weathered layer has a profound effect on geophysical data and is a major consideration in geophysical exploration in Western Australia. Therefore the effects of the weathered layer on geophysical data are reviewed in the first section of this paper.

EFFECTS OF WEATHERING ON GEOPHYSICAL EXPLORATION

Introduction

Much of Western Australia, including about 80 percent of the Yilgarn Craton, is covered by a mantle of deeply weathered rocks, or regolith, which is commonly between 30 and 60 m thick, but may reach 100 m or more (Lawrance, 1990). Laterites, silcretes and calcretes have also formed as part of this weathering process. The situation is further complicated by the presence of transported alluvium within palaeo-drainage systems. Lateritisation has affected both bedrock and alluvial cover. It is important to realise that significant mineralisation can occur within the weathered layer, such as lateritic nickel, supergene gold, and calcrete-related uranium deposits. Thus, although the effects of the weathered layer are usually treated as noise from which the bedrock signal needs to be isolated, sometimes the geophysical response

of the weathered layer is the signal.

Comprehensive descriptions of the effects of the regolith and alluvial cover on geophysical data are given by Doyle *et al.* (1981), Doyle & Lindeman (1985) and Smith & Pridmore (1989). The following is largely taken from these publications and the reader is referred to the original authors for a more detailed discussion. The influence of deep weathering upon geophysical data is varied and can be regarded as both positive and negative. Geophysical exploration is hindered in two main ways; firstly, by increasing the distance between sensor and target, and secondly, by creating geophysical noise such that the overall signal-noise-ratio is decreased. Positive effects also fall into two categories. Firstly, the physical properties of the weathered layer are partly a function of the underlying bedrock and therefore can facilitate geophysical mapping. Secondly, the gentle topography formed through long-term weathering creates less logistical and processing problems compared to areas with greater relief.

Effects on geophysical techniques

Variations in magnetic susceptibility and remanence within the weathered zone can range over six orders of magnitude. Ground magnetics are commonly dominated by short-wavelength anomalies with amplitudes of several thousand nanoTesla originating in the near-surface (Fig. 2A). The source of these anomalies is maghemite, a magnetic species formed during the lateritisation process which typically has strong remanence and susceptibility as well as superparamagnetic behaviour (Clark & Emerson, 1991). Such anomalies are suppressed in airborne data and through non-linear and low-pass wavelength filtering of ground magnetic data (Fig. 2B). Below the maghemite layer, weathering of magnetite within the regolith generally causes magnetic depletion through production of non-magnetic species (see Dentith *et al.*, 1992b) and hence tends to suppress the geological signal.

Gravity data are affected by density contrasts within the weathered layer and also by the irregular nature of the boundary between fresh and weathered material (Fig. 3). Density variations rarely exceed one order of magnitude. However, the diminished relief, caused by long-term weathering, makes the reduction of gravity data relatively simple since terrain corrections only rarely need be applied. Generally, steeply dipping stratigraphy can be mapped using gravity if density contrasts of 0.05 g/cm³ or greater are present. Variations in the density structure of the regolith and alluvial cover, such as the presence of palaeochannels, are capable of generating gravity anomalies of the same order as bedrock geological contacts.

Electrical and EM data respond to variations in bedrock and regolith conductivity. Conductivities in the weathered zone can vary over some eight orders of magnitude. Areas of conductive clay and saline groundwater typically have electrical resistivities in the range 0.3 to 100 ohm m. Regolith can have an electrical conductance up to 100 S. In addition, polarisable clays in the weathered zone can cause IP effects in EM data. Modern EM systems are capable of mapping not only strong isolated sulphide conduc-

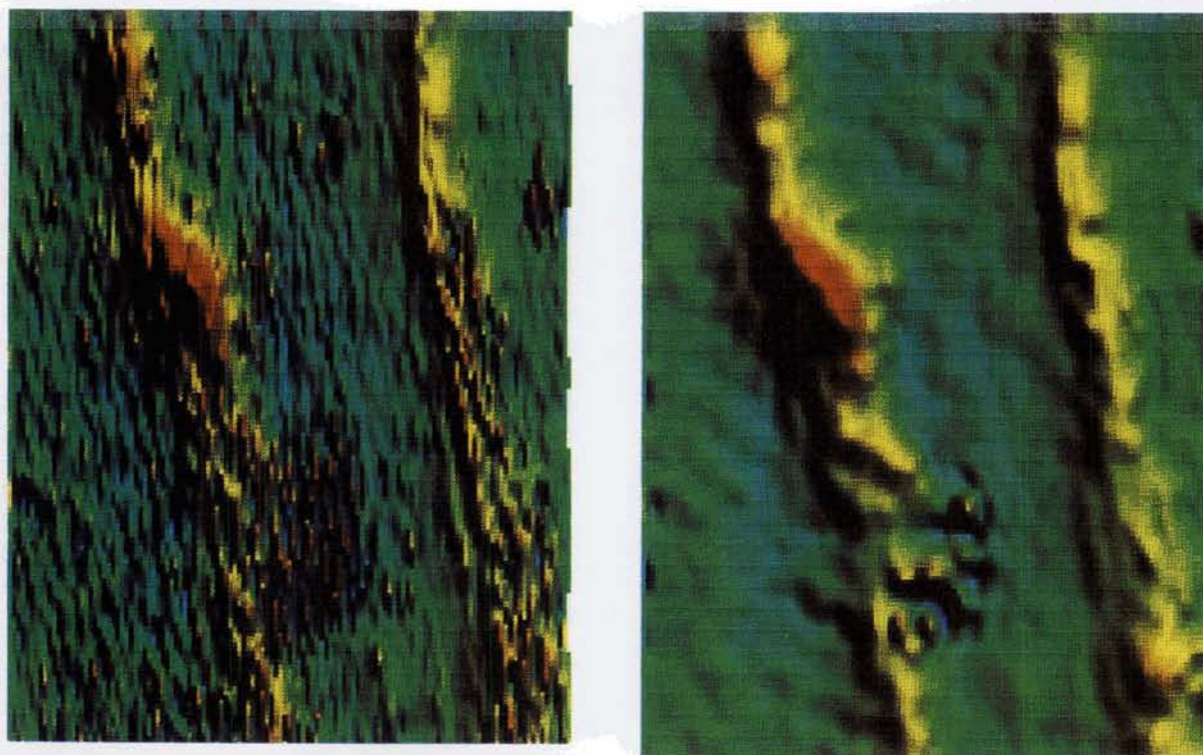


FIGURE 2 A. Image of unfiltered caesium vapour ground magnetic data showing "spiky" areas influenced by lateritic magnetic noise. Lines trend east-west, line spacing is 50 m, sampling interval is 0.5 m. North is directly "up" the page. Image is sun-illuminated from the northeast. The east-west extent of the data is about 1300 m. B. Image of filtered magnetic data from the same area as A. Note the improvement in clarity upon non-linear and low-pass filtering, but also the artefacts generated by filtering in the southern central area of the image.

tors, but also subtle changes in conductivity which accompany geological contacts. AEM systems are therefore being increasingly used for geological mapping and can reveal information not present in aeromagnetic data. Despite these advances, both airborne and ground-based systems may not be able to penetrate to bedrock resulting in the possibility of orebodies evading detection. DHEM techniques provide only a partial solution to this problem. Conventional IP surveys are strongly effected by the conductive weathered layer. These data can be completely dominated by variations in electrical properties within the weathered layer and also by variations in its thickness. When ground resistivity is low, electromagnetic coupling presents serious problems. This is exacerbated by the need for relatively large dipole sizes, required to penetrate to fresh rock.

Radiometric data both benefit and suffer from the weathering process. For instance, concentration of uranium minerals in calcrete allows direct detection using the radiometric method (e.g., Yeelirrie, see below). However, the presence of transported cover can effectively mask the radiometric response of the underlying geology. Comparatively little is known about the effect of the weathering process on uranium, thorium and potassium. Uranium and potassium are commonly concentrated in salt lakes although the mechanism of enrichment is not known. In contrast, thorium gives rise to the radiometric response from ferricretes within the laterite profile.

Summary

The deep weathering profile over Western Australia both assists and hinders geophysical exploration, although overall its effect is negative. Density, magnetisation and conductivity contrasts within the weathered layer, between transported cover and regolith, and at the irregular interface between regolith and bedrock combine to produce spurious anomalies and mask bedrock responses. Combined use of several geophysical techniques, or recourse to drillhole techniques, are means to, at least partially, overcome weathering-related geophysical effects.

ALUMINIUM

Lateritic bauxite deposits occur in two main areas in Western Australia, the Darling Ranges in the south-west of the State (e.g., Jarrahdale), and the Mitchell Plateau and Cape Bougainville in the Kimberley (Fig. 1). These deposits result from the weathering of aluminous rocks, with gibbsite being the main ore mineral. Rattigan (1990) does not mention geophysics in his description of Australian aluminium deposits, and discussions with personnel from the local industry confirm that geophysics does not play a significant role in exploration. This is partly because the major deposits were discovered in the early 1960s when geophysics played a less important role in exploration than it does today. A second factor is that exposure is such that resources in the Darling Range can be mapped easily and economically by a field geologist.

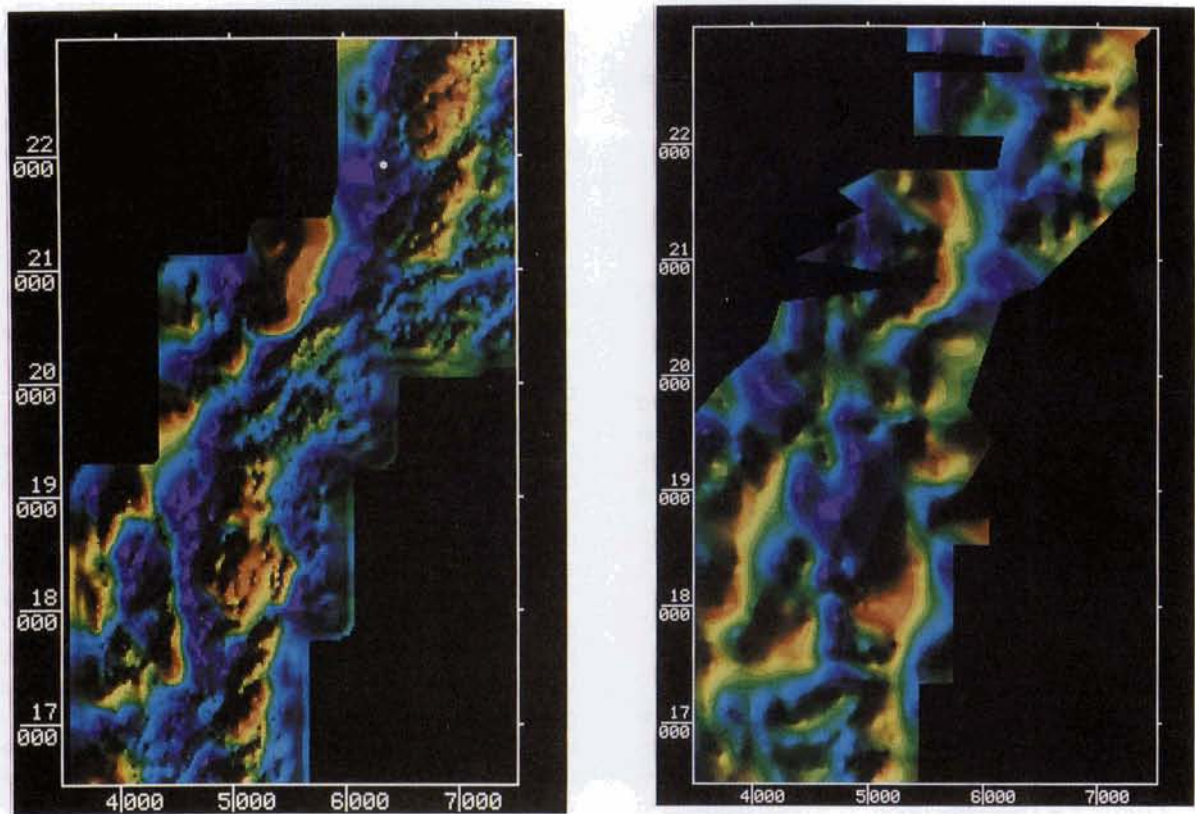


FIGURE 3 Gravity data from within the Yilgarn Craton. A. Observed gravity. B. Calculated gravity effect of the weathered layer derived from thicknesses in drillholes and assuming a constant density contrast with the fresh rock of 1.0 g/cm³. The colour range in both figures covers about 4 mGal.

In contrast, the remoteness of the Kimberley bauxite deposits makes the use of geophysics a more attractive option and Henderson *et al.* (1984) describe the use of remote-sensing data to map the Cape Bougainville deposits. Figure 4 is based on an enhanced false-colour composite image of Landsat multi-spectral scanner data. The flat-lying limonitic

bauxite laterite shows as bright green areas while the underlying basic volcanic rocks, which give rise to sloping terrain with a heavier cover of vegetation, appear red. Clearly, the bauxite deposits can be mapped in this manner. However, Henderson *et al.* (1984) comment that Landsat imagery was not able to map the Darling Range bauxites.

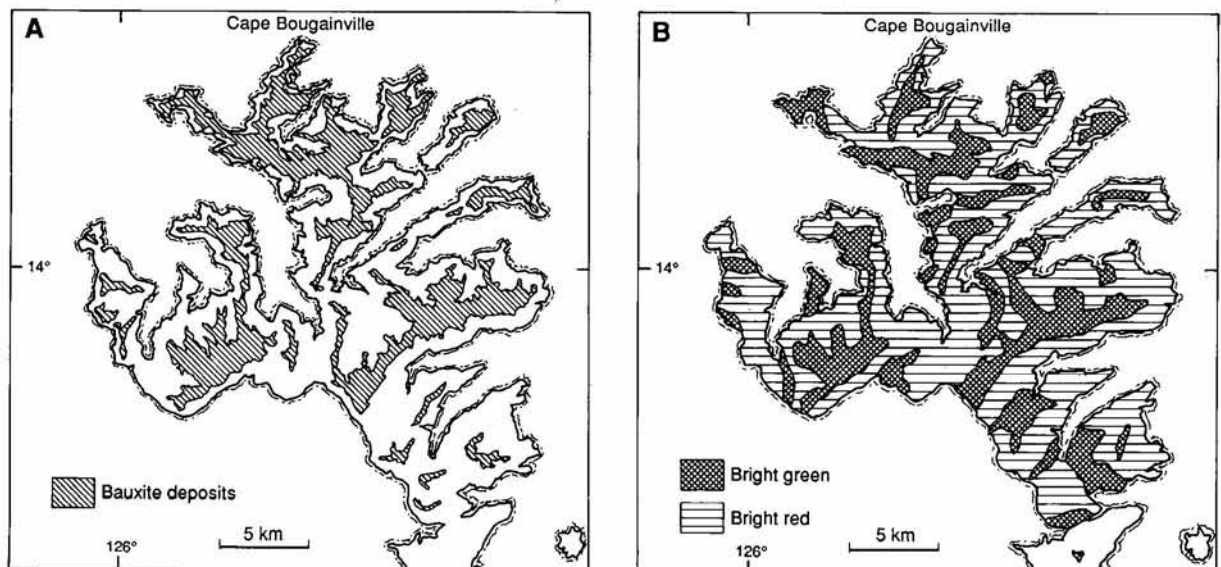


FIGURE 4 A. Distribution of bauxite deposits at Cape Bougainville. B. Landsat multi-spectral scanner enhanced false-colour-composite data from the same area. Redrawn from Henderson *et al.* (1984)

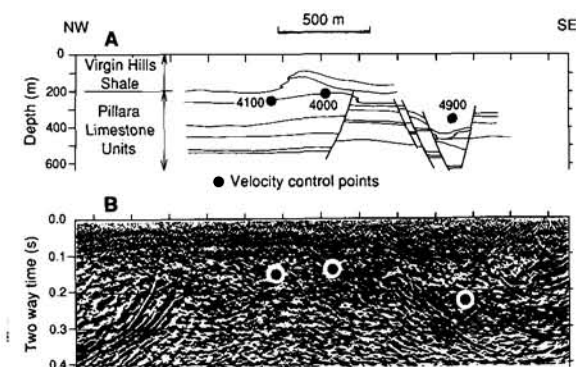


FIGURE 5 A. Geological cross-section located about 1500 m north of the Blendevale MVT deposit. Geology derived from drilling data. B. Migrated seismic reflection data along the same line. Redrawn from Isles *et al.* (1987).

COPPER, LEAD AND ZINC

Carbonate-hosted base metals

Carbonate-hosted lead-zinc deposits of Mississippi Valley-type (MVT) occur in the Canning and Bonaparte Basins (Fig. 1) in the north of Western Australia (Davies & Blockley, 1990). The main deposits in the Bonaparte Basin are at Sorby Hills. Within the Canning Basin, the majority of deposits occur on the Lennard Shelf (*e.g.*, Cadjebut, Blendevale, 12-Mile Bore, Wagon Pass and Narlarla); the exception is the Admiral Bay deposit which lies on the southwestern

margin of the Broome Arch on the southwestern side of the basin.

LENNARD SHELF

Geophysical exploration for MVT deposits on the southern part of the Lennard Shelf is summarised by Scott *et al.* (this volume). Geophysics plays an important role in an exploration strategy also involving geology, geochemistry and grid-drilling. Gravity and magnetic data are used for regional mapping. Seismic reflection data collected in the area mainly for petroleum exploration are used in a similar manner. Figure 5 shows a migrated seismic reflection section recorded about 1500 m along strike from the Blendevale deposit and the geology derived from drilling (Isles *et al.*, 1987). Faulting in the limestone units is quite well resolved, an important consideration given that Blendevale is essentially a fault-controlled deposit and many of the other deposits in the areas are associated with faults to a greater or lesser degree. The association of all known MVT deposits on the Lennard Shelf with marcasite has led to the use of IP for semi-regional-scale exploration (Scott *et al.*, this volume). However, geophysics, or for that matter geochemistry and geology, are not capable of defining individual drill targets. Instead, these data are used in combination to locate prospective areas which are then grid drilled.

The Narlarla and Wagon Pass deposits are the principal occurrences of MVT mineralisation in the northern part of the Lennard Shelf (Buchhorn, 1986; Ringrose, 1989). The Narlarla deposit was discovered early this century and was worked between 1948 and

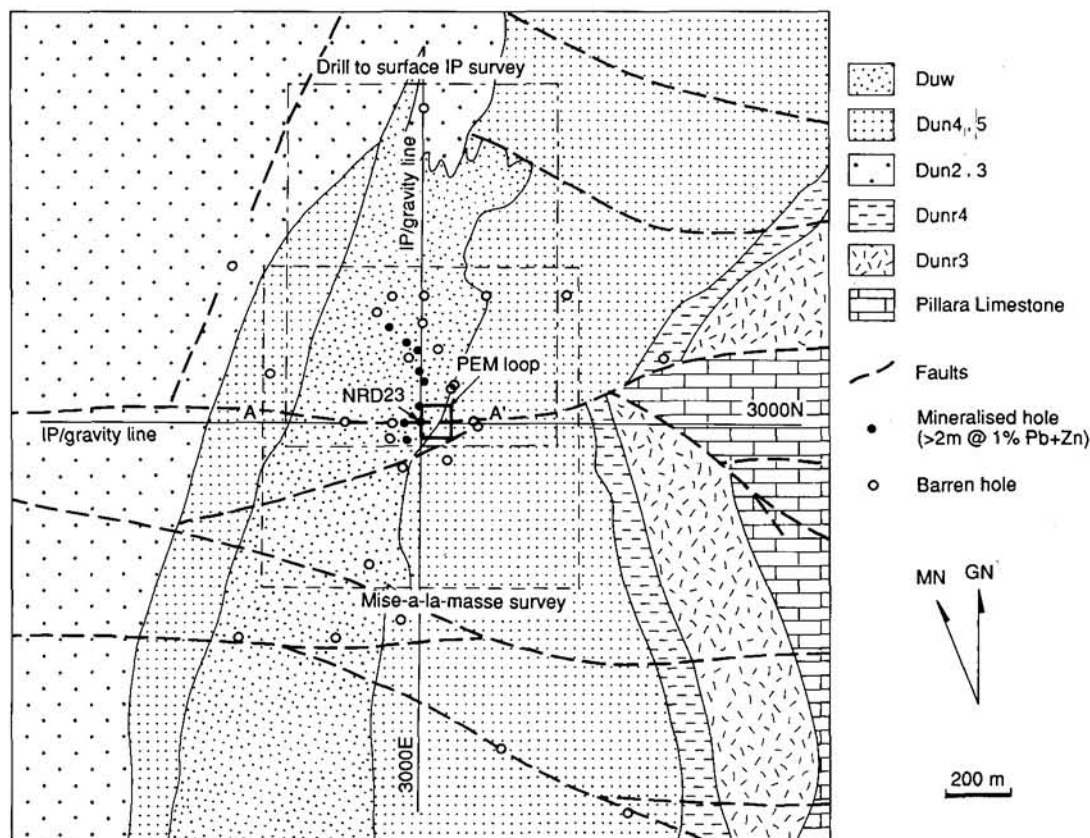


FIGURE 6 Simplified geological map of the Wagon Pass area showing locations of geophysical surveys and drillholes. Geology from Buchhorn (1986). See Figure 7 for descriptions of the geological units.

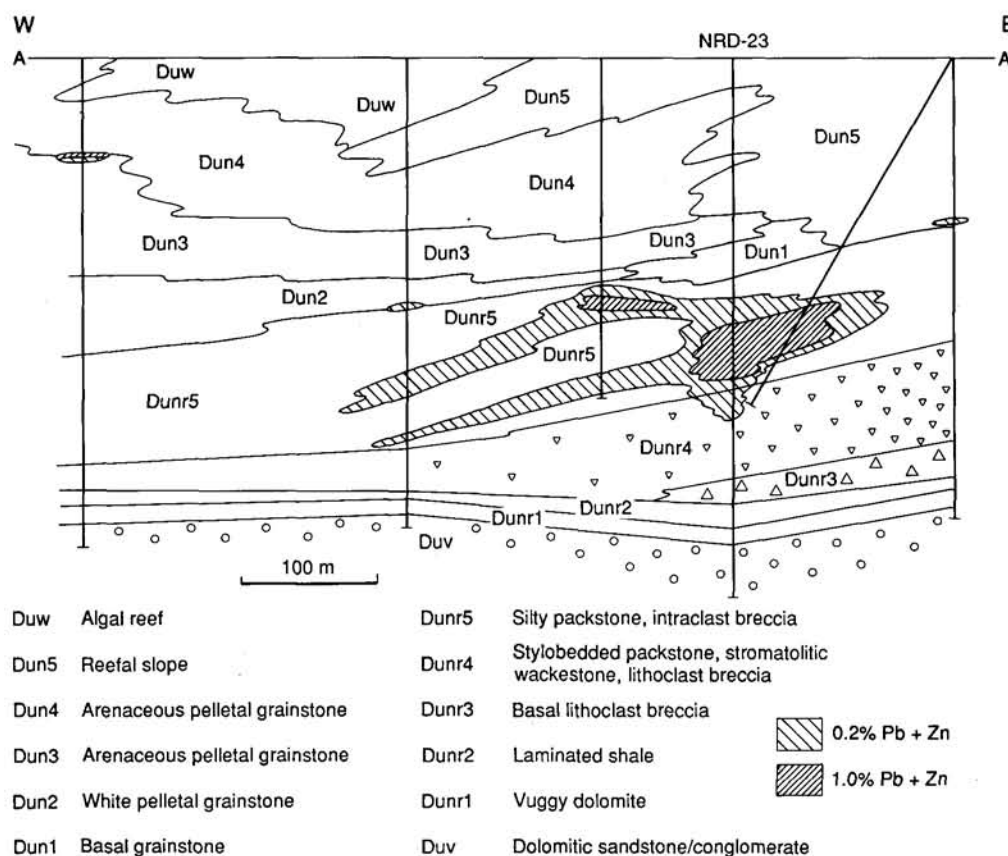


FIGURE 7 Geological cross section along 30000N, Wagon Pass deposit. NRD-23 is the discovery drillhole. Modified from Buchhorn (1986). See Figure 6 for location.

1966. To the authors' knowledge, no detailed geophysical data have been acquired around the deposit. In contrast, several types of geophysical data have been collected around the Wagon Pass deposit, primarily to test which methods can be used to locate similar mineralisation. These data and their interpretation have kindly been provided by Billiton Australia.

Wagon Pass

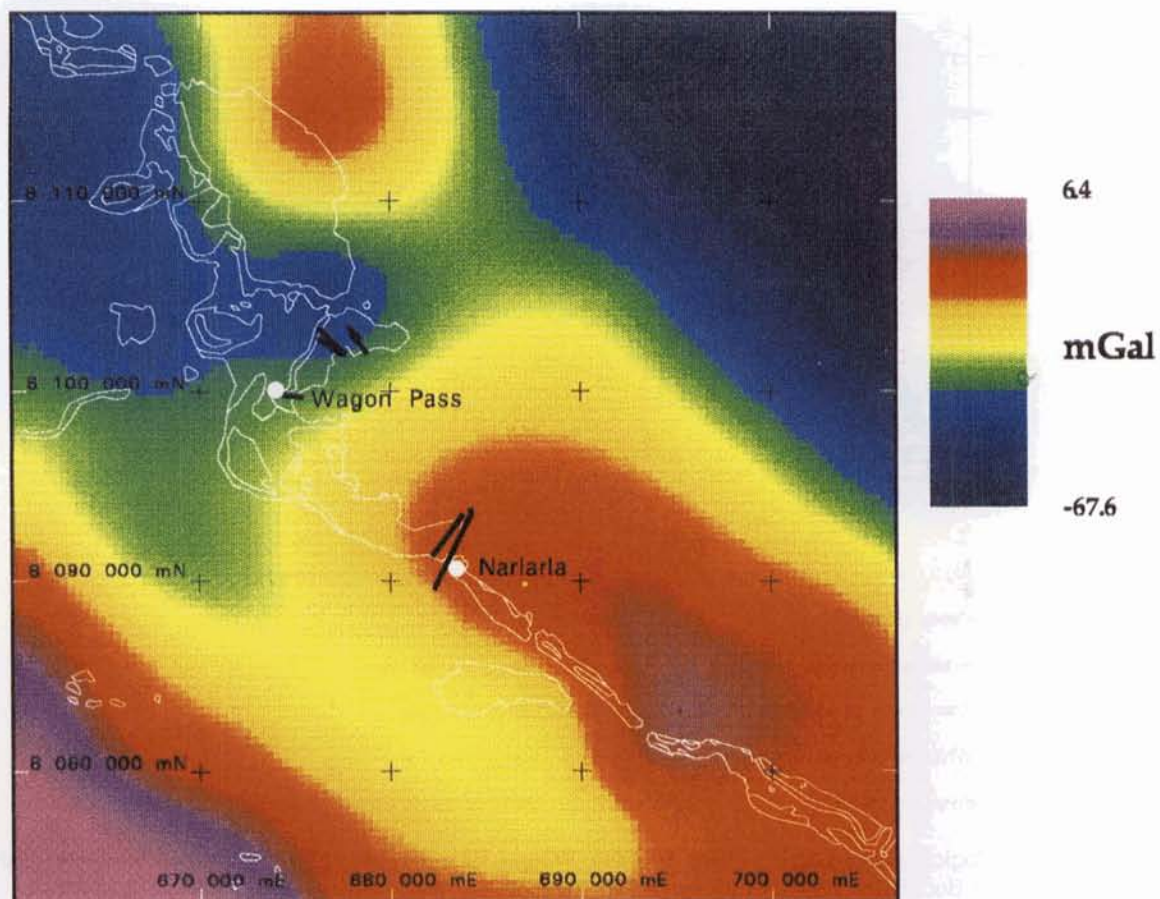
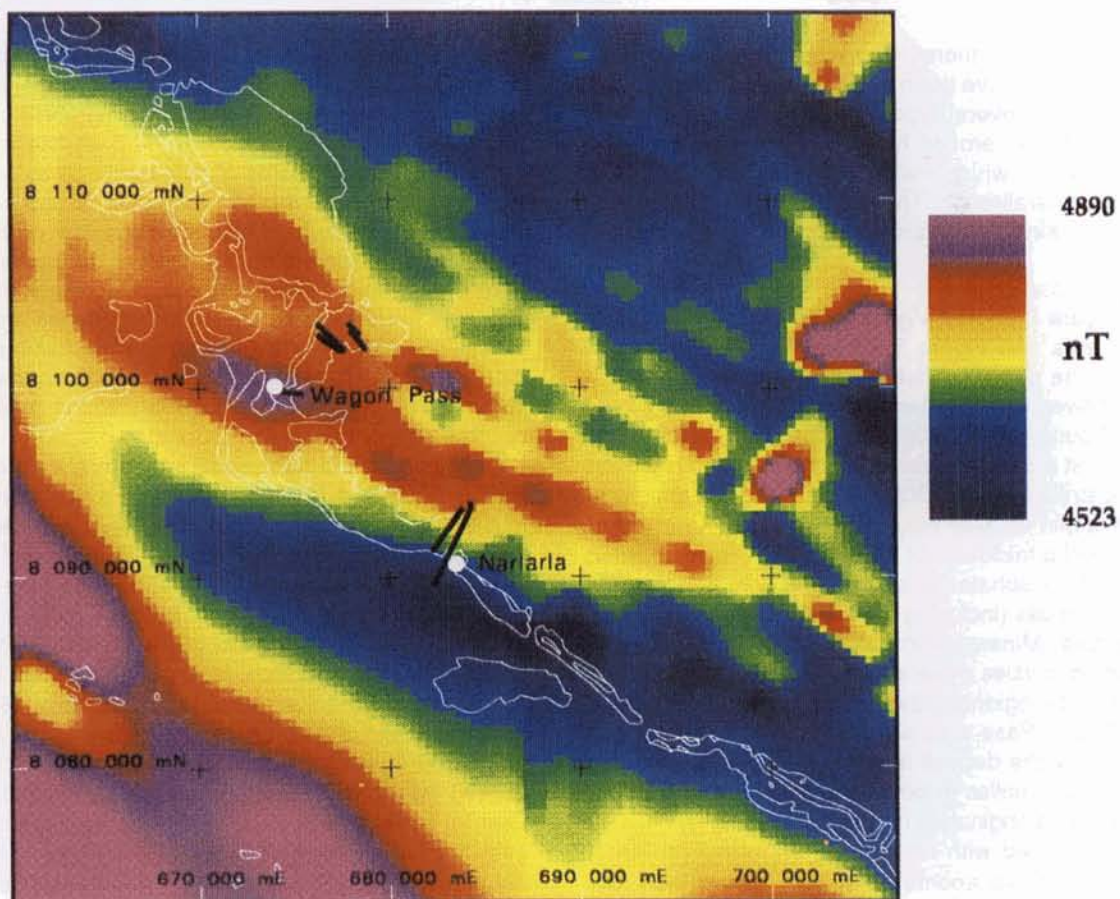
Figure 6 shows a geological map of the Wagon Pass area and Figure 7 an east-west cross-section across the deposit. Mineralisation occurs as a north-to northwest-trending lens of reticulate fracture fillings stratabound within dolomites of the Lower Napier Formation at a depth of about 220 m. The mineralisation has a strike length of 300 m (consisting of high-grade pods within weaker mineralisation), a width of 30 to 80 m and a thickness of 3 to 36 m. The mineralisation consists of sphalerite and galena with subordinate iron sulphides (including marcasite) and minor copper sulphides. Mineralisation is interpreted to have occurred in cavities generated by solution brecciation.

AGSO regional gravity and magnetic data across the Wagon Pass area are shown in Figure 8. These data show the deposit is in an area where there are positive anomalies in both datasets and these are interpreted as originating from basement highs, such as are associated with many MVT deposits. The areal extent of these anomalies differs, presumably because of variations in the distribution of density and magnetisation contrasts within the basement.

Downhole logs were recorded in drillhole NRD-

23, the discovery hole of the Wagon Pass deposit (Figs 6 & 7), to characterise the physical properties of the mineralisation and to assist in stratigraphic correlation (Fig. 9). The chargeability (M3) and resistivity logs were recorded using a pole-dipole array and a Scintrex IPR-8 receiver. Mineralisation is associated with a chargeability high and resistivity low on these logs. The approximate coincidence of the curves for each of the three electrode spacings (2, 8 and 16 m) suggests the mineralisation is homogeneous around the drillhole. There is also a high on the gamma ray data. The only effect of the mineralisation on the single-point resistivity and SP logs is that the readings become slightly higher and more stable.

Figures 10 and 11 show IP and gravity data along lines 30000N and 30000E (local grid) which intersect at NRD-23 (Fig. 6). The gravity data were collected at a spacing of 100 m, and a density of 2.5 g/cm³ was used in their reduction. The gravity response is a combination of long-wavelength features derived from basement and short-wavelength features which appear to correlate with local facies changes. The electrical data were collected using a Scintrex 15 kW transmitter and IPR-8 receiver, a dipole-dipole array and a 200 m electrode spacing. The pseudosections derived from the IP data contain anomalies that appear to be related to local facies changes with little evidence for response from the mineralisation. The IP responses beneath the depth of mineralisation are probably related to groundwater in porous sandstones known to occur at the base of the Devonian sequence [labelled Duv (the Van Emmerick Conglomerate) in

A**B**

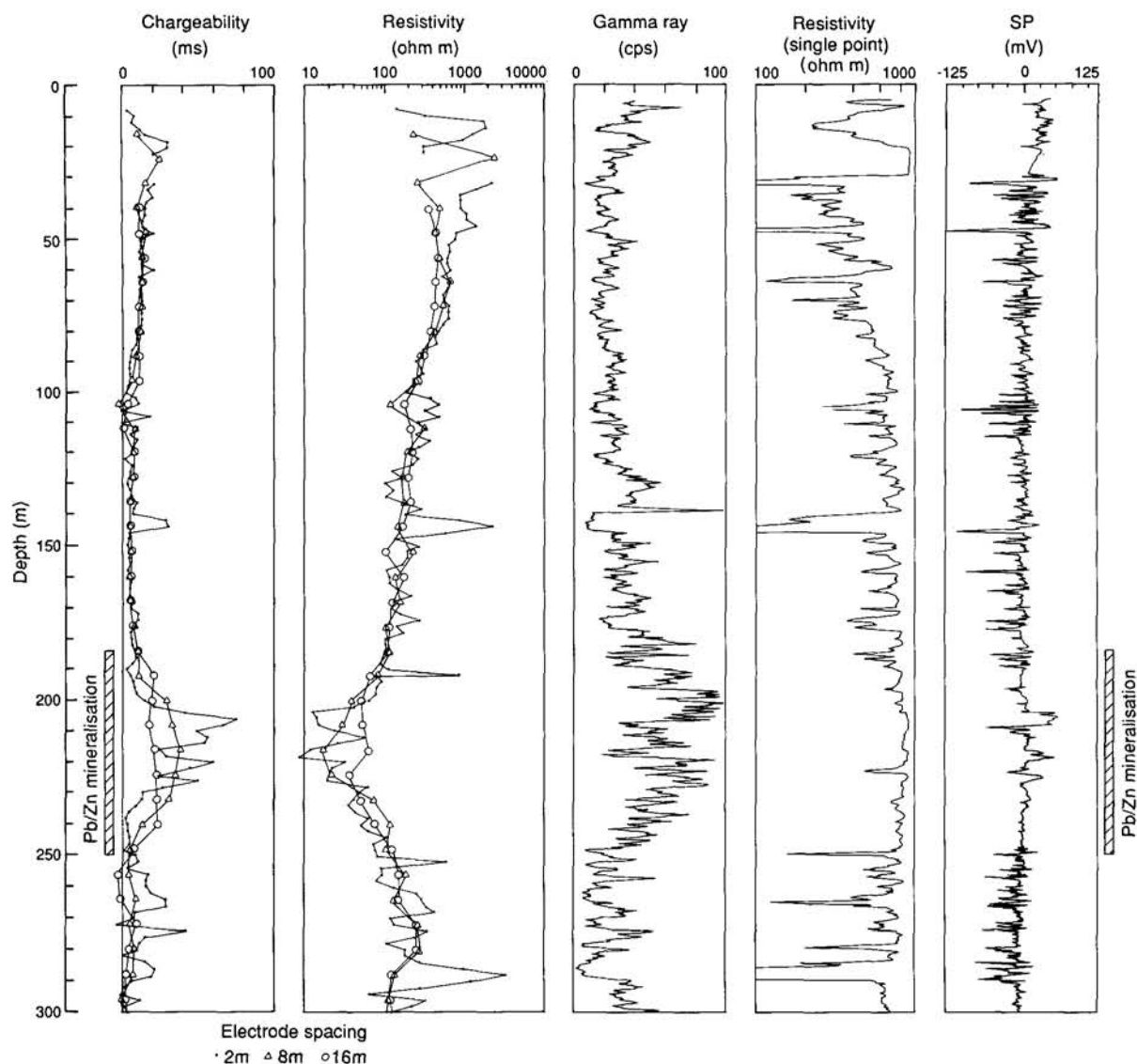


FIGURE 9 Downhole logs from the NRD-23 drillhole through the Wagon Pass deposit. See Figure 6 for location.

Fig. 7]. However, there is a chargeability anomaly on line 30000N between 29400E and 30000E which may be associated with mineralisation. Various EM systems were tested across the Wagon Pass deposit, including EM-37, Turam and EMR-16, but all failed to unequivocally detect the mineralisation, although EM-37 soundings proved capable of mapping a conductor at depth, in agreement with the electrical data. Follow-up drilling to test the deep conductor did not locate mineralisation.

Mise-a-la-masse data from NRD-23 are shown in Figure 12. In the area immediately surrounding the drillhole these data show a north-south trend similar to that of the mineralisation. However, at distances greater than 100 m, the mise-a-la-masse contours are nearly circular and there is little correspondence between the contours and the distribution of mineralisation known from nearby drillholes. This suggests that mineralisation is either not conductive or is centred on the drillhole. The distribution of mineralisation from drilling suggests the former. Trials with gradient-array IP using downhole current electrodes were undertaken. The surveys consisted of current electrodes within mineralised areas of drillholes and a surface di-

pole to measure resistivity and chargeability. In the example shown in Figures 13 and 14, a current of 2.5 to 3 A was used with electrodes in NRD-23 (210 m depth) and NRD-65 (330 m depth), which are about 1 km apart (Fig. 6). Measurements were made using a Huntect 7.5 kVA transmitter and a Huntect Mk IV receiver. Survey lines were 700 m long and oriented east-west to be perpendicular to the direction of current flow and the geological strike. Line spacing was 200 m, station spacing 50 m and a 50 m dipole was used. Contours of chargeability (Fig. 13) and normalised voltage (Fig. 14) define anomalies roughly coincident with mineralisation immediately north of NRD-23. However, the overall correlation with known mineralisation is poor and the north-south trends of the contours may well be a function of facies changes rather than mineralisation.

Downhole PEM was also tried in drillhole NRD-23, with the results shown in Figure 15. The method appears to detect the mineralisation with a subdued response on channels 1 and 2. The late-time low at 225 m is ascribed to local heterogeneities or noise. The downhole EM response of the mineralisation is insignificant from an exploration perspective.

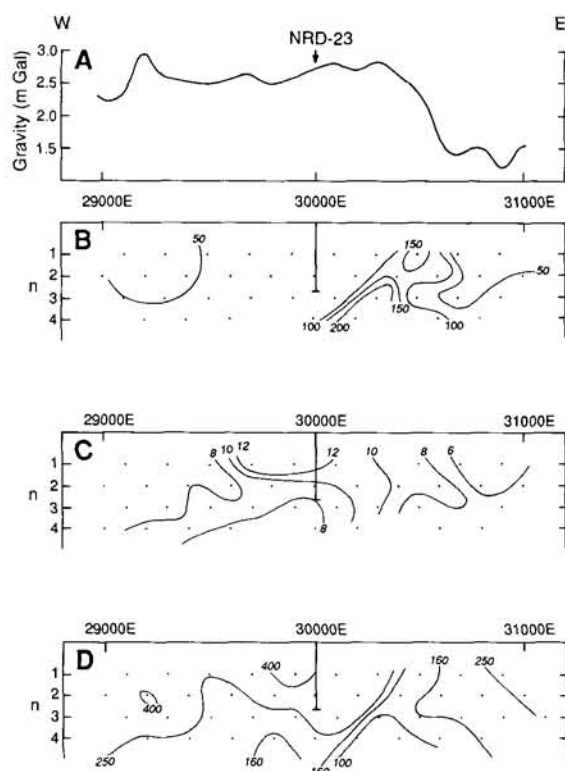


FIGURE 10 Gravity and IP data from line 30000N across the Wagon Pass deposit. A. Gravity. B. Metal factor, 2000 M/p. C. Chargeability. D. Apparent resistivity. See Figure 6 for location.

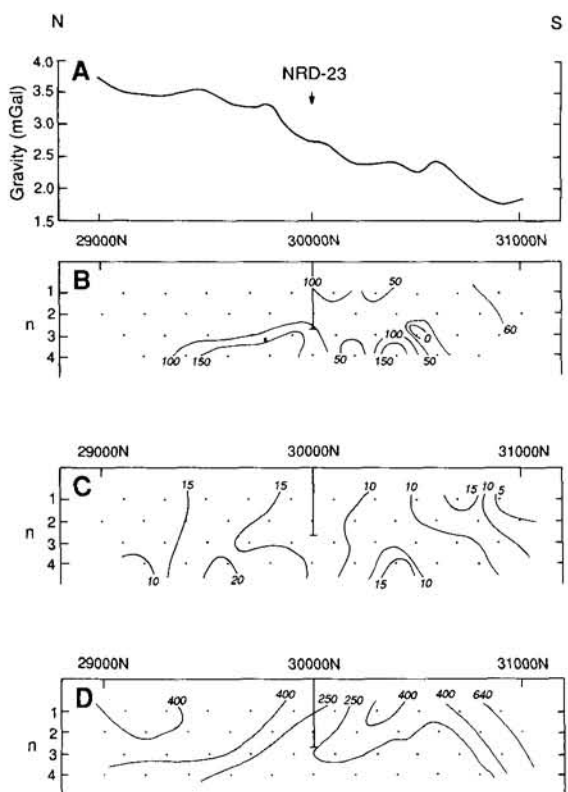


FIGURE 11 Gravity and IP data from line 30000E across the Wagon Pass deposit. A. Gravity. B. Metal factor, 2000 M/p. C. Chargeability. D. Apparent resistivity. See Figure 6 for location.

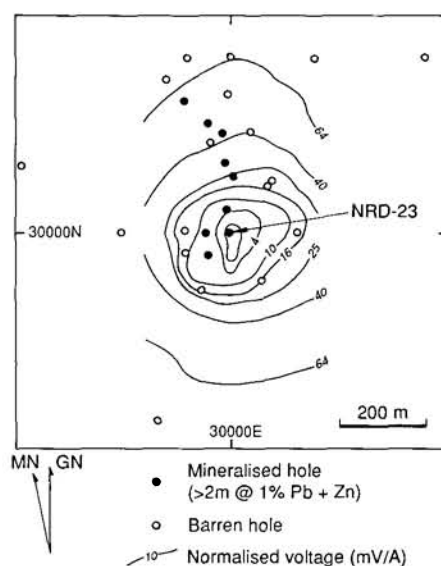


FIGURE 12 Mise-a-la-masse data from drillhole NRD-23, Wagon Pass. The reference potential electrode was positioned by the drillhole collar. GN = grid north, MN = magnetic north. See Figure 6 for location.

BONAPARTE BASIN

Sorby Hills

The Sorby Hills deposits occur over a 7 km strike-length in the southern part of the Bonaparte Basin (Lee & Rowley, 1990). Mineralisation is hosted by dolomite within a succession of carbonate and clastic rocks, and consists of a number of discrete orebodies (Fig. 16), some of which are linked by low-grade mineralisation. The average thickness of the high-grade pods is about 7 m. Bodies A to G occur on the eroded edge of a palaeosurface adjacent to north-west-trending faults and are commonly associated with palaeochannels. Bodies H to J are controlled by basement palaeohighs. In both cases the host is a stratabound sheet breccia developed along an unconformity. The Alpha and Beta trends are structurally controlled, being within tectonic and syn-sedimentary slump breccias and collapse breccias, respectively. The orebodies are vertical to subvertical in both cases. The ore mineralogy at Sorby Hills is simple, comprising galena and sphalerite at a ratio of about 10:1 with marcasite, pyrite, calcite and dolomite the gangue minerals (Jorgensen *et al.*, 1990). Mineralisation occurs beneath a thick (typically 25 m) conductive (about 0.2 S/m) cover of black alluvial soil and shale. Geophysics was a major component of the exploration programme; methods used included magnetics, gravity, various electrical methods (especially IP), seismic refraction and EM. Downhole logging, particularly gamma logging, was widely used to establish correlations between boreholes. The following description of the geophysical program is taken from various open-file reports submitted by Aquitaine Australia Minerals to the Western Australian Department of Mines.

Mineralisation was discovered at Sorby Hills by drilling bedrock geochemical anomalies. Subsequently, trial IP surveys found anomalies coincident

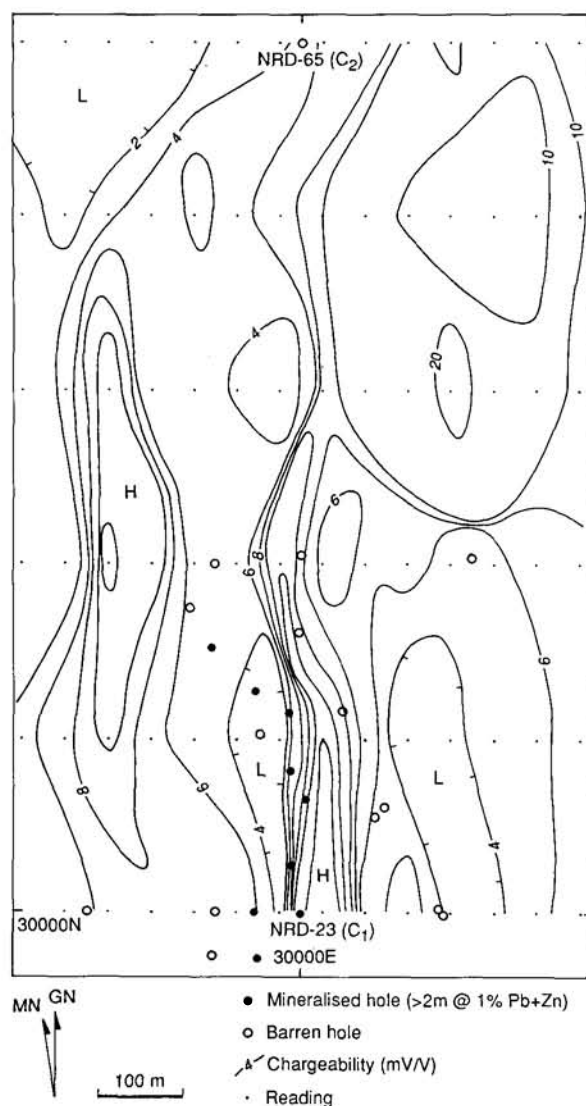


FIGURE 13 Chargeability data for Wagon Pass obtained using current electrodes (C1 and C2) in drillholes NRD-23 and NRD-65, respectively. GN = grid north, H = high, L = low, MN = magnetic north. See Figure 6 for location.

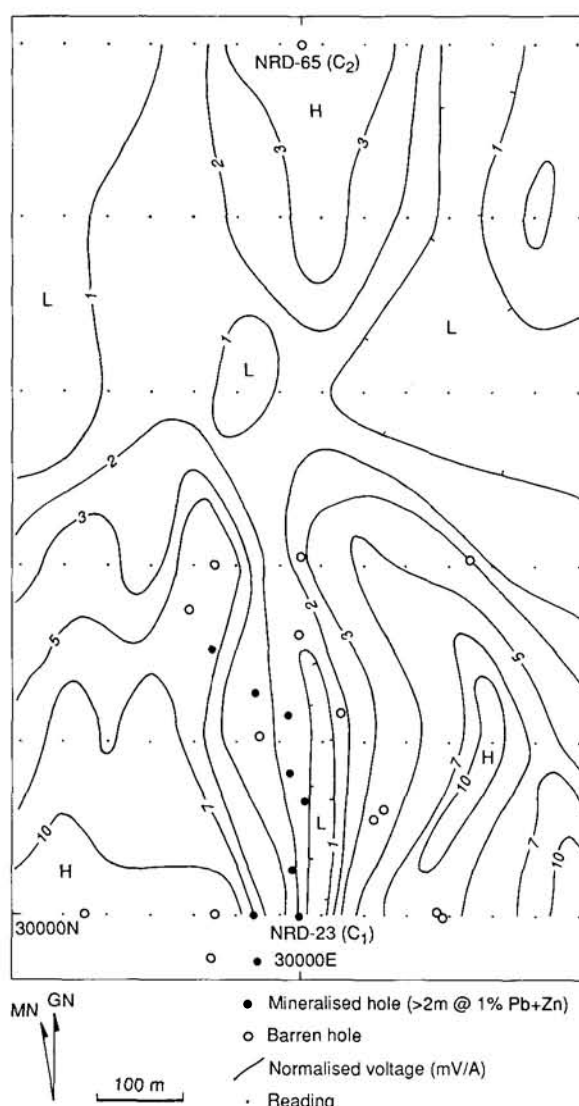


FIGURE 14 Normalised voltage data for Wagon Pass obtained using current electrodes (C1 and C2) in drillholes NRD-23 and NRD-65, respectively. GN = grid north, H = high, L = low, MN = magnetic north. See Figure 6 for location.

with known mineralisation and geochemical anomalies, and extensive tests were carried out to determine the best survey parameters for locating mineralisation in the Sorby area. The procedure adopted consisted of dipole-dipole reconnaissance surveys with 100 m dipoles and n from 1 to 4, while areas known to contain mineralisation were mapped using the gradient array with overlapping blocks. In the latter case, the current electrode spacing (AB) was selected based on electrical soundings and IP expanders. In general, a current electrode spacing of 1000 m was used, larger spacings giving rise to severe electromagnetic coupling effects, especially in areas of conductive black soil cover. The potential electrode spacing (MN) was set at 50 m and line spacing at 100 m. The two types of survey were used for these different tasks because the dipole-dipole array was found to produce the largest anomalies, but its horizontal resolution is poor. In contrast, the gradient array only gave rise to small anomalies but resolution and dip indications are good. A 7.5 kVA transmitter and Scintrex IPR-7 re-

ceiver were used in both cases.

Chargeability and apparent resistivity data from the gradient array surveys are shown in Figures 17 and 18. These data must be treated with caution for several reasons. Firstly, some blocks covered an area 400 m square whereas others covered 600 m square with AB remaining at 1000 m. In the latter case, the conductive overburden has a greater influence on the results giving rise to circular lows close to electrode positions. Secondly, the process of matching adjacent blocks by elevating or decreasing values of a particular block to match its neighbours gives rise to gradients at block boundaries. Finally, data of different vintages were collected based on different survey grids resulting in uncertainties in location. Despite these limitations, a number of observations can be made about the data. The individual pods of high-grade mineralisation are not defined by either the chargeability or apparent resistivity data. This is because changes in chargeability within individual blocks are generally due to changes in total sulphide content,

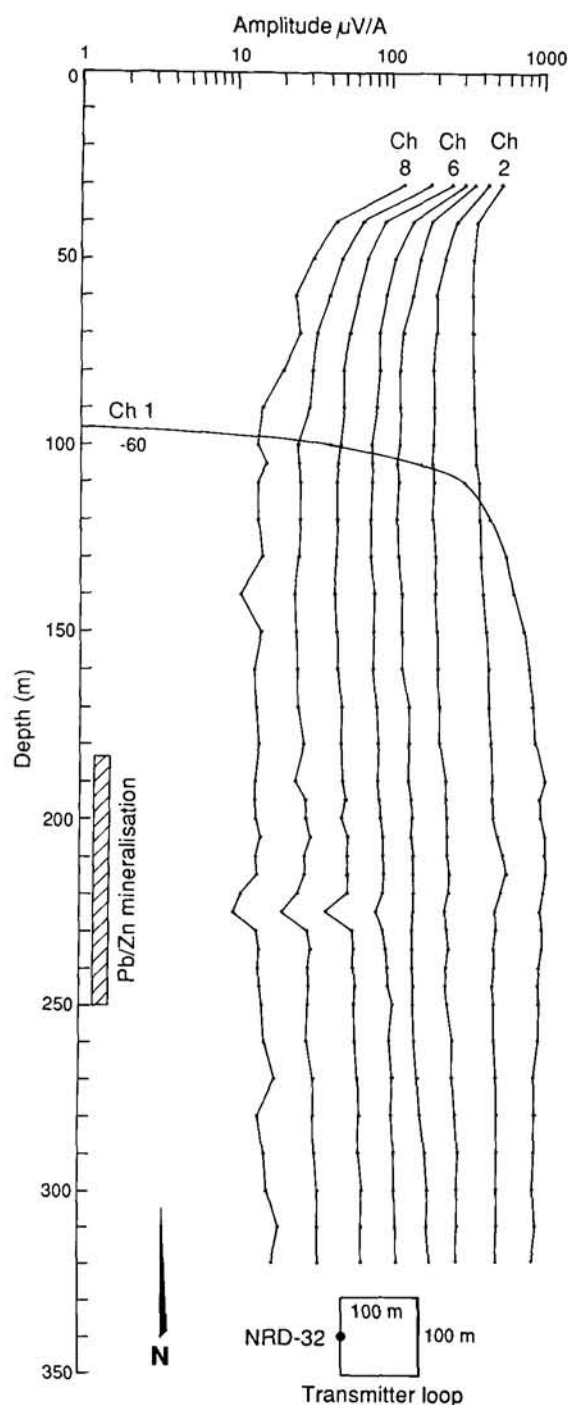


FIGURE 15 Downhole PEM data from drillhole NRD-23, Wagon Pass. See Figure 6 for location.

particularly pyrite. The relationship between pyrite and galena is not well understood but high pyrite contents seem to exclude high galena grades, hence the lack of correlation between chargeability and mineralisation. However, the gradient-array data do outline the broad zone of base-metal and pyrite mineralisation and define the local geological strike, as well as possible crosscutting faults (compare Figs 17 and 18 to Fig. 16) or perhaps facies changes. In the north of the area, where the Alpha and Beta trends occur, IP is much less successful with no IP response obtained over the Beta trend for any AB spacings. This is mainly due to a thicker conductive cover.

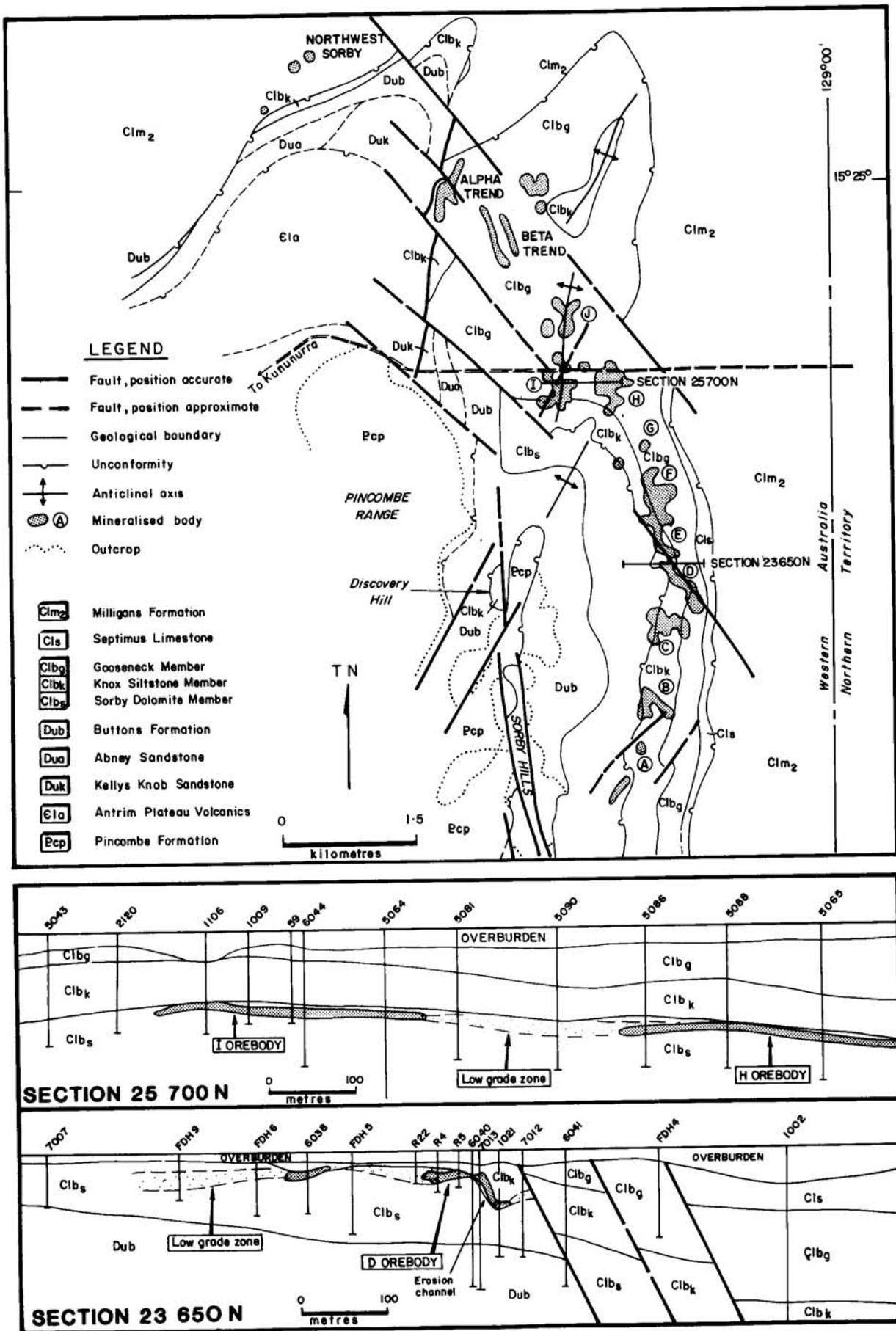
Figure 19 shows an example of a dipole-dipole reconnaissance IP line over mineralisation comprising the C pod. The mineralisation gives rise to an apparent polarisability anomaly and, to a lesser extent, a resistivity anomaly.

Given the lack of IP response in the northern part of the Sorby Hills area, a test RRMIP survey was carried out to see if such data could detect mineralisation. The survey consisted of six blocks using 1.2 km current dipoles and a frequency of 3 Hz. A 600 m dipole and 0.3 Hz frequency were also used for some blocks. Conductive zones were detected using the H_n parameter, but not equated with mineralisation because of the known poor conductivity-thickness product of the mineralisation determined by earlier PEM surveys (see below). RPS data showed quite good IP effects when the smaller dipole and lower frequency were used. The results from the western Beta trend are shown in Figure 20, with the mineralisation apparently well defined. However, the eastern Beta trend, admittedly much less well covered, is not nearly so well detected. It is arguable that the conventional IP surveys, if applied in an equally detailed fashion, would also have been as successful. Spectral IP was also tried over the Alpha and Beta trends. A dipole-dipole array was used with a 50 m dipole. Low-resistivity zones were attributed to faults and fractures, but phase data (at 0.11 Hz) did appear to detect mineralisation. Again, comparison with the conventional IP data is difficult since the latter used 100 m dipoles and obviously have lower resolution.

Aeromagnetic data were acquired and small-scale ground magnetic surveys carried out to provide structural information. Results were not particularly helpful although some basement features, such as highs and faults, were defined. Magnetic data cannot be used to directly detect mineralisation since this was found to have susceptibilities close to those of the host sedimentary rocks (Table 1).

TABLE 1 Magnetic susceptibility data from Sorby Hills. Measurements were made on cores, chips and powdered samples using a Bison 3101A susceptibility meter. They are considered accurate to about 3×10^{-5} SI.

Description	Magnetic Susceptibility (SI)
Basement	$741 \times 10^{-5} - 1257 \times 10^{-5}$
Dolomites and siltstones	$38 \times 10^{-5} - 88 \times 10^{-5}$
Massive mineralisation	0
Disseminated mineralisation	Similar to sediments
Magnetite-bearing sands	up to 251×10^{-5}


 FIGURE 16 Geological map and cross-sections of the Sorby Hills area. From Jorgensen *et al.* (1990).

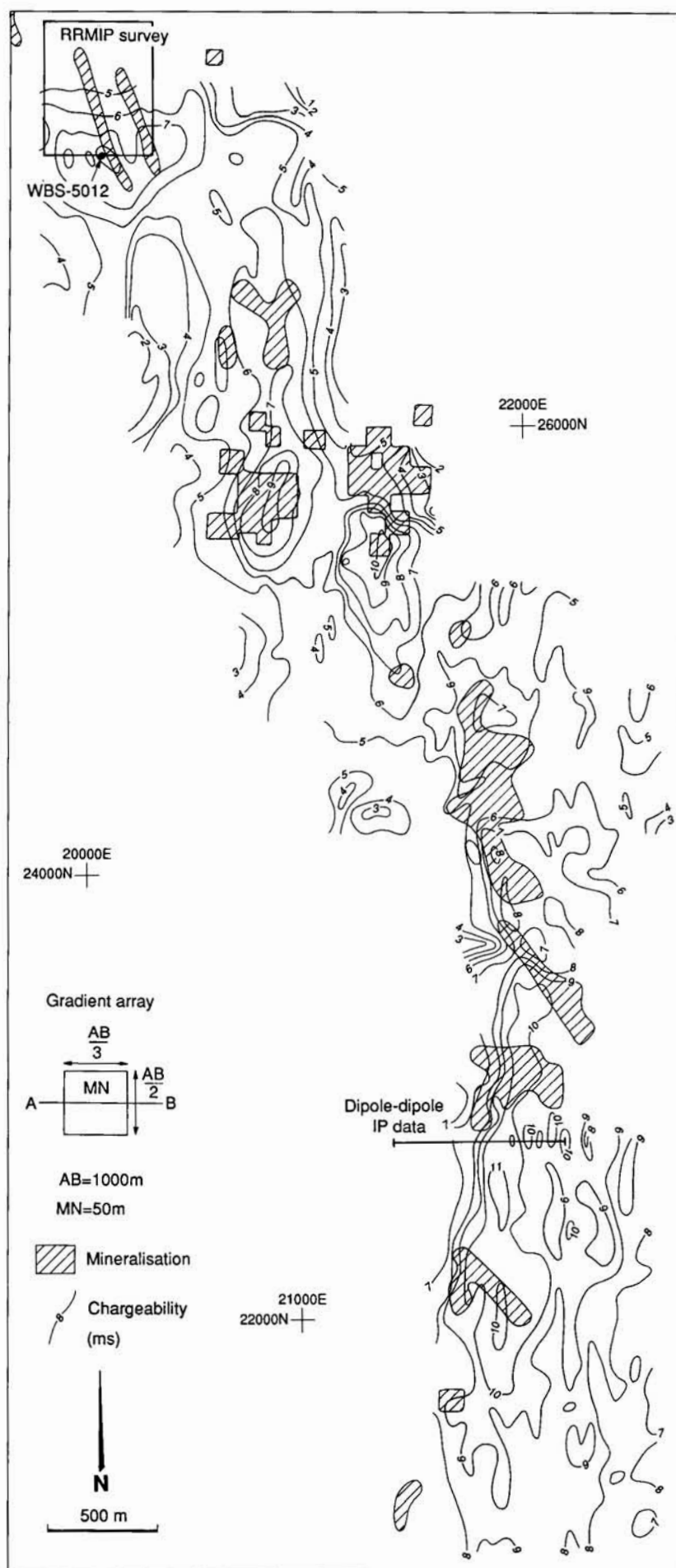


FIGURE 17 Gradient-array chargeability data, Sorby Hills.

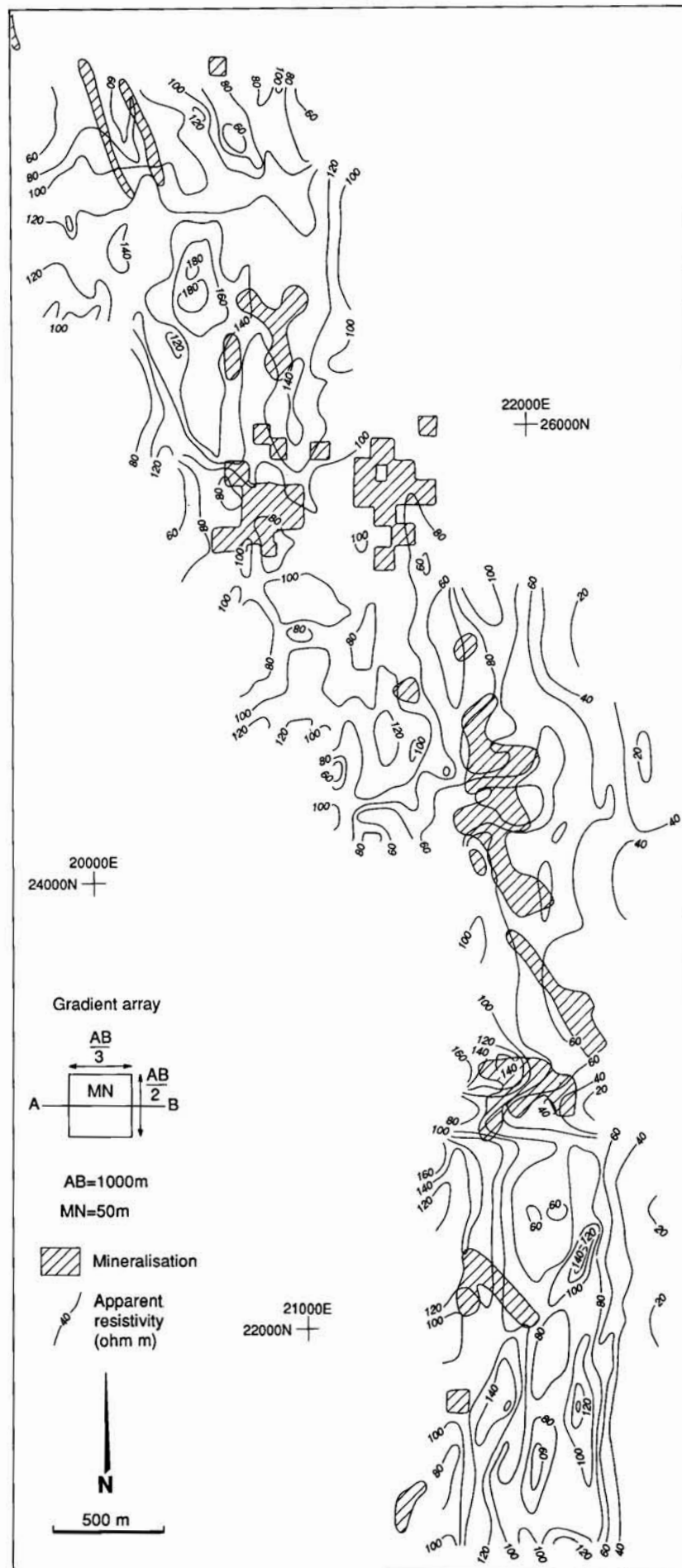


FIGURE 18 Gradient-array apparent resistivity data, Sorby Hills.

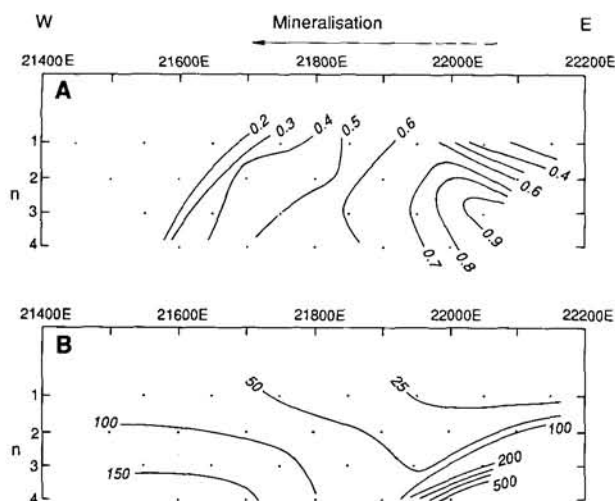


FIGURE 19 Dipole-dipole array IP data along line 22800N, Sorby Hills. A. Polarisation. B. Apparent resistivity. See Figure 17 for location.

Gravity surveying was also tried at Sorby Hills but was found to be of little use for detecting mineralisation due to problems isolating anomalies originating from the small density contrast between ore and host rock from those due to irregularities in the basement surface and facies changes within the cover. Seismic refraction data were also used as a cheaper alternative to grid drilling to determine structure between boreholes. Velocity contrasts were such that the base of the black shales and the interface between siltstone and dolomite, important in terms of the location of mineralisation (Fig. 16), could be mapped. Faults and solution features could also be detected. Velocities were sufficiently diagnostic in many areas that formations could be identified in this manner. The seismic data were also used to map hinge lines which controlled mineralisation in some areas (e.g., the Alpha trend). A trial of the seismic reflection method using Mini-Sosie was undertaken in an attempt to recognise breccia-type orebodies and general structures. The only significant reflection obtained was from the base of the black shales. The poor data were explained in terms of:

- (i) the overburden absorbing most of the seismic energy,
- (ii) lack of sufficient velocity contrasts within the underlying sequence and
- (iii) deeper reflections arriving too close behind the base of shale event to be distinguished.

The degree of success of PEM surveys at Sorby Hills is unclear. Lee & Rowley (1990) state that the method "led to the successful discovery" of the Beta trend but was less successful in other areas of flat-lying mineralisation (24000N to 26000N, local grid; see Fig. 18) where anomalies correlated with barren fault and fracture zones. However, reports submitted to the Western Australian Department of Mines suggest that good mineralisation had already been found in the Beta area prior to carrying out the PEM surveys. Nevertheless, various types of horizontal-loop survey defined two elongate conductive trends which closely coincided with the two areas of mineralisation comprising the Beta trend. Subsequent work defined

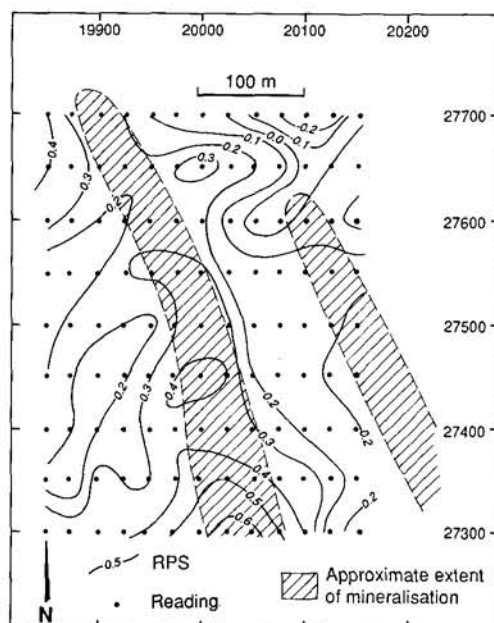


FIGURE 20 RRMIP, RPS data over the Beta trend, Sorby Hills. See Figure 17 for location.

further elongate zones of similar trend in the area but drilling yielded disappointing results, with conductive fault and fracture zones being considered responsible for the anomalies. In the area of the Alpha trend, the PEM delineated the basement-cover interface and some faults. The effectiveness of the method was, however, greatly reduced by the presence of significant thicknesses of conductive black shale. Initial soundings over known mineralisation (Beta trend) using a vertical loop again defined anomalies apparently coincident with mineralisation but, as before, subsequent drilling results were disappointing, only intersecting conductive faults and fractures. Downhole PEM was also tried, using a 100 m by 100 m loop. The results were dominated by overburden responses (Fig. 21), although in this case about 1 m of massive galena gives rise to the small anomaly between 70 and 80 m on the early channels. These data demonstrate the low conductivity-thickness product of the mineralisation relative to the host rocks and overburden, hence the poor response to PEM and the reluctance to drill conductive areas mentioned above. The Crone DEEPEM technique was also tested at Sorby Hills but only conductive overburden responses were obtained.

Several mise-a-la-masse surveys were carried out at Sorby Hills to determine the extent of mineralisation encountered in drillholes, for example in the D pod and Alpha trend. Variations in potential and chargeability sometimes showed moderately well-developed trends, although these were commonly not parallel to the main trend of the mineralisation as defined by drilling and could reflect faulting.

BROOME ARCH Admiral Bay

The Admiral Bay zinc-lead deposit (Connor, 1990) is 1280 to 1600 m below the surface and was discovered when the mineralisation was intersected by a petroleum exploration well (Fig. 22). The depth

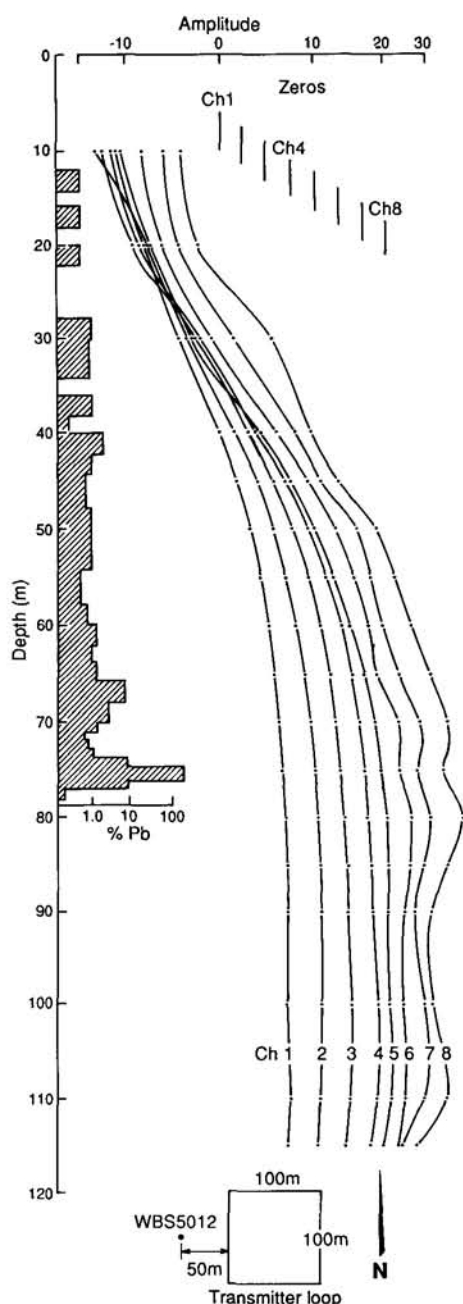


FIGURE 21 Downhole PEM and assay data from drillhole WBS-5012, Sorby Hills. See Figure 17 for location.

of the mineralisation has prevented extensive drilling to determine its extent and continuity, although a strike length of 19 km has been proved.

The following is based on Connor (1990) and additional geological and geophysical data generously made available by CRA Exploration Pty Ltd. The local succession consists of Ordovician to Silurian sedimentary rocks unconformably overlain by Permian and younger sedimentary rocks. Mineralisation occurs throughout the Lower Palaeozoic sequence but is concentrated within the Nita Formation and the lower part of the overlying Carribuddy Group and, to a lesser degree, the Goldwyer Formation (Fig. 23). The Goldwyer Formation consists of shale with minor limestone and the Nita Formation comprises limestone and dolomite with minor siltstone and shale.

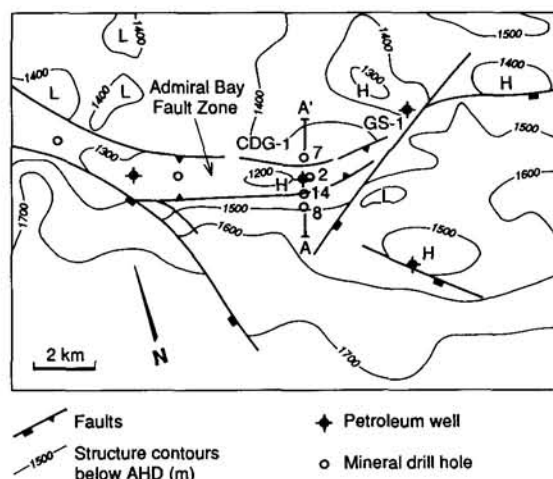


FIGURE 22 Structure contours on the top of the Nita Formation and drillhole locations, Admiral Bay area. Redrawn from Connor (1990). CDG-1 = Cudalgarra-1 petroleum well, GS-1 = Great Sandy-1 petroleum well, H = high, L = low.

The Carribuddy Group comprises claystone, shale, halite and dolomitic siltstone with minor sandstone and limestone. Low-grade mineralisation is developed over intervals ranging in thickness from 165 to 459 m within which there are higher-grade zones a few metres thick. Two styles of mineralisation are recognised (labelled 1 and 2 in Fig. 23) with the gradual boundary between the two within the Nita Formation (Connor, 1990). The lower zone (2) is at the basal contact of the Nita Formation and consists of a complex network of veins of barite, dolomite, calcite, siderite and quartz with associated galena, chalcopryite, fluorite, pyrite, marcasite, haematite, magnetite, sphalerite and hydrocarbons. There is massive galena at the top of this zone in a few drillholes. Vugs can be lined with bitumen and in places contain liquid hydrocarbons. Zone 1 is in the upper part of the Nita Formation. It has less veins than zone 2, and mineralisation has sealed porous units leading to thin stratabound mineralisation. The main ore minerals are sphalerite and galena with the gangue minerals being dolomite, barite, fluorite and hydrocarbons. In places, hydrocarbons are present in vugs, stylolites and within sandstone matrix. Beneath zone 2 is a complex area of alteration extending through most of the Goldwyer Formation (labelled 3 in Fig. 23) and consisting of barite, quartz, siderite, fluorite, dolomite, magnetite and other iron oxides with only minor galena and chalcopryite. Increased magnetic susceptibility of the zone is attributed to magnetite (Fig. 23).

The deposit is associated with the Admiral Bay Fault Zone (Fig. 22). Variations in stratigraphic thickness show this fault was active in the Ordovician and it may have controlled a local high giving rise to the algal reef assemblage of the Goldwyer Formation (Fig. 23). Later reverse movements (*i.e.*, inversion) on the fault resulted in the present-day fault-bounded high. Figure 24 shows a seismic section across the Admiral Bay deposit and Figure 25 is an interpretation of these data (S. McCracken, pers. comm., 1993). The ore itself is not visible on these data other than as a zone where seismic markers become less dis-

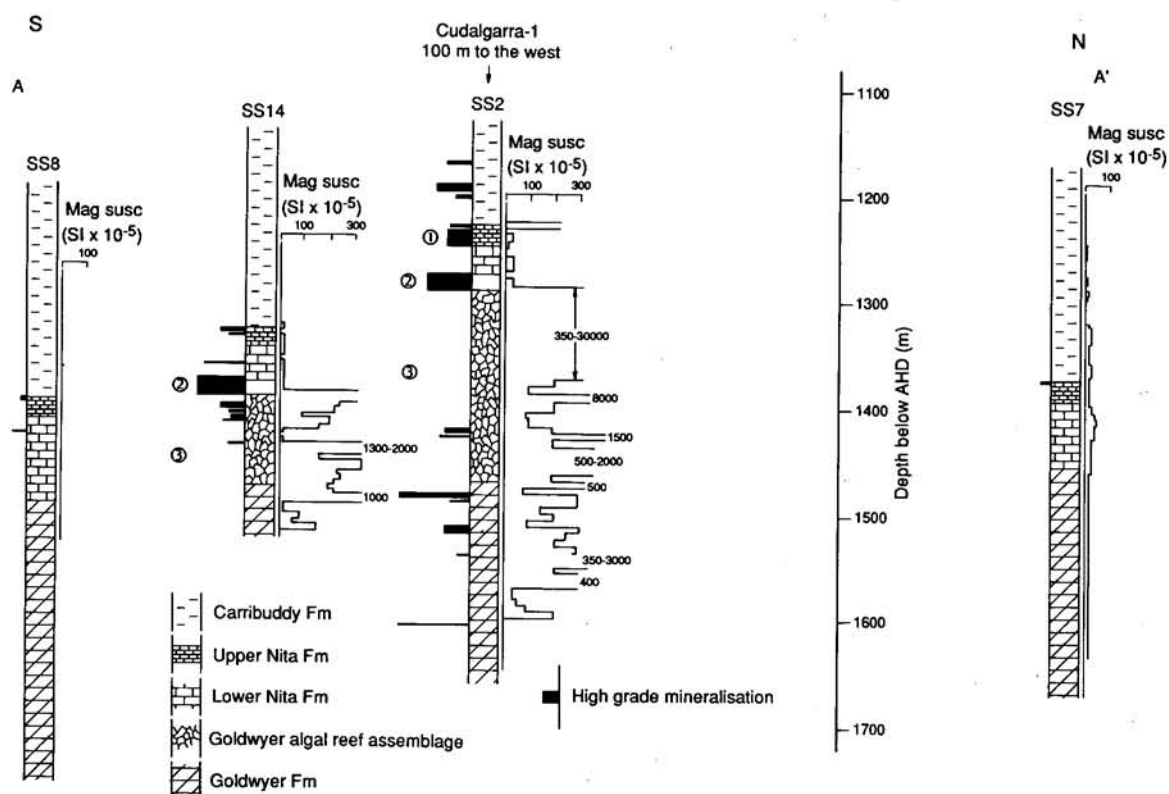
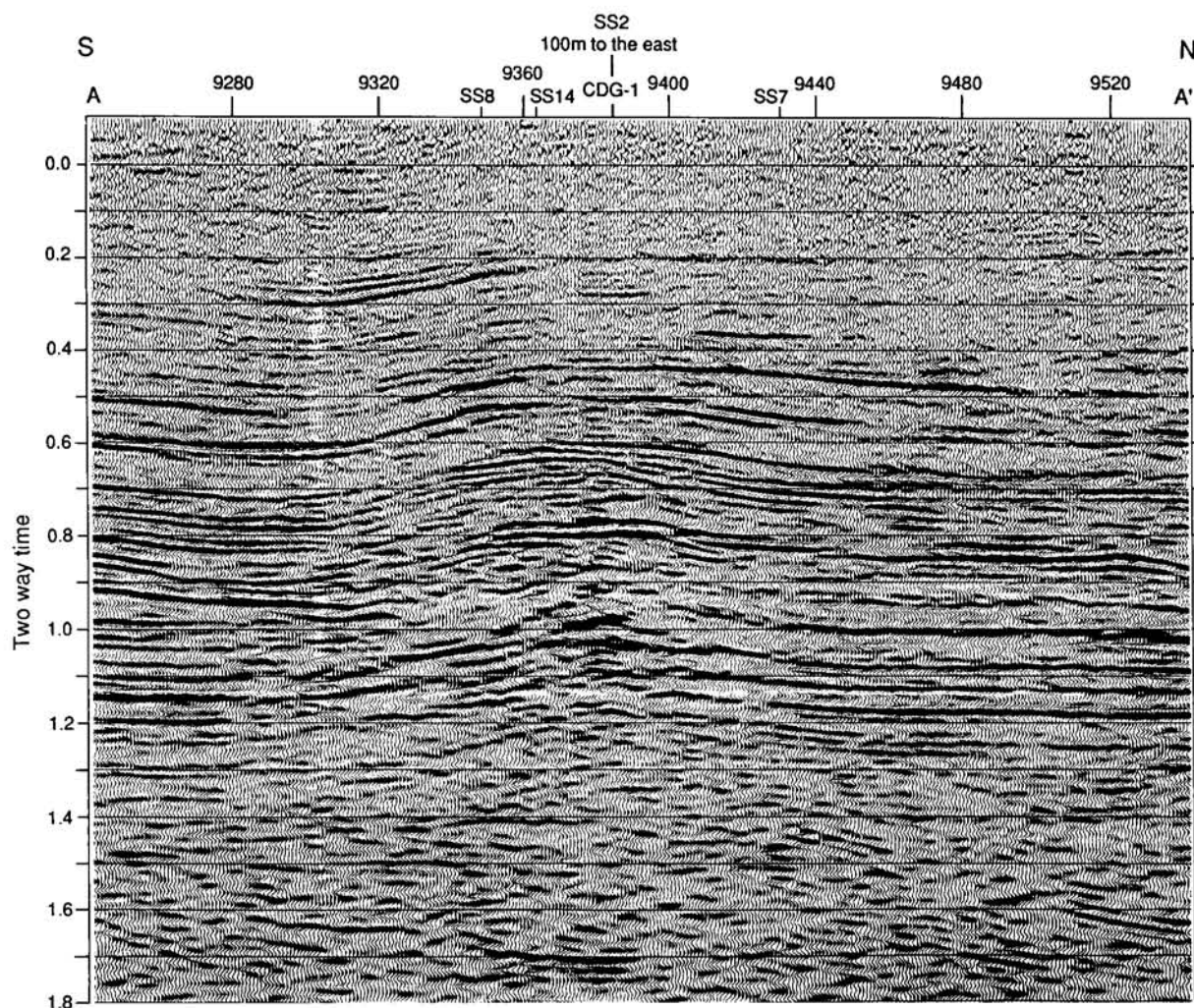


FIGURE 23 Drillhole and magnetic susceptibility data from the Admiral Bay deposit. 1 and 2 are areas of high-grade mineralisation. 3 is the zone of low-grade mineralisation. SS2, SS7, SS8 and SS14 are drillholes. See Figure 22 for location.



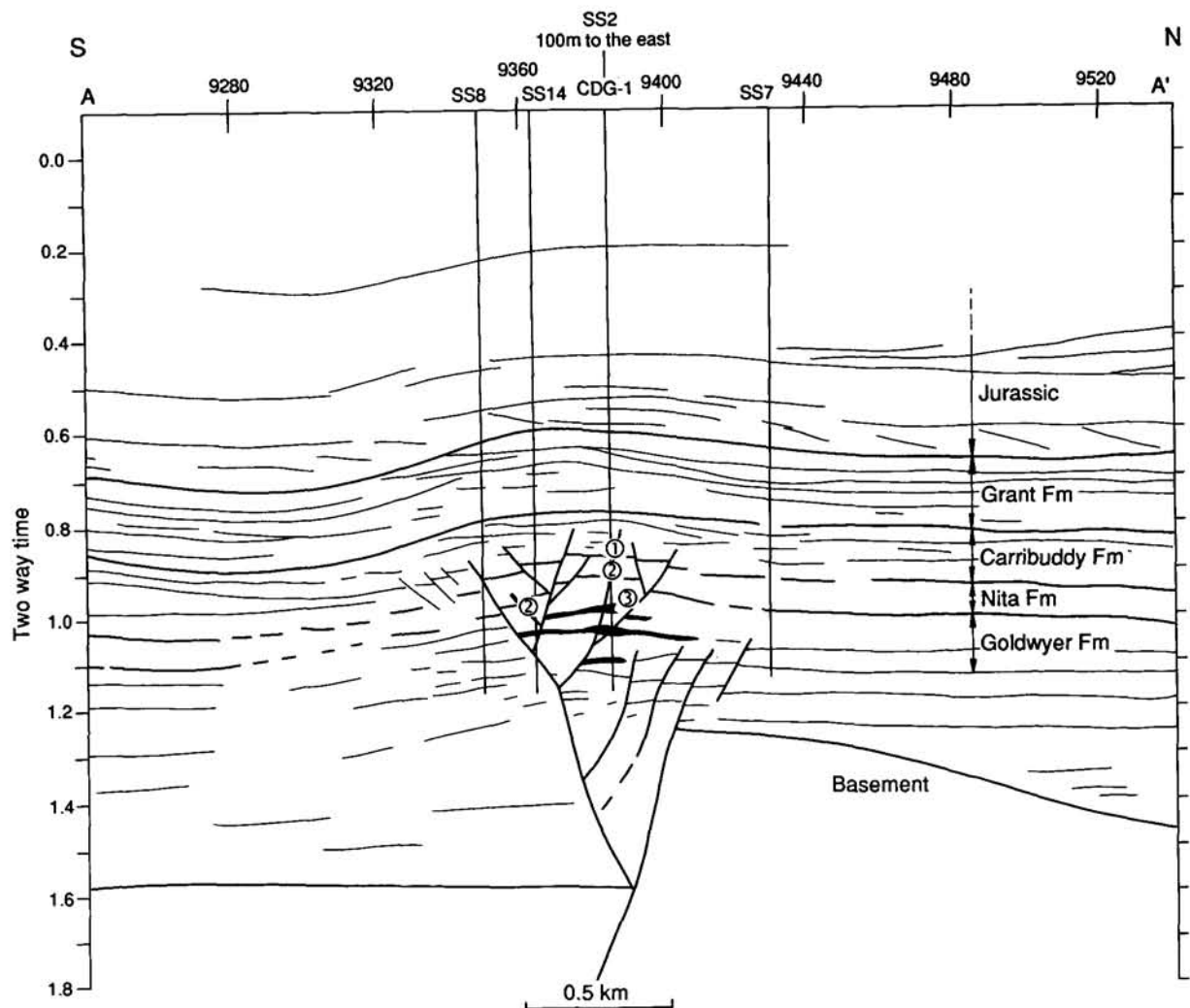


FIGURE 25 Interpretation of seismic line 88-109 (S. McCracken, pers. comm., 1993) for the Admiral Bay deposit. The seismic line is approximately coincident with the line of drillholes in Figure 23. 1 and 2 are areas of high-grade mineralisation. 3 is the zone of low-grade mineralisation and alteration and the black areas are interpreted to be more intense mineralisation within this zone. SS2, SS7, SS8 and SS14 are drillholes used to constrain the interpretation (see Fig. 23).

tinct. However, the faulted structure associated with the mineralisation is defined. The interpretation is constrained by data from the Cudalgarra-1 petroleum well and the deep diamond drillholes shown in Figures 22 and 23.

Gravity and aeromagnetic data have also been acquired in the Admiral Bay area to test whether they can be used to map the reef facies, and/or alteration comprising zone 3, of the Goldwyer Formation, which is associated with the mineralisation (Fig. 23). However, the magnetic response is very weak and not sufficient to enable drillholes to be sited. The gravity signal is indistinguishable from the effects of other density contrasts in the subsurface, such as the contrast between carbonates and shales.

A selection of the wireline logs recorded for petroleum exploration purposes in Cudalgarra-1 is shown in Figure 26. Being a petroleum well, very little core was taken, and thus the intensity and location of mineralisation is poorly known. Additional information

has been derived from the core log from the SS2 drillhole which is situated 100 m to the east (Fig. 22). The analysis of the response of the petroleum logs to the mineralisation was carried out by the authors.

In the succession above the Nita Formation, the SP and gamma logs behave as expected, showing a strong correlation resulting from the fact that both respond to sand-shale. Sand and shale lines can be defined at 0 and 30 mV, respectively, for the SP log, and 20 and 70 Gapi, respectively, for the gamma log. There is usually only a slight separation of the resistivity curves, indicating low porosity, and a positive separation between the density and neutron logs, indicating shale. There are a few areas where responses consistent with limestone horizons are observed, notably at a depth of about 1140 m. These responses are entirely consistent with the rock types comprising the Carribuddy Formation described by Connor (1990).

The effects of the mineralisation are clearly evi-

FIGURE 24 (facing page, at bottom) Migrated seismic reflection section 88-109 across the Admiral Bay deposit.

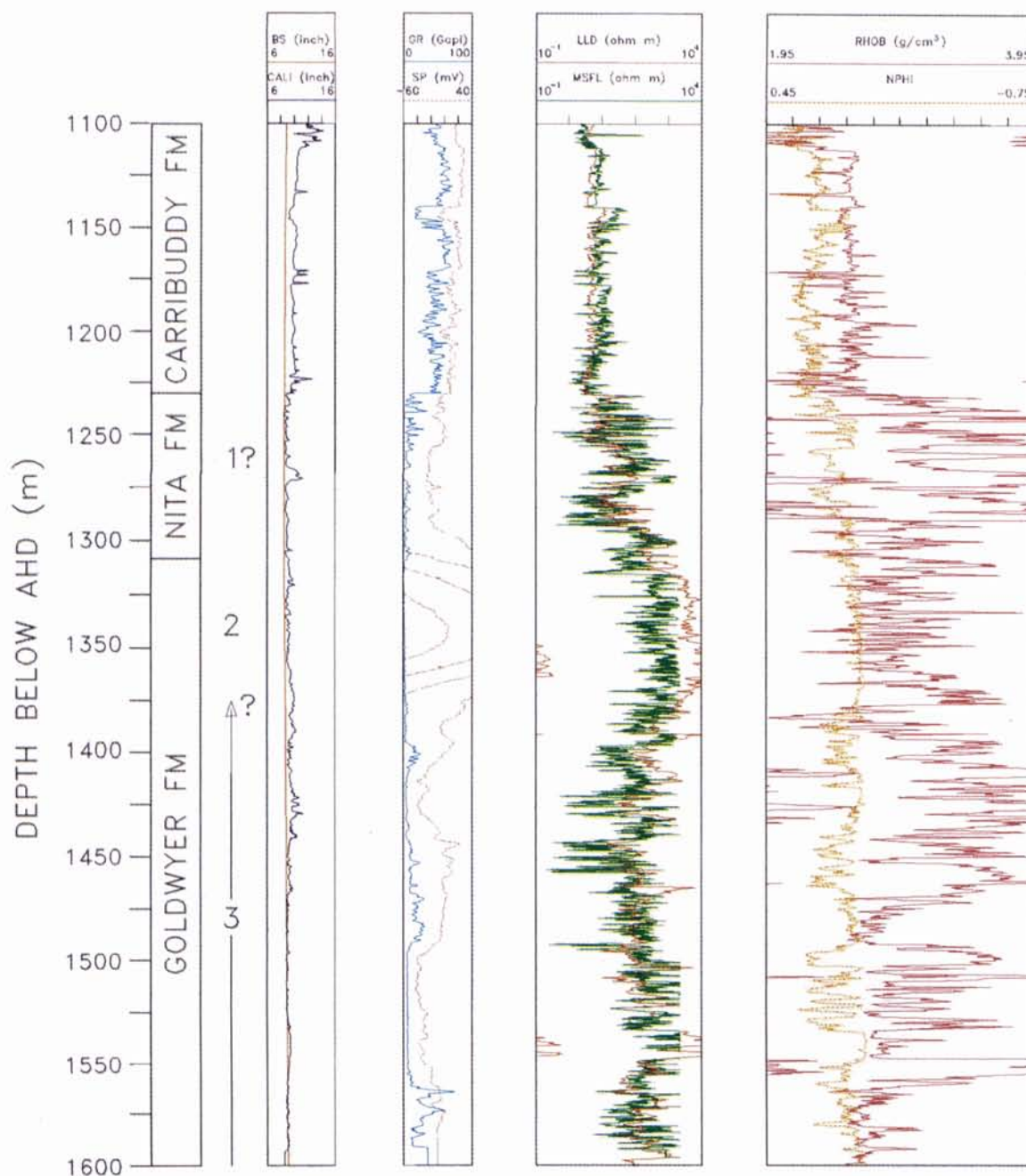


FIGURE 26 Wireline logs from the Cualgarra-1 petroleum well. 1 and 2 are areas of high-grade mineralisation. 3 is the zone of alteration and low-grade mineralisation. BS = bit size, CALI = caliper, GR = gamma ray, LLD = laterolog deep resistivity log, MSFL = micro-spherical laterolog shallow resistivity log, NPHI = neutron log, RHOB = density log, SP = self potential log. See Figure 22 for location.

dent in the Nita Formation and underlying rocks. Over most of the mineralised part of the succession the SP log has a negative deflection of between 40 and 80 mV below the sand line. Areas where this negative deflection is smaller mainly correspond to peaks on the gamma log and could be due to shales. A negative deflection of the SP log is the usual response to sulphides, however, between 1300 and 1375 m the log has a very large positive deflection with a maximum value of around 310 mV. There appears to be no correlation between the grade of mineralisation and the amplitude of the SP response, as is generally the case (Becker & Telford, 1965). Below the Carribuddy Formation, the gamma log readings are

very low. The lowest responses coincide with the largest SP deflections (both positive and negative); for example, 1300 to 1375 m, 1410 to 1430 m and 1495 to 1560 m. This supports the interpretation that the SP log is mainly responding to the mineralisation. The low gamma response is expected, given the lack of radioactive elements comprising the ore and gangue minerals. Thus, the gamma log is basically responding to host rock lithology. The results from Admiral Bay contrast with the results from Wagon Pass where there is a stabilisation of the SP response and a broad high on the gamma log associated with the mineralisation.

Shallow, intermediate and deep resistivity logs

were all recorded in Cudalgarra-1, although for clarity only the shallow (MSFL) and deep (LLD) logs are shown in Figure 26. Mineralisation at Wagon Pass is associated with a low on the shallow, intermediate and deep resistivity logs. This is not the case at Admiral Bay where mineralisation generally has high resistivity, reaching as much as 10,000 ohm m. The positive SP deflection is associated with particularly high resistivities. There is a second zone of very high resistivities at around 1540 m and an associated negative SP deflection. The caliper log shows caving in the middle of this zone so the cause of the resistivity high may not be entirely geological. Throughout the mineralised part of the succession, the lack of separation of the deep and shallow resistivity curves shows the mineralised zone to be impermeable. However, the positive SP deflection coincides with a separation of the curves. The high resistivities within the Nita and Goldwyer Formations are expected, given the relatively low proportion of conductive minerals comprising the mineralisation.

The neutron log is fairly consistent in the mineralised areas, apart from a slight increase and stabilisation where the positive SP deflection occurs. The density log has high values in the mineralised areas, as expected given the nature of the mineralisation. Typical density values lie between 3 and 4 g/cm³ with peaks to 4.5 g/cm³. Density is relatively low where the positive SP deflection occurs, between 1475 and 1490 m where no other log has an anomalous response, and between 1,535 and 1,545 m where there are anomalously high resistivities (see above). Again, the effects of caving may be significant. The density responses can be explained in terms of changes in the proportions of ore minerals, especially galena ($\rho = 7.5 \text{ g/cm}^3$), sphalerite ($\rho = 4.1 \text{ g/cm}^3$) and, to a lesser extent, barite ($\rho = 4.5 \text{ g/cm}^3$).

The zone 1 mineralisation is not obvious on the logs but its location is interpreted from a local increase in resistivity and density (Fig. 26). The positive SP deflection occurs at about the depth where the lower mineralised zone (2) is in SS2. According to Becker & Telford (1965), a positive deflection of the SP occurs in the presence of sulphides where the hole has passed close to, but not intersected, mineralisation. Perhaps the SP log is responding to the high-grade mineralisation comprising zone 2 in SS2, but the high-grade material does not extend as far as the Cudalgarra-1 well, hence the off-hole response of the log. The high resistivities, separation of the resistivity curves and low density in this area are interpreted in terms of the well intersecting porous, relatively low-grade mineralisation, possibly with hydrocarbons in the pore space. In support of this interpretation we note that Connor (1990) states that zone 2 mineralisation is not present in all drillholes, and vugs and hydrocarbons have been observed in core.

The zone 3 mineralisation and alteration does not produce a consistent response on the logs. This is because the zone is highly variable and each log is responding to a different aspect of the mineralisation. Hence, there is no reason why the specific properties affecting each log should change sympathetically.

SUMMARY

The association of MVT mineralisation with

faults, basement highs and, in some cases on the Lennard Shelf, reef carbonates concealed beneath basinal sedimentary rocks, means that both gravity and magnetic data play an important role in regional mapping to define prospective areas.

In general, geophysical techniques cannot be used to directly detect MVT mineralisation. The ore is non-magnetic and has poor electrical conductivity. There is usually a strong contrast in density between mineralisation and host rocks, but the orebodies are usually too small to cause a gravity anomaly that can be recognised among those due to other geological causes. Various forms of IP are the only methods that have been at all successful in detecting mineralisation. However, on the southern Lennard Shelf, it is the marcasite which is commonly associated with the lead-zinc mineralisation that is being detected, rather than the base metals themselves (Scott *et al.*, this volume). At Sorby Hills, the IP is described as detecting pyrite mineralisation (Lee & Rowley, 1990), the distribution of which is only broadly related to base-metal mineralisation, rather than the base-metal sulphides themselves. Marcasite is described by Jorgensen *et al.* (1990) as a common gangue mineral at Sorby Hills. It is possible that marcasite is the major source of IP anomalies in this region as well. IP surveys at Wagon Pass were capable of defining porous zones but responded poorly to mineralisation itself, despite the presence of marcasite. The same is true for EM-37 data. Drillhole electrical surveys gave results that seem to be more a function of the local geology than the distribution of mineralisation.

Admiral Bay is obviously an atypical geophysical target due to its depth and the geophysical data available reflect this. Based on data available to date, direct detection of the mineralisation is not possible even with high-resolution seismic data. Clearly, the suite of well logs respond to the mineralisation but only provide very local information, with the possible exception of the SP log.

Volcanic-hosted base metals

There are volcanogenic massive-sulphide (VMS) deposits containing potential resources of copper, zinc, lead, silver and gold in the Archaean granitoid-greenstone terrains of Western Australia (Barley, 1992). These deposits occur both in the Pilbara and Yilgarn Cratons, although the number of deposits in the Yilgarn is small compared to similar terrains elsewhere (*e.g.*, the Canadian shield; Groves *et al.*, this volume). No doubt this is partly due to lack of outcrop, although Barley (1992) suggests that few greenstone belts which contain favourable volcanic assemblages have been adequately explored using modern methods. There is a quite extensive literature on geophysical exploration for VMS deposits in Western Australia; see Bishop & Lewis (1992) for a recent review. This literature highlights the variability of their geophysical responses. Published descriptions of data from a number of examples are reviewed below.

PILBARA CRATON

There are several barite-rich zinc-lead-copper VMS deposits in the eastern Pilbara, including the recently discovered Panarama deposit (Fig. 1). Nothing has been published regarding the geophysical re-

TABLE 2 Survey specifications at Salt Creek as outlined by Gunn & Chisholm (1984).

Survey	Description
EM37	25 Hz time base, 300 x 600 m loop
UTEM	Operating frequency 22.5 Hz
SIROTEM	100 x 100 m loop
IP	Dipole-dipole array, 50 m dipole, Scintrex IPR-11 receiver, 12 kVA generator, 2 s pulse cycle
MIP	IPR11 receiver

sponses of these deposits, apart from a comment by Gunn & Chisholm (1984) that the Big Stubby deposit (Fig. 1) does not respond to TEM, specifically INPUT, Crone PEM or EM-37. A significant amount of geophysical data (e.g., magnetics, GEOTEM, SIROTEM, gradient and dipole-dipole IP and mise-a-la-masse) has been collected at Panarama but these data are currently considered too sensitive to be made available. However, according to M. Doepel (pers. comm., 1993), by far the most useful exploration method in the area has been geological mapping and prospecting with follow-up drilling of targets.

More data are available for deposits in the western Pilbara, such as Mons Cupri and Salt Creek (Fig. 1).

Mons Cupri

Gunn & Chisholm (1984) describe geophysical surveys at the Mons Cupri deposit. However, Lebel & Fallon (this volume) provide a much more comprehensive review of results from this deposit. Numerous types of ground and airborne EM data have been collected over Mons Cupri but no response attributable to mineralisation was obtained by any of them. The deposit also gives rise to no magnetic response; a small anomaly which roughly coincides with mineralisation is thought to originate from a chlorite-alteration

pipe. Stockwork mineralisation caused a slight resistivity low on IP data but a resistivity high on MIP data. However, the mineralisation did generate PFE, chargeability and RPS anomalies on IP data. Lebel & Fallon (this volume) attribute the poor EM response to low sulphide content, the depth of massive-sulphide mineralisation and poor electrical continuity.

Salt Creek

The Salt Creek deposit (Gunn & Chisholm, 1984) consists of stratabound zinc-lead-copper mineralisation hosted by pyritic sedimentary rocks which immediately overlie volcanic and volcanic clastic rocks. Massive chalcopryite, galena, sphalerite and pyrite mineralisation is subvertical, about 12 m thick, 125 m in strike length, and extends to a depth of more than 200 m (Fig. 27A). There is disseminated stringer mineralisation, consisting of chalcopryite and pyrite, stratigraphically beneath the massive mineralisation. Weathering extends to a depth of 65 m. Salt Creek was not a geophysical discovery but various surveys were carried out over the deposit to define a geophysical signature (Table 2). Examples of IP and EM-37 data are shown in Figures 27 and 28. Gunn &

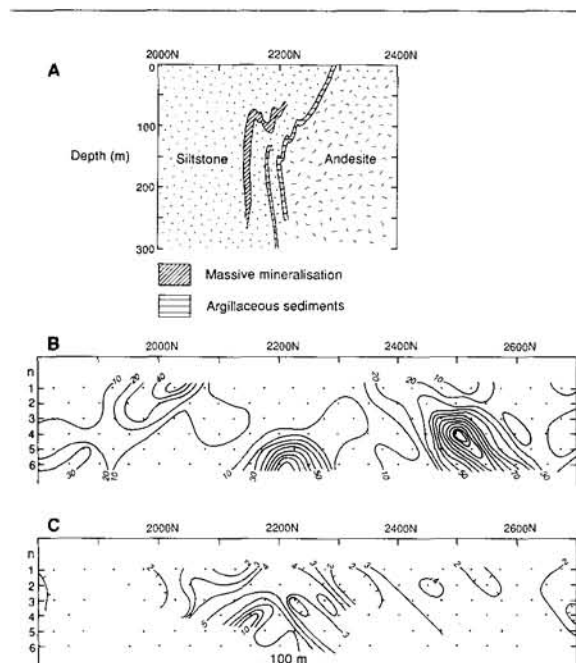
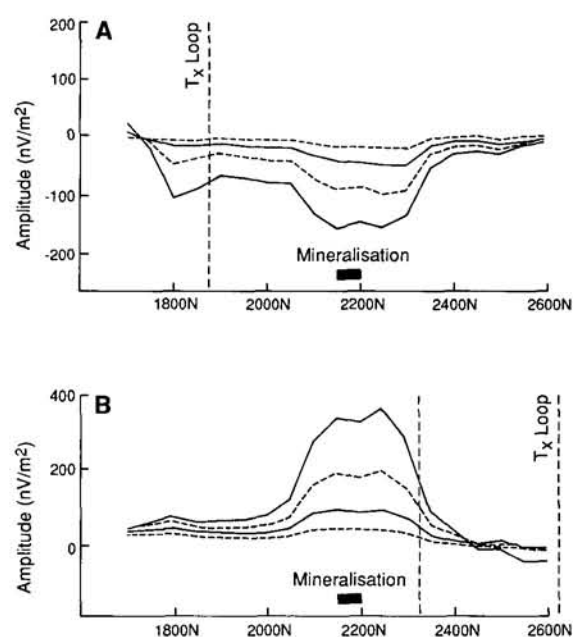


FIGURE 27 Dipole-dipole IP data from Salt Creek. A. geology, B. apparent resistivity, C. chargeability. Redrawn from Gunn & Chisholm (1984).



Chisholm (1984) use results from a barren area to highlight responses due to mineralisation. This enabled conductive responses on the EM data around 2200N (local grid) to be identified as originating within the weathered layer. This is supported by SIROTEM apparent resistivity data and by the dipole-dipole apparent resistivity results which show depth-limited low values at $n=1$ in the locations of the EM conductors. Downhole PEM surveys confirmed the resistive nature of the mineralisation. The chargeability pseudosection, based on data collected between 90 and 1220 ms, has a distinct anomaly coincident with mineralisation. The MIP H_n parameter locates the same shallow conductors as the EM surveys. MIP chargeability data (M3) were effected by the near-surface conductors and bear little resemblance to the electrical IP chargeabilities. They produce similar responses in barren and mineralised areas. Finally, the Salt Creek mineralisation gives rise to neither gravity or magnetic anomalies, the former being expected due to its small size, the latter due to its mineralogy.

YILGARN CRATON

As previously stated, occurrences of VMS-type mineralisation are comparatively rare in the Yilgarn Craton. The most important example, and only currently operating mine, is in the Golden Grove belt in the Murchison Province (Fig. 1). The Scuddles deposit at Golden Grove gives clear ground EM and magnetic responses but only a subtle gravity response which is difficult to distinguish from overburden effects (Boyd & Frankcombe, this volume). An IP anomaly over the deposit could be caused by shallow mineralisation and deep mineralisation is probably not detectable in this manner.

The Teutonic Bore deposit in the Eastern Goldfields Province was also mined, although operations ceased in 1984. There are numerous small prospects across the craton. Examples for which geophysical data are available include Freddie Well in the Murchison Province and the Nangaroo deposit in the Eastern Goldfields Province.

Teutonic Bore

Teutonic Bore is located in the Eastern Goldfields Province (Fig. 1). Massive and disseminated lead-zinc-copper mineralisation in the form of sphalerite, pyrite, chalcopyrite and galena occurs in a basaltic sequence about 100 m above the contact with felsic volcanics (Grieg, 1984). The massive mineralisation forms a steeply-dipping lens about 320 m long, 280 m deep and up to 30 m thick. The disseminated mineralisation occurs in an irregular zone beneath the massive lens (Barley, 1992). There is oxidation to about 85 m depth.

Geophysical surveys over Teutonic Bore are summarised by Fritz & Sheehan (1984) from whom the following summary is largely taken. The deposit has no magnetic expression and, based on petrophysical and local geological considerations, gravity is considered unlikely to detect it. However, the estimated 10000:1 conductivity contrast between ore and host rock suggests electrical and EM methods are applicable.

Figure 29 shows resistivity and chargeability pseudosections across the deposit. The data were

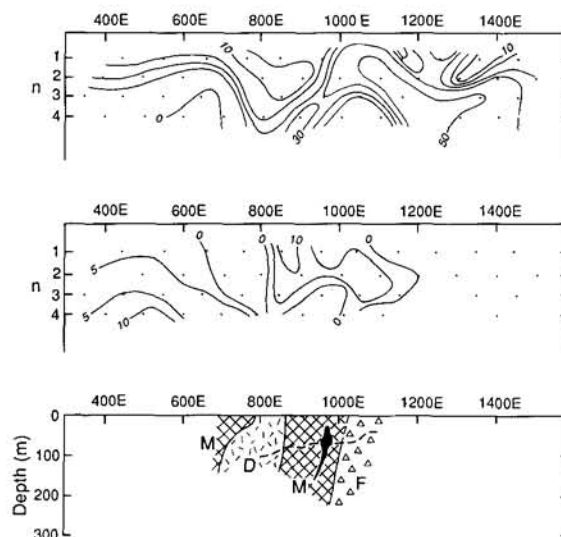


FIGURE 29 Dipole-dipole IP data from Teutonic Bore. A. Apparent resistivity. B. Chargeability. C. Geology. M = mafic volcanic rocks, F = felsic volcanic rocks, D = dolerite. The dotted line is the base of weathering. Mineralisation is shown in black. See Figure 30 for location. Redrawn from Fritz & Sheehan (1984).

collected using a dipole-dipole array with 100 m dipoles, and a Scintrex IPR-7 receiver and a 2.5 kVA transmitter. Overburden effects are evident but a deep resistivity low at 1000E to 1100E (local grid) could be due to mineralisation. MIP data were also acquired across the deposit using a 400 m electrode spacing and again a response is detected, but, as before, it is uncertain if it is related to the orebody. Three mise-a-la-masse surveys were undertaken using a current electrode:

- (i) in the massive mineralisation;
- (ii) in a surface gossan; and
- (iii) in an auger hole in the hangingwall away from mineralisation, but within the deposit's geochemical halo.

All three surveys successfully delineated the northern portion of the deposit and also areas of stringer sulphides and geochemical anomalies associated with subeconomic mineralisation. Data from the survey with the electrode in massive mineralisation are shown in Figure 30.

Several types of EM surveys have been carried out over Teutonic Bore (Buselli *et al.*, 1986; Fritz & Sheehan, 1984). VLF data only detected weathering responses and the PEM response is equivocal. The MPPO-1 system and SIROTEM were much more successful. The former detected the deposit using several loop sizes and configurations. SIROTEM data were collected using 100 and 50 m coincident loops. Figure 31 shows that there is a strong response from the mineralisation on the 100 m data. The 50 m data were noisy but, again, a response was obtained, although modelling suggests this is due to a shallow source rather than the main mineralisation.

Nangaroo

The Nangaroo copper-zinc deposit (Fig. 1) consists of massive pyrite with variable amounts of

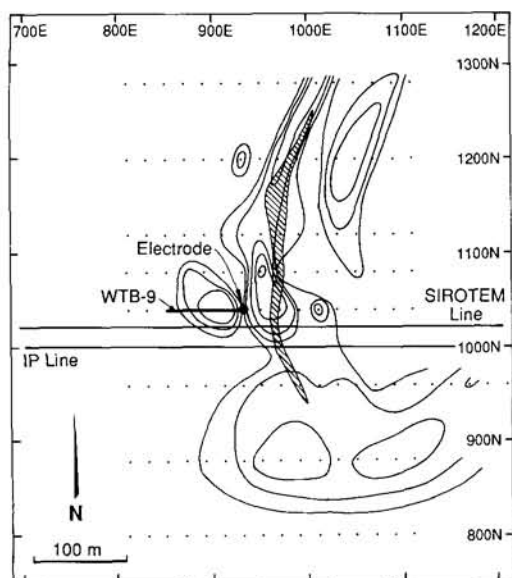


FIGURE 30 Mise-a-la-masse data from Teutonic Bore. The solid line is the surface projection of WTB-9, the drillhole containing the electrode. Mineralisation is shown hatched. Redrawn from Fritz & Sheehan (1984).

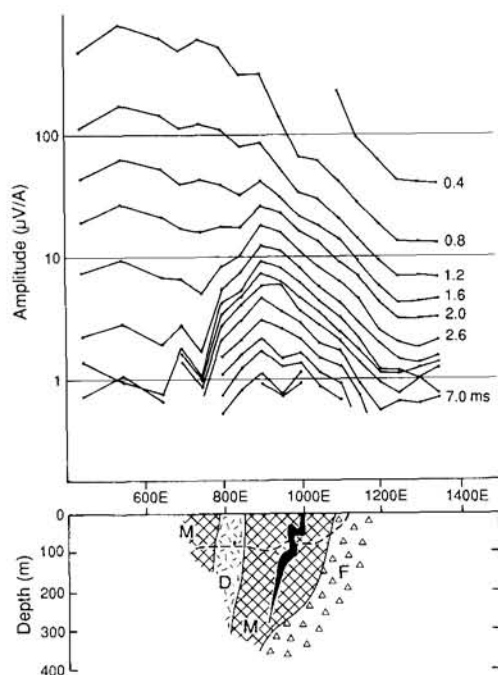


FIGURE 31 100 m coincident-loop SIROTEM data from Teutonic Bore. M = mafic volcanic rocks, F = felsic volcanic rocks, D = dolerite. The dotted line is the base of weathering. Mineralisation is shown in black. See Figure 30 for location. Redrawn from Fritz & Sheehan (1984).

chalcopyrite and sphalerite hosted by acid igneous rocks, usually close to contacts with basic rocks. Brecciated sulphides can also occur within volcanic and sedimentary breccias. The local stratigraphy dips steeply to the west. Weathering reaches more than 30 m depth. A geophysical case study from the area is presented by Cowan *et al.* (1975) with discussion

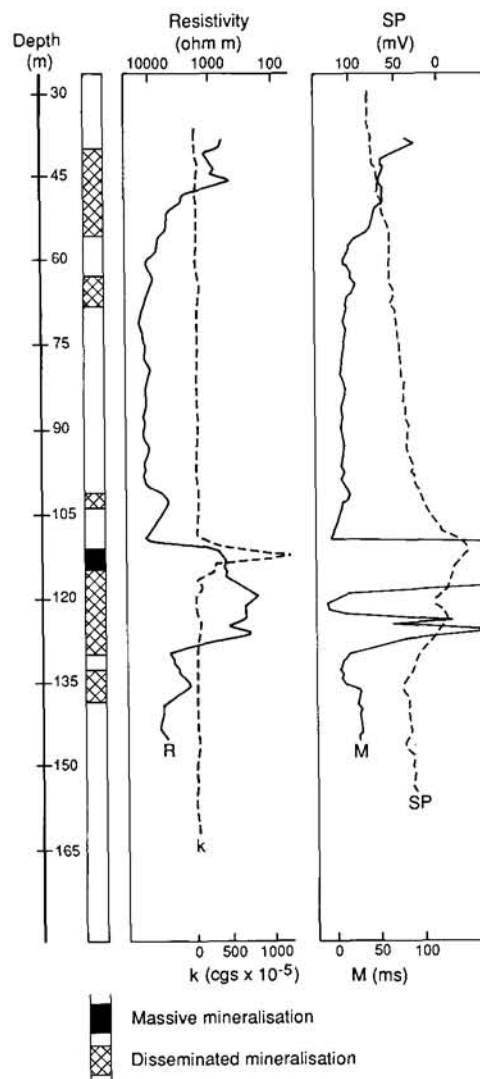


FIGURE 32 Downhole logs from drillhole DDH-11, Nangaroo. k = magnetic susceptibility, M = chargeability, R = resistivity, SP = self potential. Redrawn from Cowan *et al.* (1975)

from Roth (1977) and reply by Cowan (1977). The following summary is based on these papers. Dipole-dipole IP and VLF EM surveys were initially carried out at Nangaroo but failed to detect the mineralisation so a programme of downhole electrical surveys was undertaken.

Measurements of SP, apparent resistivity, chargeability and magnetic susceptibility were made every metre in drillhole DDH/11. Electrical logging used a Schlumberger array with current electrodes spaced at 20 m and potential electrodes spaced at 1 m. The downhole logs defined two main anomalous mineralised zones at 40 to 56 m and 110 to 131 m (Fig. 32). The shallower zone consists of weak disseminated mineralisation in acid volcanic rocks and is associated with increased chargeability and moderate resistivity, but no SP or susceptibility effects. The deeper zone corresponds to massive sulphides in its upper part and heavy disseminated mineralisation in acid volcanic rocks lower down. Anomalously high susceptibility (due to pyrrhotite), low resistivity, high chargeability and high SP responses are recorded here.

Other zones of weak disseminated mineralisation are also detected by the logs.

Mise-a-la-masse surveys were carried out using a current electrode located in the massive mineralisation in DDH/11. Measurements of both potential difference and chargeability at 450 ms were made using a mobile potential dipole, with the data referenced to a fixed potential electrode located at the top of the drillhole. A Scintrex IPR-7 receiver was used with a Huntex 7.5 kVA transmitter. IP potential was calculated by multiplying the chargeability values at 450 ms by the corresponding potential difference. The derived values were referenced against the fixed potential electrode. The resulting value represents a quantity approximately proportional to the IP potential at about 600 ms. Contoured maps of electrical and IP potential are shown in Figures 33A and 33B. The contour distribution is similar in both cases, with a single elongate asymmetric high centred south of DDH/11. These data are interpreted by Cowan *et al.* (1975) in terms of body dipping to the west with a moderate plunge to the north. The contours are offset by two apparently linear features. The axis of the anomalies is considered to coincide with the vertical projection of the massive mineralisation. A surface gradient-array IP survey was also undertaken using the same equipment as the mise-a-la-masse surveys. Current electrode spacing was 1000 m with potential electrodes spaced at 60 m and a station spacing of 30 m. Chargeability was determined over a 0.45 to 1.1 s window. The apparent resistivity and chargeability maps derived from the surface IP survey are shown in Figures 33C and 33D. Both datasets define two elongate north-south-trending anomalies, although these are not coincident, and also the offsets seen in the mise-a-la-masse data. The westernmost of the two chargeability zones is associated with a resistive area and is interpreted by Cowan *et al.* (1975) as due to the shallow disseminated mineralisation seen in the downhole logs. The eastern chargeable zone coincides with a conductive region and is interpreted as due to the main massive mineralisation. The discontinuities in the data are attributed to a fault and a dyke. Subsequent surveys using Crone shootback, with a coil spacing of 122 m and frequency of 825 Hz, detected a conductor coincident with the mineralisation. An INPUT Mk 2 survey also detected a conductor over the mineralisation, but the response was similar to those due to graphitic shales elsewhere in the area.

Freddie Well

The geology of the Freddie Well deposit (Fig. 1) is briefly described by Marston (1979). Zinc-copper mineralisation is hosted by felsic schists adjacent to a metamorphosed layered gabbroic intrusion. The schists are about 500 m wide and lie between the intrusion and adjacent granitoids. Mineralisation occurs within the schists as layered quartz-sulphide(-magnetite) rock (freddite). Sulphides include pyrrhotite, pyrite, sphalerite and chalcopyrite. There are also mineralised breccias of schist and mafic rocks. Weathering is comparatively shallow, extending to only about 10 m depth. Two main "zones" of mineralisation are known, of which the "D zone" is most significant. Here there are two parallel shoots 8 m apart, 120 m long,

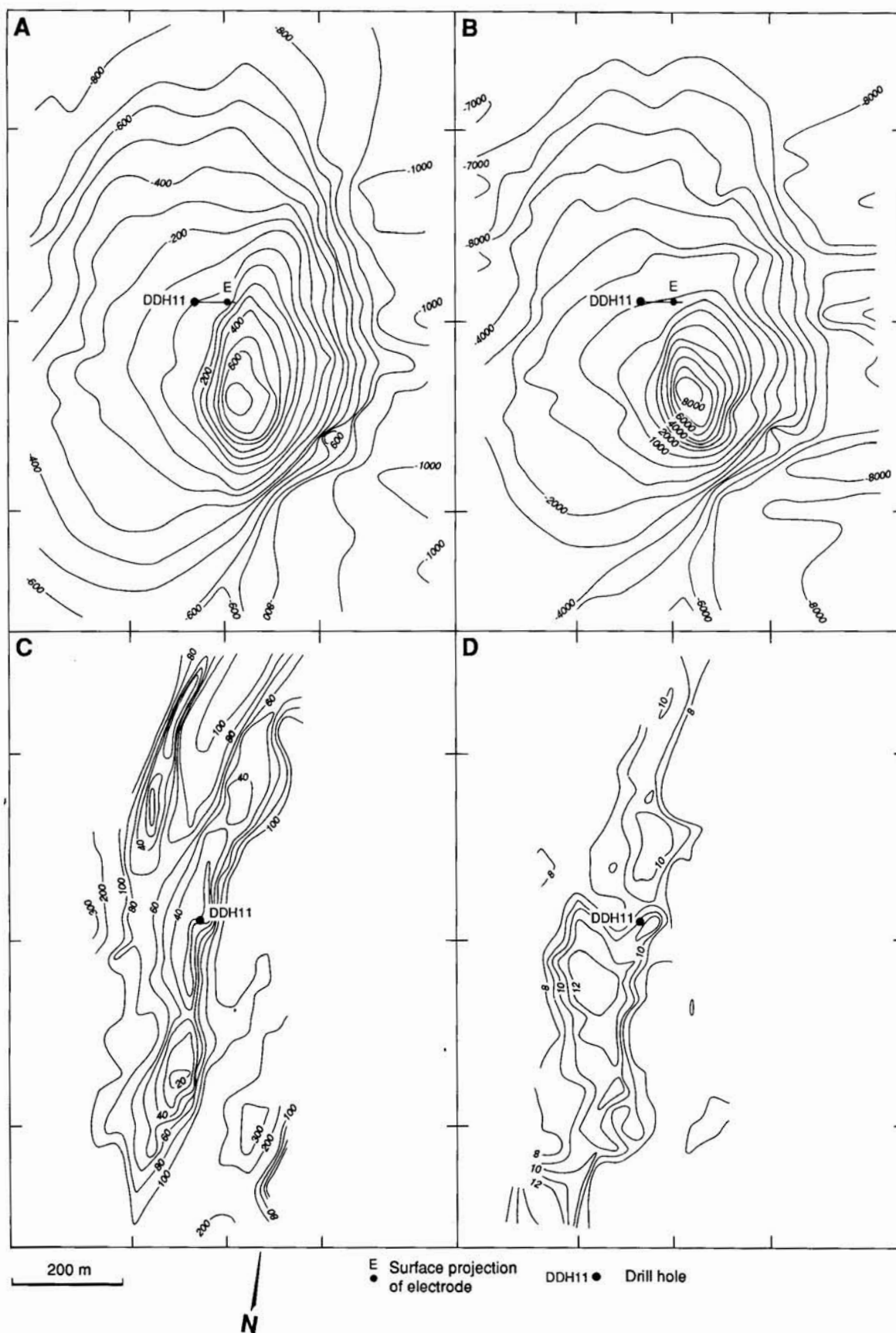
and 5 to 6 m wide which strike parallel to the contact between gabbro and schist. The much smaller "A zone" is a folded inclusion, entirely within the mafic intrusion.

Reports describing geophysical exploration at Freddie Well have been submitted to the Western Australian Department of Mines by Conwest (Australia) NL and CRA Exploration Pty Ltd. Turair surveys were used by Conwest to see if there were conductive bodies coincident with gossans and geochemical anomalies. Aeromagnetics were flown in conjunction with the AEM. Numerous AEM anomalies were detected but these were resolved into five conductors considered worthy of ground follow-up. Two of these zones correlated with areas highlighted by geological methods and drilling confirmed a sulphide source. One of these zones was the D zone. The A zone is not crossed by a flight line but there is evidence for a weak response on the data. The source of the other anomalies, which are not associated with anomalous geochemistry, remains unclear even after ground follow-up surveys (see below). The response of the Freddie Well deposit to INPUT and QUESTEM AEM surveys is described by Butt (1985), Smith & Pridmore (1989), Annan & Lockwood (1991), and Bullock & Isles (this volume). It is not clear whether the surveys are over the A or D zone. The surveys are dominated by the response of conductive overburden adjacent to the deposit, but a response due to the mineralisation is seen as a shoulder on this anomaly.

Ground EM surveys of selected areas were carried out by Conwest using a McPhar VHEM unit with a vertical coil configuration and frequencies of 600 and 2400 Hz. Both broadside and fan surveys were carried out along lines spaced at 200 ft (61 m). The A zone was detected by broadside surveys, with a fairly strong conductor coinciding with the surface gossan and the projected strike extension of the mineralisation. The successful detection of this relatively small body was attributed to the very shallow weathering in the area. Surveys over the D zone defined a pronounced anomaly extending for around 1 km. PEM surveys recorded a strong response from the D zone but nothing over the A zone. CRA Exploration report that EM-37 and SIROTEM surveys delineated conductors at Freddie Well.

The aeromagnetic data flown by Conwest defined several anomalies, one of which was associated with exposed gabbro to the east of mineralisation. Small anomalies were found to correspond to iron formation within the schists. A subsequent more detailed survey by CRA Exploration, using a sensor height of 80 m and line spacing of 250 m, mapped the internal structure of the gabbroic rocks. Ground magnetic surveys reported by Conwest mapped the gabbro and iron formation within the schists. Despite the presence of pyrrhotite, an anomaly associated with D zone was not detected but it could have been masked by the response from the nearby magnetic gabbro. Drilling of a magnetic anomaly coincident with A zone intersected both pyrrhotite and iron formation, and the nature of its source is unclear. A gravity survey by CRA Exploration showed the gabbroic intrusion to be a sill-like body.

IP surveys by Conwest over the D zone with both 100 ft (30 m) and 200 ft (61 m) electrode spacings



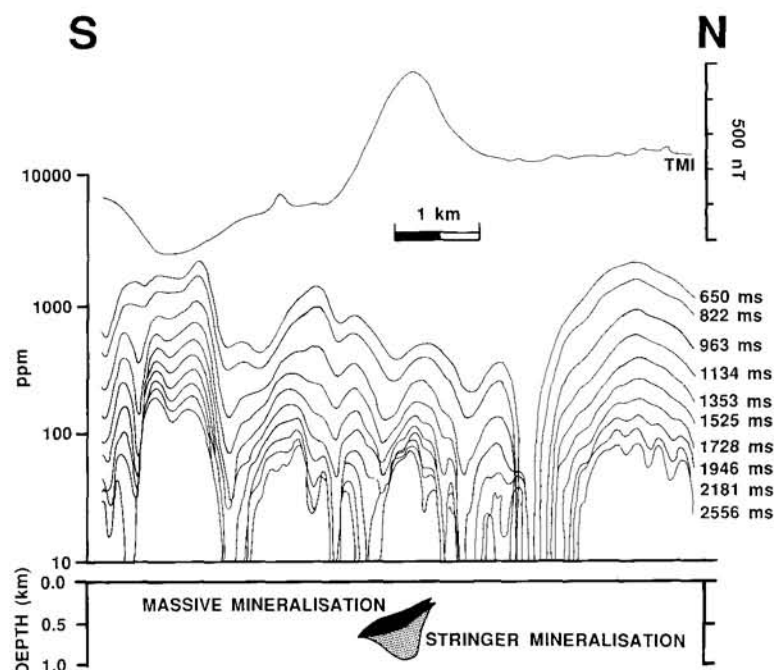


FIGURE 34 Geological, aeromagnetic and GEOTEM (channels 3-12) data over the Abra deposit. The geological cross-section through the deposit is an approximation of that along the line of flight. Geophysical data redrawn from Wolfram *et al.* (1992). Geological data based on McInerney *et al.* (this volume).

appeared to detect the mineralisation. MIP surveys to the north of D zone carried out by CRA Exploration defined numerous chargeability anomalies. However, since there are numerous potential sources in the area, both mineralised and barren, the significance of the anomalies is unclear.

SUMMARY

There is obviously considerable variation in the geophysical responses of VMS deposits in Western Australia. Deposits such as Scuddles and Nangaroare magnetic but other examples are not. The Salt Creek mineralisation resembles its neighbour at Mons Cupri in that it is chargeable but does not give rise to EM and magnetic anomalies. Teutonic Bore is highly conductive but apparently not very chargeable. The Golden Grove orebodies are chargeable and highly conductive and can be detected with ground EM but give a poor IP response (Craven *et al.*, 1985; Bishop & Lewis, 1992). Clearly, geophysical exploration for VMS targets requires multiple methods: regional exploration using only airborne magnetics and EM could miss mineralisation and, therefore, areas that have been surveyed in this manner cannot be discounted in terms of containing mineralisation. This is especially true with older data, given the steady improvements in AEM technology (Annan & Lockwood, 1991; Bullock & Isles, this volume). On a prospect scale, trials of IP and EM data are required to assess which is more successful. Once mineralisation has been intersected by drilling, *mise-a-la-masse* is apparently consistently successful for mapping its extent.

Other types of base-metal deposit ABRA

The Abra deposit (Fig. 1), located in the Bange-mall Basin and described by McInerney *et al.* (this

volume), is an example of a sedimentary exhalative deposit. Mineralisation contains iron, barite, lead, silver, copper and gold at low grades (Boddington, 1990). The deposit is blind and was discovered by drilling coincident positive gravity and aeromagnetic anomalies. The deposit also produces ground TEM responses both at the surface and downhole. Wolfram *et al.* (1992) describe the results of an aeromagnetic and AEM survey over the Abra deposit using the GEOTEM system with a base frequency of 125 Hz and a aircraft height of 120 m (Fig. 34). The magnetic anomaly from the deposit is clear but the AEM response is weak, mainly due to the shallow part of the mineralisation, and it is not significantly different to anomalies from areas to the north and south where there is no known mineralisation. Contouring of time constants calculated from the AEM data defines a "bull's eye" anomaly over the shallowest part of the Abra mineralisation; these data reflect conductivity-thickness product rather than channel amplitude. However, once again, there are numerous similar anomalies in barren areas.

ONEDIN

The Koongie Park area in the Halls Creek Orogen also contains base-metal mineralisation. The following description of the geology and geophysics of the Onedin Prospect (Fig. 1) is based on Cole (1991), and these and additional data have generously made available by Billiton Australia and Anglo Australia Resources. The Onedin Prospect lies about 2 km north-northeast of Koongie Park. The local geology consists of Palaeoproterozoic volcanic and sedimentary rocks of the Biscay Formation. The succession is steeply dipping and locally inverted, and consists of felsic volcanic rocks, volcanoclastic rocks, and chemical and argillaceous sedimentary rocks (Fig. 35B). The

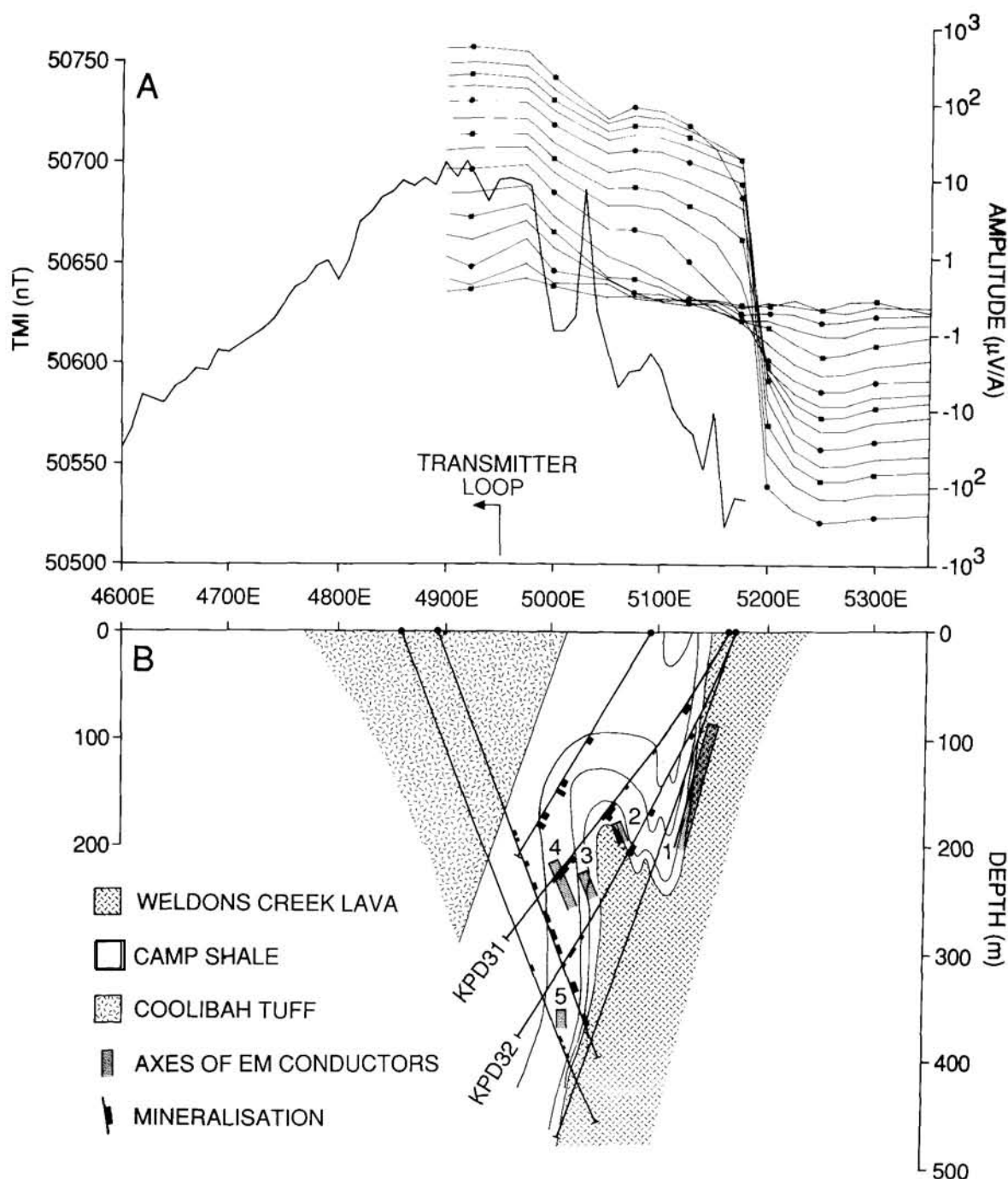


FIGURE 35 A. Ground magnetic and SIROTEM data across the Onedin prospect. B. Composite geological cross-section along line 19900N (local grid). EM conductor 1 is interpreted from the SIROTEM data in A. Conductors 2, 3 and 4 are interpreted from DHEM data from drillhole KPD31 (see Fig. 37). Conductor 5 is interpreted from DHEM data from drillhole KPD32.

footwall to mineralisation is the felsic Coolibah Tuff. The stratigraphically overlying Camp Shale consists of tuffs, chert, shales and siltstones which are commonly carbonate rich and cleaved. Massive mineralisation occurs mainly within cherts and a calc-silicate horizon. There is disseminated mineralisation in surrounding tuffs. Gossans are present at the surface. Intermediate volcanic rocks of the Weldons Creek Lava stratigraphically overlie the Camp Shale. The succession is folded with axes trending northeast, and minor faulting is common. Weathering in the area extends to a depth of several tens of metres.

Limited gravity data suggest that surface gossans can produce gravity lows of up to 1 mGal. Ground magnetic data show a positive anomaly over the Camp Shale sequence (Fig. 35A). Limited drill-hole susceptibility data show susceptibilities as high as 15×10^{-3} SI, with mineralised areas generally coinciding with enhanced susceptibilities, although barren areas may also be susceptible (Fig. 36). The ground magnetic data, collected at 10 m station spacing, define an anomaly with a wavelength of about 800 m and amplitude of around 150 nT. Superimposed on this anomaly are spikes originating at shallow depth.

There may be anomalies related to mineralisation but it is difficult to be certain. Cole (1991) modelled the long wavelength component of the magnetic anomaly and suggests it originates at a few hundred metres depth. A significant component of remanent magnetisation is required to model the anomaly in a manner consistent with the known geology. Cole (1991) suggests the source of the anomaly is zones of magnetite within the Camp Shale succession which have been intersected by several boreholes.

TEM data were collected using a SIROTEM Mk 3 unit with a 800 m by 500 m transmitter loop and a roving vector receiver. Readings were made at 50 m intervals with in-filling at 25 m intervals in anomalous areas. Data from line 19900N (local grid) are shown in Figure 35A. The clear crossover at 5175E is consistent with a conductor that dips steeply to the west at a depth of no greater than 100 m (conductor 1 in Fig. 35B). The surface EM data were supplemented by DHEM surveys using a 200 m by 200 m transmitter loop in two to four positions around the drillhole collars. Again, a SIROTEM Mk 3 unit was used, in conjunction with a SIROTEM probe, with data recorded at 10 m intervals. Data from drillholes KPD31 and KPD32 (Fig. 35B) showed similar responses from the different loop positions. One of the datasets from KPD31 is shown in Figure 37. These data define anomalies at 210 m, 285 m and 310 m which also coincide with known mineralisation. Cole (1991) interprets the deepest anomaly in terms of an intersection with the edge of a conductor (conductor 4 in Fig. 35B) and the other two anomalies as predominantly off-hole responses (conductors 2 and 3 in Fig. 35B). A single off-hole conductor was interpreted from the data from KPD32 (conductor 5 in Fig. 35B). The favoured interpretation, combining geological data with

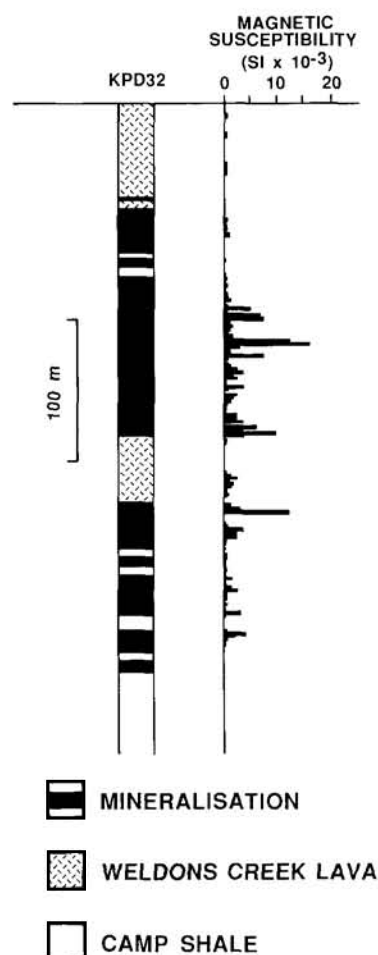


FIGURE 36 Comparison between geology, mineralisation and magnetic susceptibility in drillhole KPD32 (see Fig. 35).

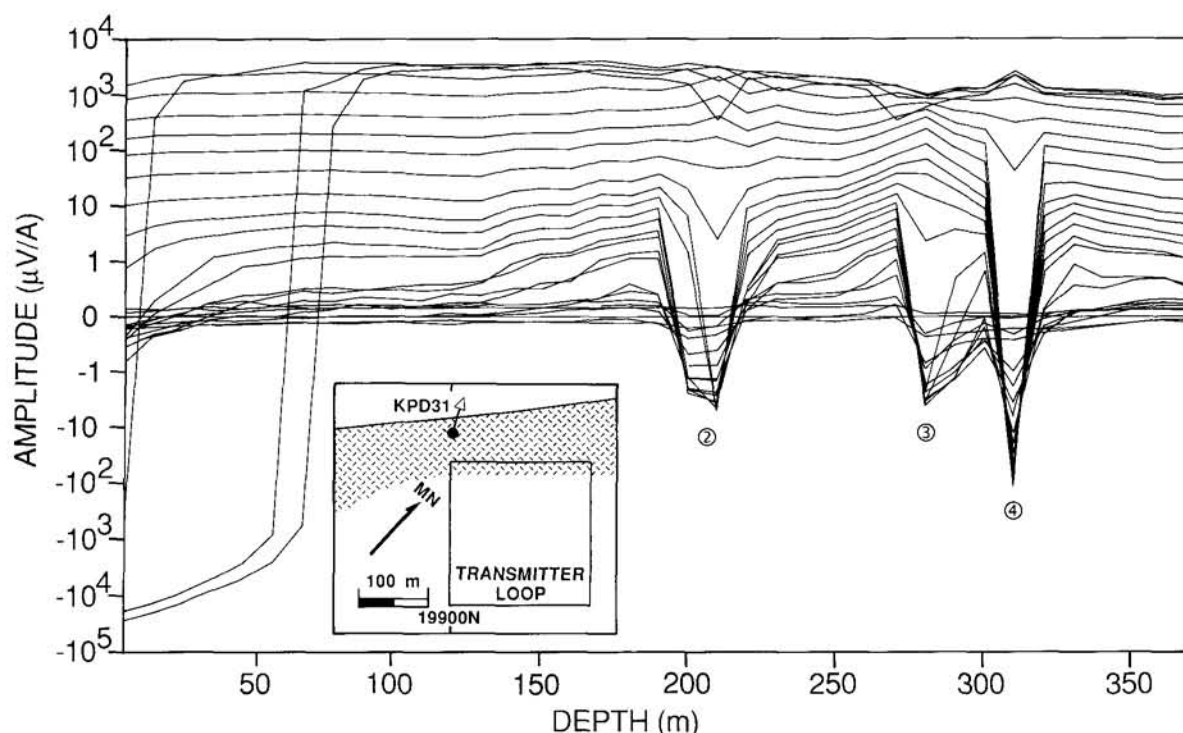


FIGURE 37 DHEM data from drillhole KPD31 (see Fig. 35). Anomalies 2, 3 and 4 are attributed to the equivalent conductors in Figure 35B. Inset shows position of loop and drillhole relative to the local geology. See Figure 35 for definition of lithological units. MN = magnetic north. Redrawn from Cole (1991).

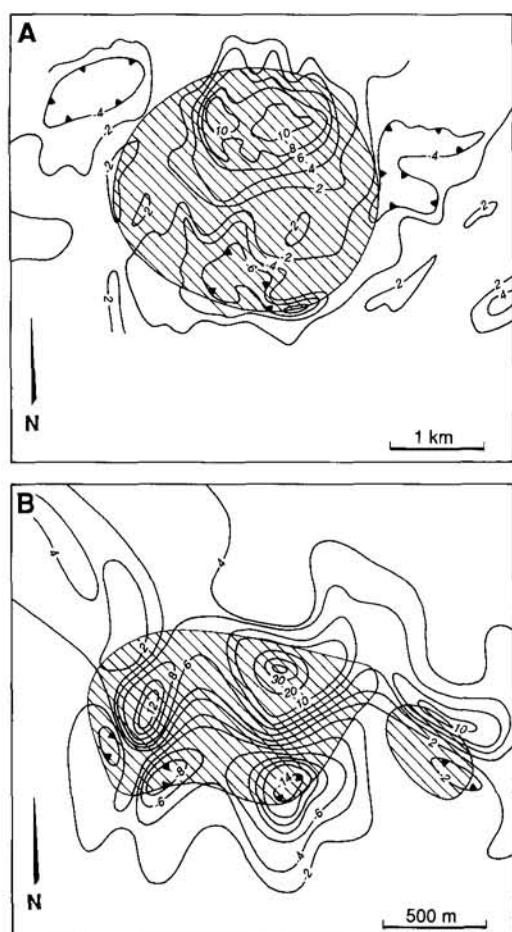


FIGURE 38 Contoured residual aeromagnetic data from Walgidee Hills (A) and Ellendale 4 (B). Hatched areas are the approximate extent of the zoned pluton and lamproite pipe, respectively. See text for description of survey specifications and processing. See Figure 1 for locations. Redrawn from Gregory (1984).

graphical modelling of the surface and downhole EM anomalies, is shown in Figure 35B. Comparison of the inferred conductor locations with the known geology and mineralisation shows reasonable correspondence. Differences are probably a function of the simple modelling methods, the presence of multiple conductors, ambiguities in their interpretation, and the complexity of the local geology.

NIFTY

Another important base-metal deposit in Western Australia is the Nifty deposit in the Paterson Orogen. No geophysical data are presently available from this locality, although geophysics did play a significant role in the discovery of the deposit.

DIAMONDS

Geophysical data from the two main diamondiferous provinces in Western Australia, Ellendale in the west Kimberley (Fig. 1) and Argyle in the east Kimberley (Fig. 1), are described, respectively, by Jenke (1983) and Jenke & Cowan (this volume), and Drew (1986) and Drew & Cowan (this volume). Since both

the major occurrences of diamonds in Western Australia are the subject of case-study papers, only a short summary of the role of geophysics in diamond exploration in the State is given here. This exploration concentrates on the detection of the intrusive pipes in which most of the diamonds occur.

Exploration techniques

The principal method of regional exploration employed in the Kimberley is stream sampling, and both the Ellendale and Argyle deposits were discovered in this way, although the Ellendale pipes were located by earlier magnetic surveys but the anomalies were not followed up (Smith *et al.*, 1990). Following the identification of the specific tributary giving rise to indicator minerals, geophysics can be used to delineate the source pipe.

BIG SPRING

The Big Spring olivine-lamproite pipes were some of the first to be discovered in the west Kimberley (Smith *et al.*, 1990). The pipes are diamondiferous but all the diamonds are very small. However, the Big Spring occurrences were used to assess the usefulness of various geophysical methods (Jenke, 1983). A ground magnetic survey defined an 80 nT anomaly over a small area in the centre of the pipe, but a gravity survey failed to define a prominent response. Resistivity soundings showed the pipe to be less resistive than its surrounds (10 ohm m versus 35 ohm m) within the uppermost 40 m. However, below this depth, the pipe was more resistive than the country rock (>100 ohm m versus 50 ohm m). These contrasts allowed the pipe to be delineated with Turam surveys using frequencies of 200 and 800 Hz. The pipe was also found to produce small anomalies on airborne magnetic and radiometric data. The magnetic and conductivity contrasts between pipes and host rocks have generally been confirmed by subsequent studies (but see Drew & Cowan, this volume with respect to Argyle), although variations in the conductivity of the host rocks reduces the effectiveness of the EM method.

GEOPHYSICAL EXPLORATION

The results from Big Spring show that airborne geophysics, particularly magnetics and to a lesser extent EM, has a significant role to play in regional exploration, especially where climatic conditions are not amenable to the cheaper drainage-sampling methods. Typical aeromagnetic survey specifications are 80 m flight height and 200 to 300 m line spacing (Smith *et al.*, 1990), based on the expectation that economic targets must exceed 300 m in diameter and that these are only likely to give rise to anomalies of around 10 nT amplitude. However, Gregory (1984) prefers a 50 m flight height and 250 m line spacing for reconnaissance surveys, with a simple derivative filter used to remove regional gradients. The resultant data are contoured at 2 nT intervals. Such filtered data from two olivine-lamproite pipes are shown in Figure 38. It is interesting that Gregory (1984) does not mention the use of stacked profiles, rather than contour maps, given the relatively small size of the targets. Jenke (1983) does, however, mention their use. The main AEM technique used in Western Australia was

INPUT, although digital systems are now used. Provided the host rocks have sufficiently low conductivity, clear responses are seen. Gregory (1984) reports that airborne VLF surveys gave inconclusive results. In addition to conventional airborne geophysics, satellite-borne remote sensing may also be used. Agar (this volume) describes the appearance of the Aries kimberlite pipe (Fig. 1), located in the central Kimberley, on remote-sensing data. The pipe itself gives rise to no signature, but sediments in the depression caused by the preferential weathering of the kimberlite are detectable.

Ground geophysical surveys are used to accurately delineate the sources of the anomalies detected using the airborne methods. Ground magnetic anomalies are typically around a few tens of nanoTesla. The pipes are not uniformly magnetised and, in some cases, remanent magnetisation can dominate. Jenke (1983) states that Koenigsberger ratios may be as high as 10. VLF, SIROTEM and Turam surveys have all been successfully used in Western Australia, but again are dependent on the local conditions.

Argyle and Ellendale

The Argyle and Ellendale deposits are both in olivine-lamproite pipes. These rocks are susceptible to weathering and hence do not usually outcrop. The Argyle pipe is a poor geophysical target being only weakly magnetic and conductive, a situation which is exacerbated by the severity of the local topography. The Ellendale pipes give rise to clear magnetic and EM anomalies, and, in some cases, radiometric anomalies, although the presence of conductive soil cover may mask the EM response.

Summary

Clearly, geophysics, especially airborne methods, has a major role to play in the location of potentially diamondiferous kimberlites and lamproites. Much of the Kimberley area has been covered by high-resolution aeromagnetic data. However, significant improvements in the resolution of such surveys have been made since the early 1980s when the bulk of these surveys were flown. Jenke (1983) describes surveys designed such that the peak-to-peak noise envelope was less than 1 nT. Bullock & Isles (this volume) describe improvements in the acquisition and processing of aeromagnetic data that allow anomalies as small as 1 to 2 nT to be considered geologically meaningful. However, the authors are aware of examples of anomalies as small as 0.25 nT which are consistent from line to line, in data recorded in 1980, which have been successfully used to locate lamproitic intrusions. There have also been significant improvements in AEM systems since the early 1980s (Annan & Lockwood, 1991; Bullock & Isles, this volume). These improvements in resolution, coupled with the weak anomalies associated with the pipes, suggest that as yet undiscovered diamondiferous pipes could exist, even in well-explored areas of Western Australia.

Whether shallow geophysical techniques has a role in exploration for submarine diamond deposits in Western Australia remains to be seen.

GOLD

Since economic gold grades can be as low as a few grams per tonne, direct detection of the gold itself by geophysical means is not yet possible. Thus, like diamond exploration, geophysical exploration for gold is based on indirect means. Most gold deposits in Western Australia are epigenetic lode-gold deposits in Archaean granitoid-greenstone terrains. However, there are a number of deposits in Precambrian sedimentary sequences and also placer deposits. Supergene deposits usually associated with the first two categories of mineralisation have assumed major importance in recent years. Descriptions of the geophysical signatures of numerous gold deposits encompassing all three of these types are described in the case-study section of this volume and, therefore, only an abbreviated summary is included here. The locations of gold deposits referred to in this paper are shown in Figure 1.

Deposits in granitoid-greenstone terrains

There is a great deal of variation among the lode-gold deposits in the granitoid-greenstone terrains in terms of their structural setting, host rock, ore mineralisation, metamorphic grade and associated alteration (Fig. 39) (Groves *et al.*, 1990). However, in many cases, one or more of these variables give rise to some form of geophysical response. This, coupled with the particularly poor outcrop in the richly mineralised Yilgarn Craton, has meant that geophysics has become an essential tool in exploration for these types of gold deposit (Isles *et al.*, 1989; Bullock & Isles, this volume).

STRUCTURE AND HOST ROCK

The single most important factor controlling the location of the gold deposits is structure (Groves *et al.*, 1990). This control ranges from craton-scale mega-structures down to relatively minor shear zones that control individual ore shoots. Since gold mineralisation is concentrated in areas where changes in the orientation of structures caused fluid focussing, the accurate mapping of these features is a priority. This is assisted by the fact that many structures occur along lithological contacts, due to strength contrasts between different rock types. The relative importance of different host rocks is summarised in Figure 5 of Groves *et al.* (this volume). Mafic igneous rocks are seen to be the most important hosts by some margin, especially in greenschist-facies areas. In the differentiated dolerite intrusion that hosts the deposits of the Golden Mile at Kalgoorlie, the magnetic phases of the intrusion are preferentially mineralised (Isles *et al.*, 1990). Banded iron-formation (BIF) is also an important host rock, especially at higher (amphibolite facies) metamorphic grades. Felsic porphyries, "internal" granitoids and sedimentary rocks can also host gold mineralisation. The fact that the majority of deposits are associated with magnetite-rich rocks means that magnetic data have become a vital tool in mapping host sequences. Modern high-resolution aeromagnetic data (60 m flight height or less) are capable of detecting changes in magnetite content as small as 0.002 vol. % (Pridmore *et al.*, 1988). Moreo-

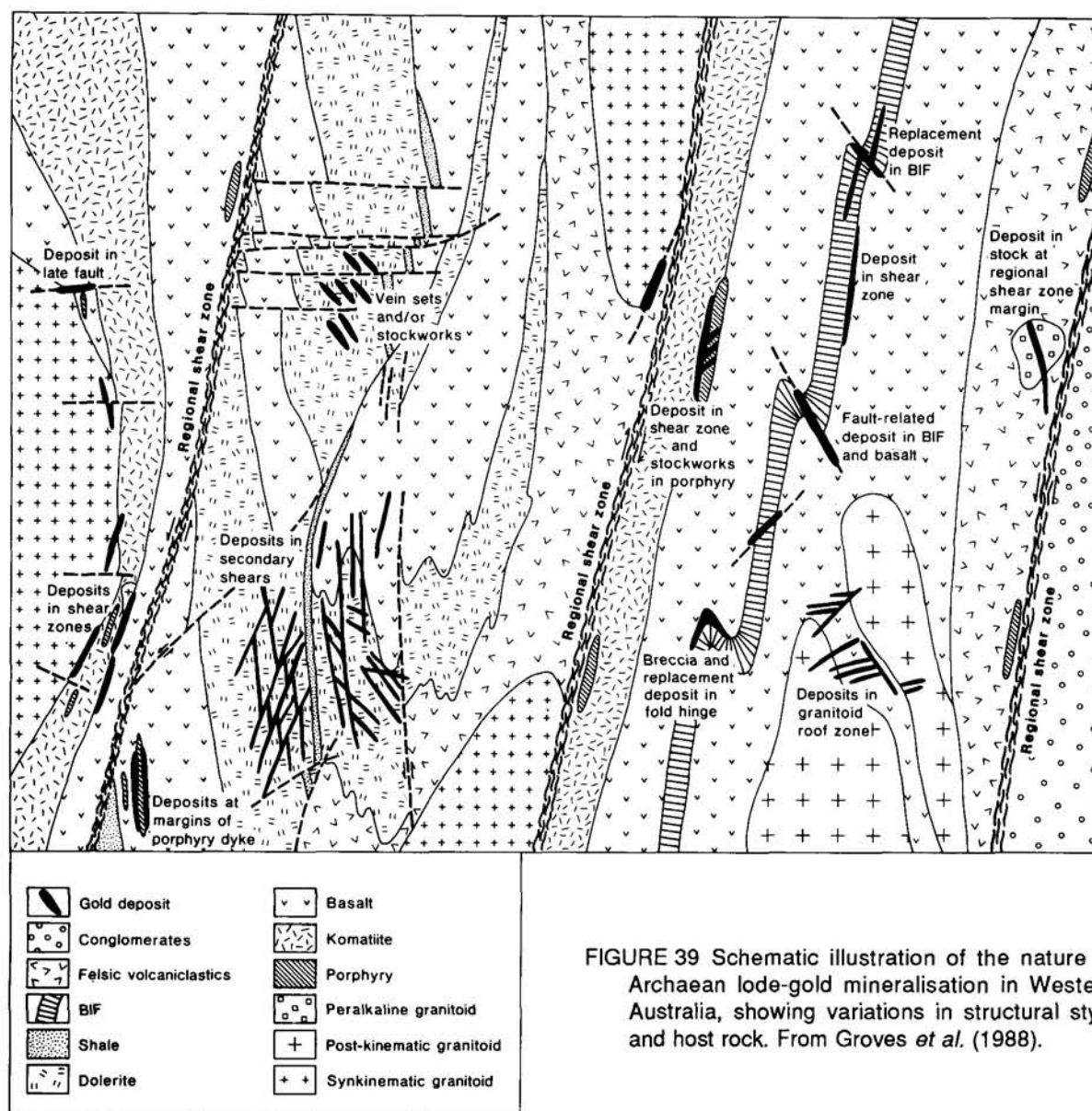


FIGURE 39 Schematic illustration of the nature of Archaean lode-gold mineralisation in Western Australia, showing variations in structural style and host rock. From Groves *et al.* (1988).

ver, favourable structures can also be mapped either because they affect rocks with different magnetisations (a good example is BIFs in a mafic sequence) or because the shear zones themselves have been sites for preferential deposition or destruction of magnetite. Figure 40 is a schematic illustration summarising the relationship between gold mineralisation and magnetic anomalies. The importance of aeromagnetic data in modern exploration for gold is demonstrated by the description of the use of such data in every case-study paper describing a gold deposit in this publication. Although mapping using aeromagnetic data is most common, virtually every other mineral exploration geophysical technique has been used for this purpose; the other techniques tending to be used for tracing an individual horizon associated with mineralisation rather than mapping the overall geology. Dentith *et al.* (1992b), Fallon & Backo (this volume), McMickan *et al.* (this volume) and Vella (this volume) all describe examples of geophysical mapping, using techniques other than aeromagnetism, for gold exploration.

ORE MINERALOGY

Ore mineralogy in the gold deposits is relatively simple (Groves *et al.*, 1990). Native gold can occur alone, or be associated with pyrite±pyrrhotite±arsenopyrite. Other associated minerals of geophysical significance, usually only present in minor amounts although they can be locally abundant, include the sulphides stibnite, tetrahedrite, molybdenite, galena, sphalerite and chalcopyrite, and the iron oxides magnetite and haematite. The relative abundance of these ore-related minerals is summarised in Figure 41. Obviously, if magnetite is present in sufficient quantities then it can be detected using the magnetic method (see below) but, as shown in the figure, it is not commonly abundant. Far more significant is the presence of sulphides. Several of the case-study papers on gold deposits describe the successful use of electrical and EM techniques to locate sulphides (*e.g.*, Coggon & Rutherford, this volume; Sheard *et al.*, this volume). Unfortunately, however, it is common for sulphides to occur without associated gold (*e.g.*, Howland-Rose, 1984; Coggon, 1984; Coggon & Rutherford, this volume). An important con-

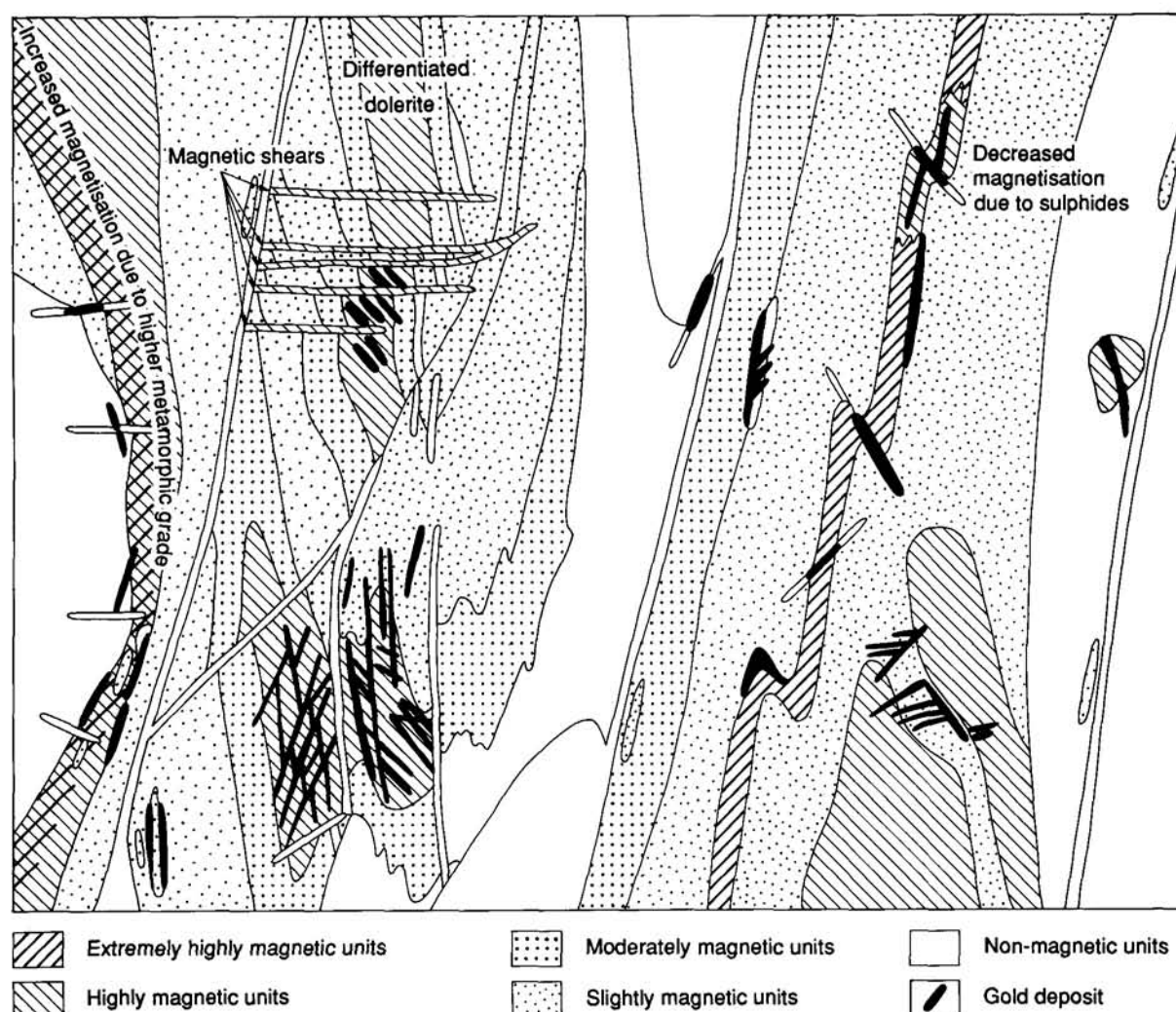


FIGURE 40 Schematic illustration showing how Figure 39 would appear on aeromagnetic data. Only changes in amplitude are shown. Units of similar magnetisation can commonly be differentiated from the texture of the magnetic data. Clearly there is an association between many types of deposit and magnetic units, or contacts between units of different magnetisation. Units have been classified according to strength of magnetisation. Note that this classification is only generalised; for example, sedimentary rocks can be moderately magnetic and basalts can be non-magnetic. *Extremely magnetic units*: BIF. *Highly magnetic units*: komatiites, post-kinematic granitoids, peralkaline granitoids and the magnetic zones of differentiated dolerites. *Moderately magnetic units*: dolerites, non-magnetic zones of differentiated dolerites. *Slightly magnetic units*: basalts, porphyry. *Non-magnetic units*: felsic volcanic rocks, shale, conglomerate, syn-kinematic granitoids.

trol on sulphide mineralogy is metamorphic grade. In greenschist-facies deposits, ore mineralogy is dominated by pyrite and/or arsenopyrite. An exception is the Water Tank Hill deposit described below. In areas metamorphosed to amphibolite facies, either pyrite or pyrrhotite can be the dominant sulphide, although pyrrhotite is more abundant than in lower-grade deposits. The association of disseminated sulphides with gold mineralisation means that the IP method can also be used to locate areas of possible mineralisation (e.g., Howland-Rose, 1984; Lindeman, 1984). Apart from sulphides allowing the use of electrical and EM techniques to locate mineralisation, BIF-hosted gold deposits commonly involve replacement of oxide-facies BIF by sulphides and gold. This can cause a decrease in the magnetic anomaly associated with the BIF, particularly where pyrrhotite is not the major sulphide phase. However, given that the magnetic susceptibility of monoclinic pyrrhotite is approximately one quarter that of magnetite, a relative diminution of

the magnetic signal is still to be expected in higher-grade areas. Fallon & Backo (this volume) argue for a decrease in the magnetic anomaly associated with mineralised BIF at Mount Morgans, but point out that other factors could also cause such an effect. Dockery (1984) describes exploration at the Lady Susan prospect where gold mineralisation is associated with disseminated pyrrhotite which is responsible, at least in part, for positive magnetic anomalies in the area.

HYDROTHERMAL ALTERATION

Metasomatic alteration of wallrock is a feature of gold mineralisation (Groves *et al.*, 1990). The mineralogical expression of this alteration is a function of host-rock lithology and metamorphic grade. In greenschist-facies deposits there is a wide zone of pervasive carbonate alteration containing a central core of ankerite, ferroan dolomite or dolomite that grades into an outer area of calcite, commonly asso-

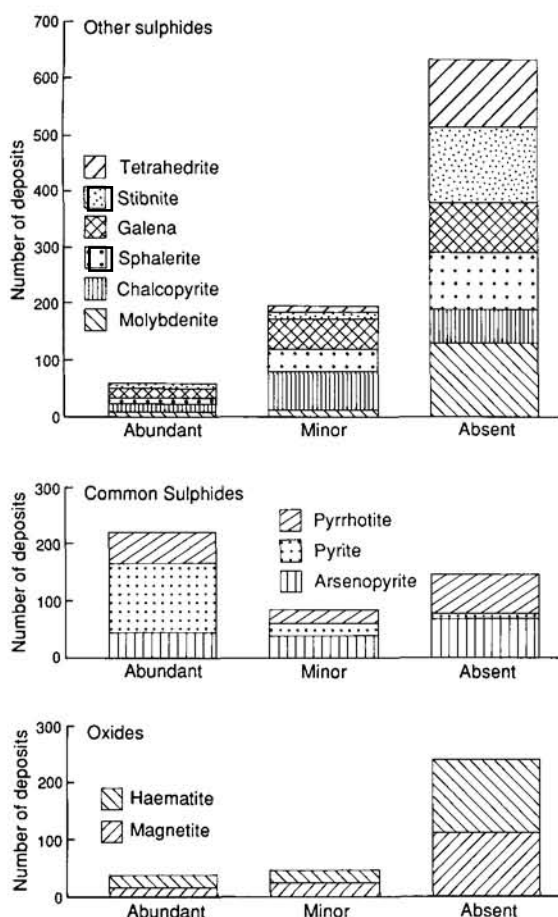


FIGURE 41 Histograms showing relative abundance of selected oxide and sulphide minerals in gold mineralisation in the Yilgarn Craton. Data from Groves *et al.* (1990).

ciated with chlorite and sometimes magnetite. In the strongly mineralised parts of the alteration zone, potassium-micas (biotite and sericite) are common, although they are absent in low-alumina rocks such as BIF. At amphibolite-facies grade, the geochemistry of the metasomatic alteration is similar but is reflected by a higher-grade mineral assemblage. Minerals normally present include chloritoid, staurolite, cordierite, garnet, andalusite, sillimanite, kyanite, diopside-hedenbergite and various amphiboles. From a geophysical perspective, the presence of potassic minerals and magnetite imply that the alteration associated with mineralisation may be detectable. Perry & Wilson (this volume) describe the radiometric detection of potassic alteration associated with gold mineralisation at the South Venus and Leviathon deposits: note that, due to the nature of the alteration, only the potassium-channel data were useful in this respect. Pridmore *et al.* (1988) state that airborne radiometric surveys, with a flight height of 60 m and a 16.8 l sodium-iodide crystal, can detect absolute changes of 0.3 wt % K_2O or 3 wt % sericite extending over several hectares. The extent to which much more localised changes associated with mineralisation can be detected is difficult to assess, especially given the ease with which radioactive sources can be masked by cover. Spencer *et al.* (1989) describe image processing of aeromagnetic and radiometric data to highlight areas of possible sericitic alteration. The potassium data are normalised by the thorium data in an attempt to remove the effects of variable transported overburden on the amplitude of the potassium signal. The data are then integrated with the magnetic data, which is better for mapping structure. The resulting image thus reflects two important characteristics of

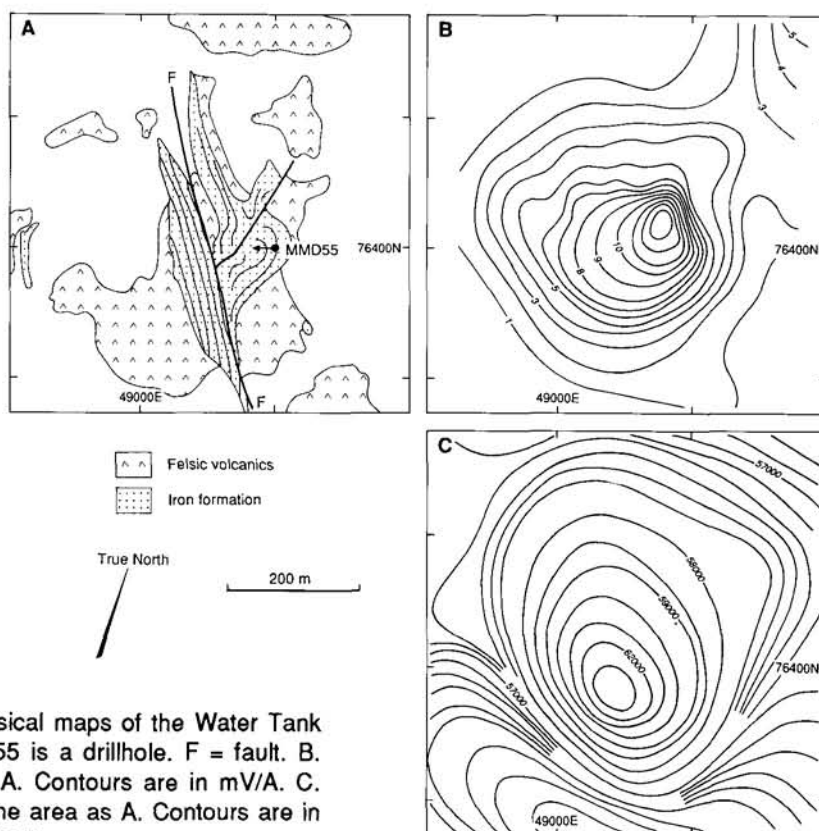


FIGURE 42 Geological and geophysical maps of the Water Tank Hill deposit. A. Geology. MMD55 is a drillhole. F = fault. B. TEM data from same area as A. Contours are in mV/A. C. Ground magnetic data from same area as A. Contours are in nT. Redrawn from Lindeman (1984).

gold mineralisation. Bullock & Isles (this volume) also describe processing of radiometric data to enhance effects due to potassic alteration.

The association of magnetite with gold has obvious implications for exploration. Elias (1990) notes that the presence of positive magnetic anomalies led to the discovery of the Defiance, Revenge and North Orchin orebodies of the Victory-Defiance gold camp. Williams (this volume) shows that the source of the anomalies at Revenge and North Orchin is magnetite-stable alteration associated with gold mineralisation. In contrast, the anomaly at the nearby Orion deposit is due to highly magnetised sedimentary rocks, within a shear zone, which are associated with gold mineralisation. Magnetite within alteration zones is also described from the Hunt mine and from the Golden Mile deposits at Kalgoorlie. Leaman (this volume) also argues for magnetic anomalies associated with gold mineralisation at Bottle Creek being produced by magnetite-stable alteration.

WATER TANK HILL

A good example of the direct detection of an Archaean lode-gold deposit by geophysics is the discovery of the Water Tank Hill deposit (Lindeman, 1984). The Water Tank Hill deposit is one of several deposits within the Hill 50 gold camp, the majority of mineralisation occurring within BIF. The exploration which discovered the Water Tank Hill deposit was designed to find other occurrences of Hill 50-type mineralisation, that is, mineralisation within a BIF host, concentrated by crosscutting fractures and associated with sulphides. The BIFs in the area were mapped using surface and photo-geology combined with semi-regional aeromagnetic data (line spacing 800 m, flight height 90 m). Subsequent exploration was concentrated in areas of BIF, with reconnaissance TEM data being collected using either a MPPO-1 or MPPO-3 (in areas of cultural noise) instrument and a 200 m loop size. Anomalous areas were followed up using 100 m or 50 m loop TEM, frequency-domain IP (dipole-dipole array, 50 m dipoles) and ground magnetics. The TEM anomalies that were confirmed to originate from within BIF were drilled. Figure 42 summarises the geological and geophysical data from the Water Tank Hill area. The TEM data were acquired with the MPPO-3 instrument using 100 m loops and 100 m station spacing. Figure 42B shows contours at 6 ms. The ground magnetic data (Fig. 42C) were collected at a station spacing of 10 m with a line spacing of 100 m. The anomaly defined has a peak amplitude of over 7000 nT above background. Modelling of these data suggested a source dipping at 70° towards grid west. IP data were collected along lines spaced at 50 m. Data from a traverse across the Water Tank Hill orebody, together with the relevant geological, TEM and magnetic data, are shown in Figure 43. There is a resistivity high associated with the BIF, as described elsewhere (e.g., Vella, this volume). The mineralisation gives rise to anomalous PFE values. Note that the gold-bearing horizon does not outcrop, so the deposit is blind. Subsequent exploration and mining show the Water Tank Hill deposit is within a tight, steeply plunging synform of BIF surrounded by felsic debris flows. Mineralisation occurs as a number of shoots and is associated with pyrrhotite replacing

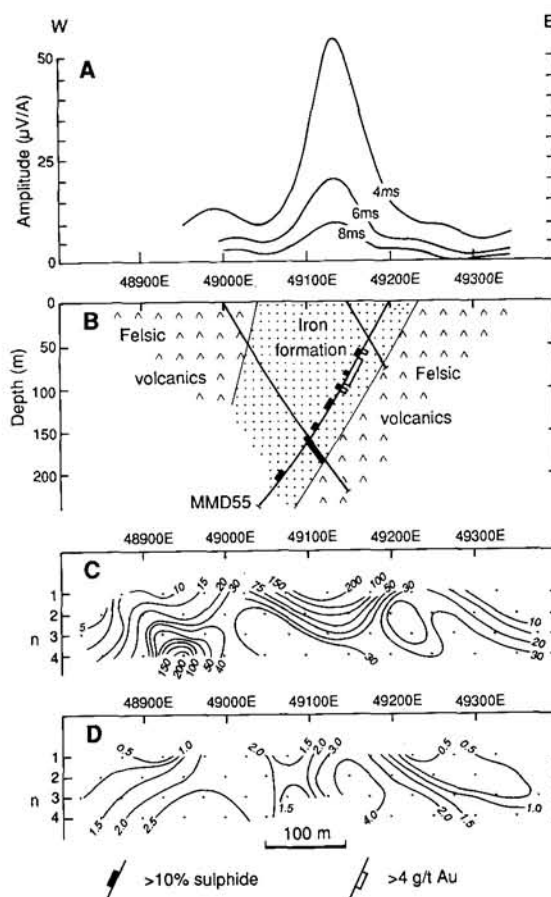


FIGURE 43 Ground geophysical data and geological cross section across the Water Tank Hill deposit. A. TEM data. B. Geology. C. Apparent resistivity (ohm m) D. PFE. Drillhole MMD55 is located in Figure 42. Redrawn from Lindeman (1984).

magnetite and, to some extent, crosscutting fractures (Thompson *et al.*, 1990).

Deposits in Precambrian sedimentary sequences

Epigenetic gold deposits within Precambrian sedimentary sequences occur in several areas in the north and northwest of Western Australia, but only those within the Capricorn and Paterson Orogens (Fig. 1) are significant. Mineralisation occurs as pyritic, copper-bearing, stratabound lodes (Blockley & Myers, 1990). Supergene mineralisation is an important component of these deposits. The most important gold deposit in Precambrian sedimentary rocks is at Telfer, where mineralisation occurs as saddle-reefs hosted by sandstones and shales, and as supergene ore in faults and in the footwall of the main reef. Sexton (this volume) describes the geophysical signature of the Telfer mineralisation and its environs. The major use of geophysics at Telfer has been as a mapping tool, with gravity and magnetic data being used to map regional structure, whereas electrical and, to a lesser extent, EM data are used to map the reefs.

The largest gold deposits within the Capricorn Orogen (e.g., Fortnum, Peak Hill, Labouchere and Horseshoe) are in the Nabberu Basin (Fig. 1). Mineralisation is commonly associated with silicic sedimentary rocks or sericite schists and is associated with pyrite (Hanna & Ivey, 1990; Hill & Cranney, 1990;

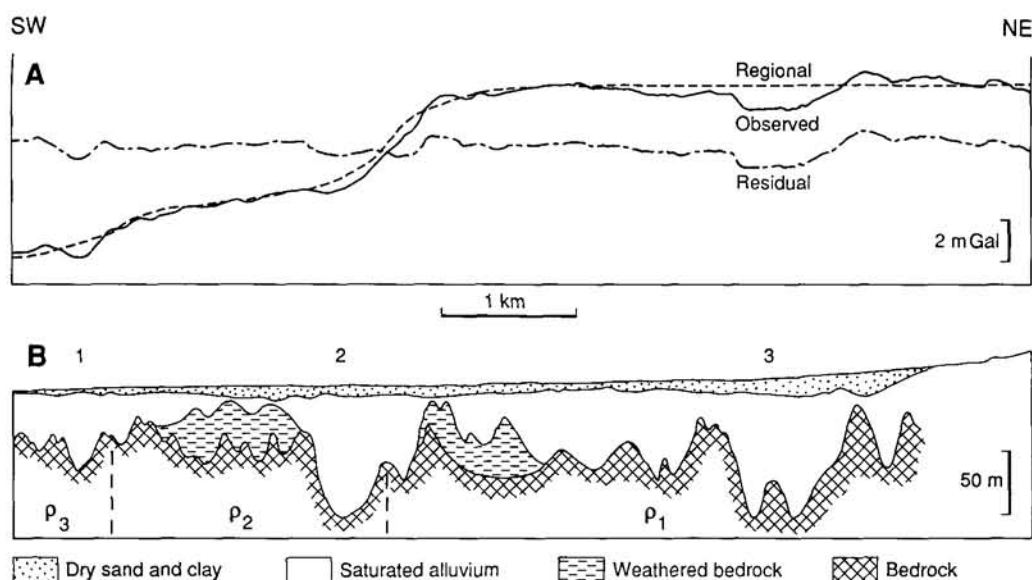


FIGURE 44 Section across palaeochannels southeast of Kalgoorlie. The geological section is obtained from interpretation of seismic refraction data. ρ_1 etc. are assumed bedrock density contrasts used to calculate the gravity "regional". $\rho_1 - \rho_2 = 0.2 \text{ g/cm}^3$, $\rho_2 - \rho_3 = 0.1 \text{ g/cm}^3$. 1, 2 and 3 are the locations of palaeochannels inferred from the seismic and gravity data. Redrawn from Urquhart (1956).

Parker & Brown, 1990). At Horseshoe, the mineralisation may be within a VMS deposit.

There is little published information on the use of geophysics in exploration for the gold deposits in the Napperu Basin. The presence of sericite alteration suggests the use of radiometrics but weathering is very deep and the cover thick, so the signature could well be completely hidden. The widespread occurrence of sulphides suggests the use of electrical and EM techniques, especially in the case of Horseshoe, and the stratigraphic control on mineralisation suggests a mapping role for geophysics. The application of geophysics in the Fortnum area is described by Hill (this volume). As at Telfer, geophysics was used primarily as a mapping tool, with gravity, magnetic and electrical data being utilised. The last-mentioned method was useful for delineating resistive jasperoid units which host mineralisation, provided they are beneath less than about 25 m of cover. IP was unable to detect sulphide mineralisation.

Mineralisation is also found within the Ashburton Basin. For example, Agar (this volume) describes the use remote-sensing data in exploration for Carlin-style mineralisation near Kazput Pool (Fig. 1).

Palaeochannel deposits

Small quantities of gold have been won from channels, ranging from Precambrian to Tertiary in age, from throughout Western Australia. Urquhart (1956) describes an early example of the delineation of palaeochannels using gravity and seismic refraction data. Data were collected along three traverses, southeast of Kalgoorlie (Fig. 1), and the results for one are shown in Figure 44. Gravity data were collected at 100 ft (30.5 m) intervals using a Heiland gravimeter which was capable of measuring changes in gravity of up to 1 mGal with an accuracy of ± 0.05 mGal. Seismic refraction data were collected with a Heiland 6-channel seismograph. Geophone spreads of 300 ft (91 m) were used at intervals of about 1000 ft

(305 m). In areas where channels were indicated, additional data were collected in order to define a continuous refraction profile. Short spreads were also used to map a shallow surface layer which varied in thickness from 1.5 to 15 m. Refractor depths were calculated, using the reciprocal method, beneath each of the four central geophones in each spread.

Three layers are recognised and interpreted as sand and clay (1000-2500 ft/s, 305-762 m/s), water-logged alluvium (4000-8000 ft/s, 1219-2438 m/s) and bedrock (11000-22000 ft/s, 3353-6706 m/s). A fourth layer (9000-11000 ft/s, 2743-3353 m/s), interpreted as weathered bedrock, was identified in a few places. Urquhart (1956) suggests this layer actually extends over a considerable part of the area. Three palaeochannels are interpreted based on increased depth to the bedrock layer. However, the assignment of rock type and correlation of layers based solely on velocity is clearly unreliable given the complexity of the regolith. Thus, the interpreted section must be treated with caution. The gravity data along the same traverse define a long-wavelength negative anomaly which is interpreted as originating from within the bedrock, probably due to sediments (Fig. 44). Superimposed on this anomaly are shorter-wavelength negative features. The bedrock was divided into a number of areas of different density which were assumed to be separated by vertical boundaries (Fig. 44). The gravity effect of these areas was used by Urquhart (1956) to define the "regional" value. On the resulting "residual" profile, the small negative anomalies have amplitudes of about 1 mGal and coincide, in terms of position and width, with the channels defined by the refraction data. It appears that, even with the relatively crude equipment available at the time, channels could be relatively easily mapped, although no drilling data are presented by Urquhart (1956) to confirm the interpretation.

A more recent description of the use of geophysics to study palaeochannels in the Yilgarn Block is

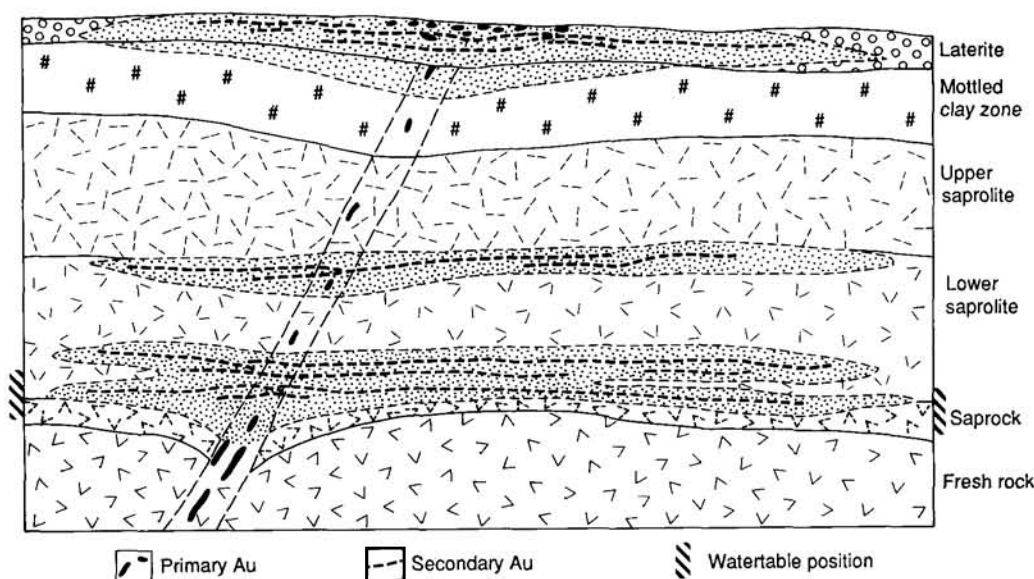


FIGURE 45 Schematic illustration of the distribution of supergene gold within the regolith. Redrawn from Lawrance (1990).

provided by Smyth & Barrett (this volume). These authors favoured the use of remote-sensing data to locate the channels. Follow-up gravity and TEM surveys were then used to define both the shape of the channel and, to lesser extent, the stratigraphy of the overlying sediments. Seismic methods were also tested but were considered to be too expensive and were unable to define the contact between sediments and saprolite.

Supergene deposits

Supergene gold deposits, formed by remobilisation of gold by chemical and/or physical processes, make a significant contribution to gold production in Western Australia. During weathering of primary mineralised zones, the carbonate and sulphidic alteration, together with faults and shear zones, allow comparatively easy access by fluids and hence result in relatively deep weathering. During this process, both gold and ore-associated elements are mobilised and dispersed (Lawrance, 1990), a process that tends to separate gold from these elements. There are two major zones of gold dispersion within the regolith; these occur in the laterite and lower saprolite zones and are usually separated by a depleted zone which is 5 to 20 m thick (Fig. 45). There may be more than one such zone within the lower saprolite horizon, depending on fluctuations of the water table and associated redox front. Below the saprolite zone, gold is generally only found within the host unit.

Geophysical exploration directed at supergene gold depends on the interpretation of signal from the regolith. This situation is complicated by the fact that the regolith response is complex, and also because the gold has been separated from the associated mineralogy that could produce a geophysical response. For these reasons it is common to direct the geophysics towards the primary mineralisation within the underlying protolith. Clearly, for geophysics to play a significant role in exploration for supergene gold, it is necessary to map the thickness and, especially, the

internal structure of the regolith. The thickness of the regolith is routinely mapped using the seismic refraction method and this is also possible using many other geophysical techniques, such as magnetics (Dentith *et al.*, 1992a). Recently, the internal structure of the regolith and overlying sediments has been successfully mapped using early-time TEM equipment such as the PROTEM EM-47. Figure 46A shows a resistivity-depth section through regolith in an area within the Eastern Goldfields Province of the Yilgarn Craton, derived by inversion of such TEM data (Mayes, 1992). Figure 46B shows the known geology from drilling. These data have kindly been made available by Plutonic Operations Ltd. The laterite and mottled clay zone coincide with an area of high resistivity, allowing them to be mapped below the cover of colluvium. The resistivity high at 8800N coincides with a zone of ironstone within the regolith. The underlying bedrock is also clearly mapped as an increase in resistivity.

Finally, remote-sensing data have also been used to map regolith landforms as an aid to exploration for supergene gold (*e.g.*, Chan, 1988).

Summary

Although direct geophysical detection of gold mineralisation is currently not possible, geophysical exploration has played a vital role in the increased exploration activity seen in the last few years. The need for greater resolution and accuracy, compared to exploration for most other commodities, has been the impetus for many of the recent developments in geophysical technology, notably high-resolution aeromagnetic surveys (Bullock & Isles, this volume) and recent initiatives to better understand the regolith from a geophysical perspective.

IRON

The vast majority of Western Australia's commercial iron-ore deposits are in the Pilbara Craton, where

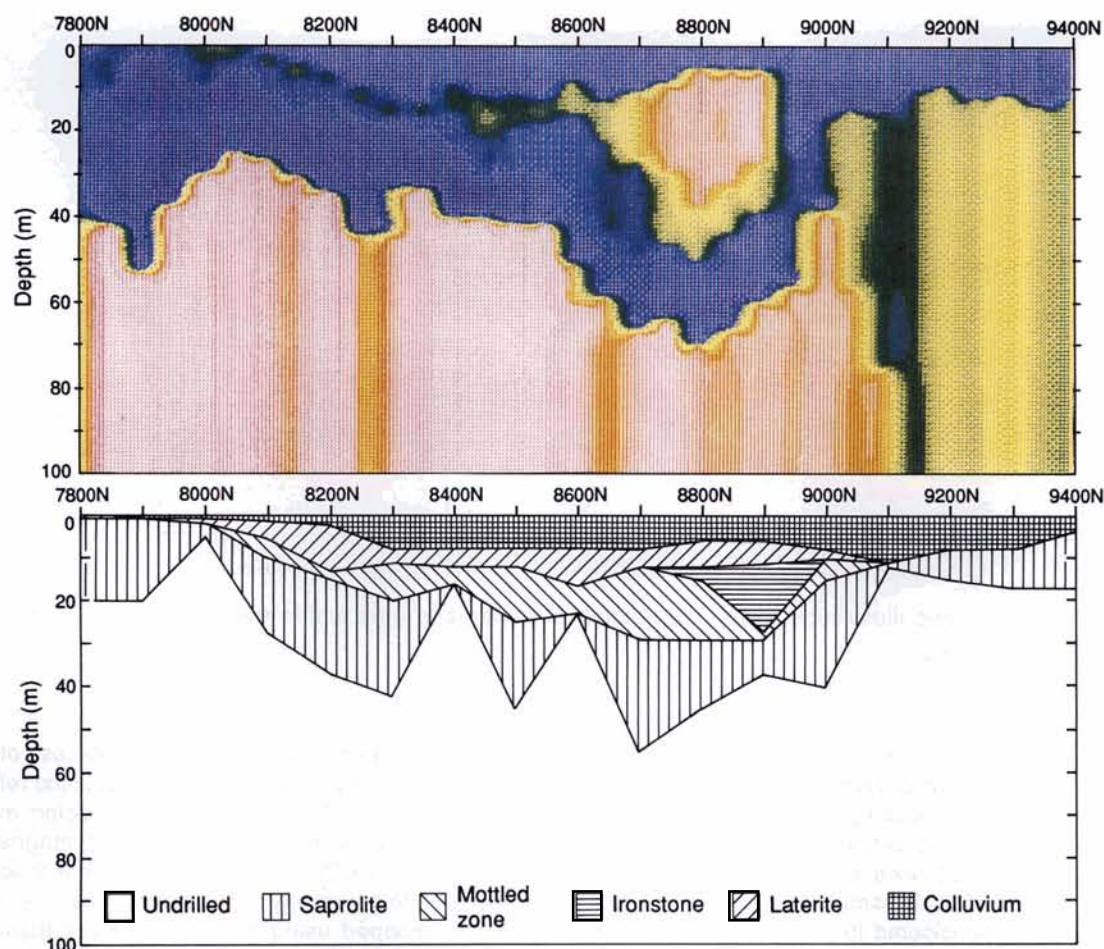


FIGURE 46 Structure of the regolith near Lawlers. A. True resistivity depth section obtained from inversion of PROTEM data. Red = high resistivity, blue = low resistivity. B. Simplified geological cross-section from drilling. Redrawn from Mayes (1992).

there is extensive BIF within the Proterozoic Hamersley Basin (Blockley, 1990) and, to a lesser extent, the Archaean Pilbara Supergroup (Fig. 47). The Archaean BIFs occur within the Gorge Creek Group which consists mainly of clastic sedimentary rocks but with a thick (about 1 km) BIF succession comprising the Cleaverville Formation. The Hamersley Group is the middle of three groups making up the Mount Bruce Supergroup which comprises the succession within the Hamersley Basin. The group is about 2.5 km thick and consists almost entirely of BIF with minor shales, dolomites and felsic volcanic rocks. It is important to realise that here the term "shale" is not used in the normal sense of the word, it describes what is in effect iron-formation with lower iron and higher sheet-silicate and carbonate contents. These shale "macrobands" are important stratigraphic marker horizons within the BIF succession and some examples can be traced over hundreds of kilometres. Mineralisation occurs at three stratigraphic levels within the Hamersley Group, these being the Dales Gorge and Joffre Members of the Brockman Iron Formation, and the Mount Newman Member of the Marra Mamba Iron Formation (Fig. 48). The Brockman Iron Formation iron ores tend to be haematite rich but those in the Marra Mamba Iron Formation are more limonitic.

Mineralisation

The most commercially significant iron ores formed by supergene enrichment of the BIFs. The ores in the Hamersley Basin typically consist of primary haematite, martite after primary magnetite, and goethite replacing primary chert and silicates. Platy haematite replacing goethite is seen in some of the more mature ores. Both the Archaean and Proterozoic orebodies are associated with structures that have focussed the flow of fluids, commonly synclines and/or faults. There are chemically precipitated limonite ores within Tertiary palaeochannels which drained the area comprising the Hamersley Group. The ore consists of pisoliths composed of varying proportions of limonite, goethite, maghemite and haematite. Deposits of this type are particularly well developed in the western Pilbara.

Geophysical exploration

The iron ore industry in Western Australia is extremely secretive and it is very difficult to find information on the use of geophysics in exploration. However, this may be due in part to the fact that, with the possible exception of aeromagnetics, geophysics appears to have played a relatively minor role in exploration for iron deposits, at least until recently. This is probably because the stratigraphic control on the ores, combined with the stratigraphic consistency in

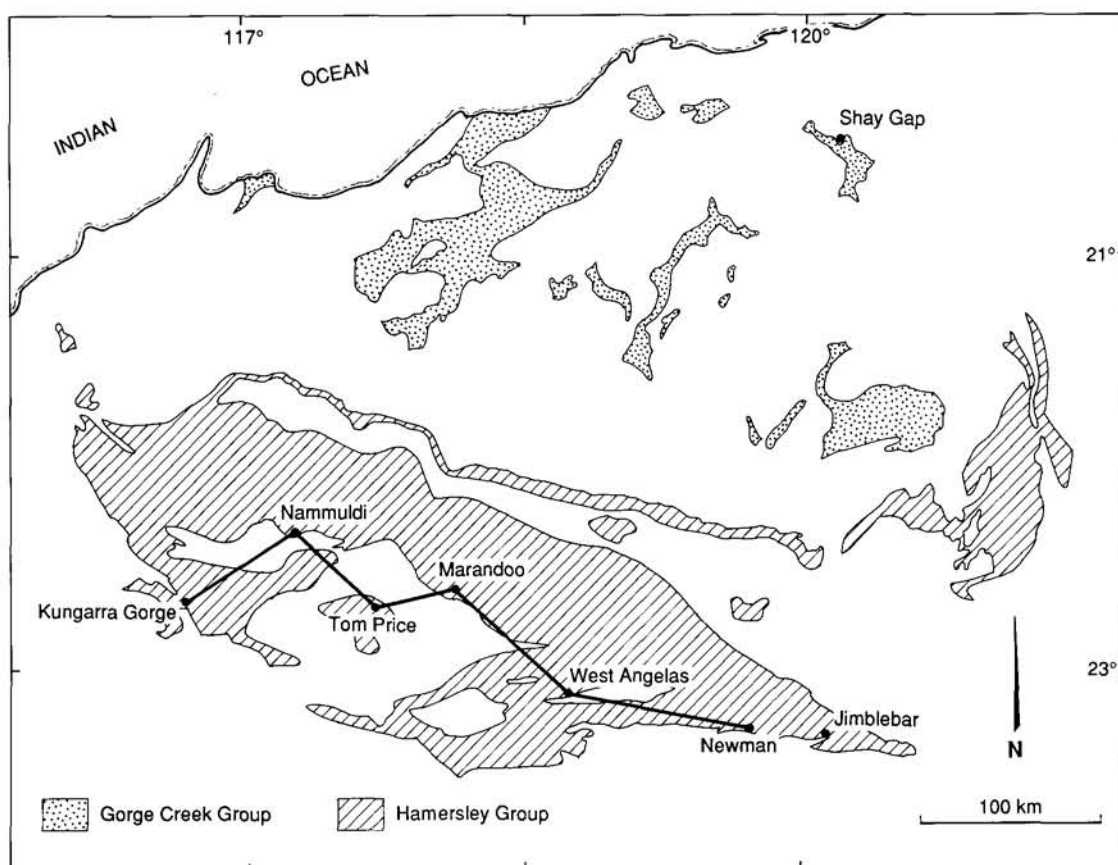


FIGURE 47 Geological map of the Pilbara region showing the distribution of the Gorge Creek and Hamersley Groups. The figure uses data from Blockley (1979), Griffin (1990) and Trendall (1990). The line from Kungarra Gorge to Newman shows the positions of sections and logs correlated in Figure 49.

the Hamersley Basin and good outcrop, makes it relatively easily to identify favourable areas without resorting to geophysical methods. The fact that the more obvious orebodies have now been located explains the increased use of geophysics. The most important geophysical methods are downhole logging to improve stratigraphic correlations and aeromagnetic surveying; the formation of the supergene-enrichment ores involves destruction of magnetite, and its location is structurally and stratigraphically controlled, so there are obvious implications in this respect. Typical survey specifications for aeromagnetic data are a line spacing between 100 and 400 m and a flight height between 60 and 100 m. The use of aeromagnetic data and downhole logging are described by Kerr *et al.* (this volume) with respect to exploration for both Archaean and Proterozoic iron ore in the Pilbara. The magnetic data confirm the structural and stratigraphic control on mineralisation, and also suggest that mineralisation can be associated with magnetic lows. However, discriminating lows due to mineralisation from others is difficult. As pointed out by Clarke & Schmidt (this volume), geological interpretation of structures in BIFs is complicated by their strongly anisotropic magnetic susceptibilities and the effects of pre- and post-folding remanent magnetisation.

Lord & Trendall (1976) and Blockley *et al.* (1990) mention the use of gravity surveying, in conjunction with magnetic surveys, in exploration for ore in the Marra Mamba Formation. The ores are particularly friable and porous in this formation but the resulting

density contrast with the host is small. However, "moderate success" in defining sub-surface extensions of known orebodies is claimed. In addition to the gravity work, seismic and resistivity surveys are reported to have been used, largely unsuccessfully, in the search for blind limonite deposits. Landsat data and the GEOTEM AEM system have been used to map the channels in which these deposits occur, and spectral analysis of remote-sensing data has also been used to locate haematite iron-ore deposits.

DOWNHOLE LOGGING

Downhole logging is perhaps the major use of geophysics in the iron ore industry of Western Australia. Blockley *et al.* (1990) mention the use of resistivity logging, Eisler *et al.* (1979) describe neutron-activation logging and Kerr *et al.* (this volume) mention density logging. Magnetic susceptibility and resistivity logs can be used to distinguish ore types, and cross-hole seismic surveys have been tested to define the structure of ore zones. However, natural gamma logging is the most important technique. The monotonous nature of the BIF succession in the Hamersley Basin and the regular occurrence of shale bands makes stratigraphic correlation between drillholes very difficult. The problem is particularly acute in the southern and eastern parts of the Basin where folding and faulting cause stratigraphic breaks and duplication (Blockley *et al.*, 1990). The shale bands produce characteristic gamma responses, even where the surrounding iron formation has been enriched to ore. As

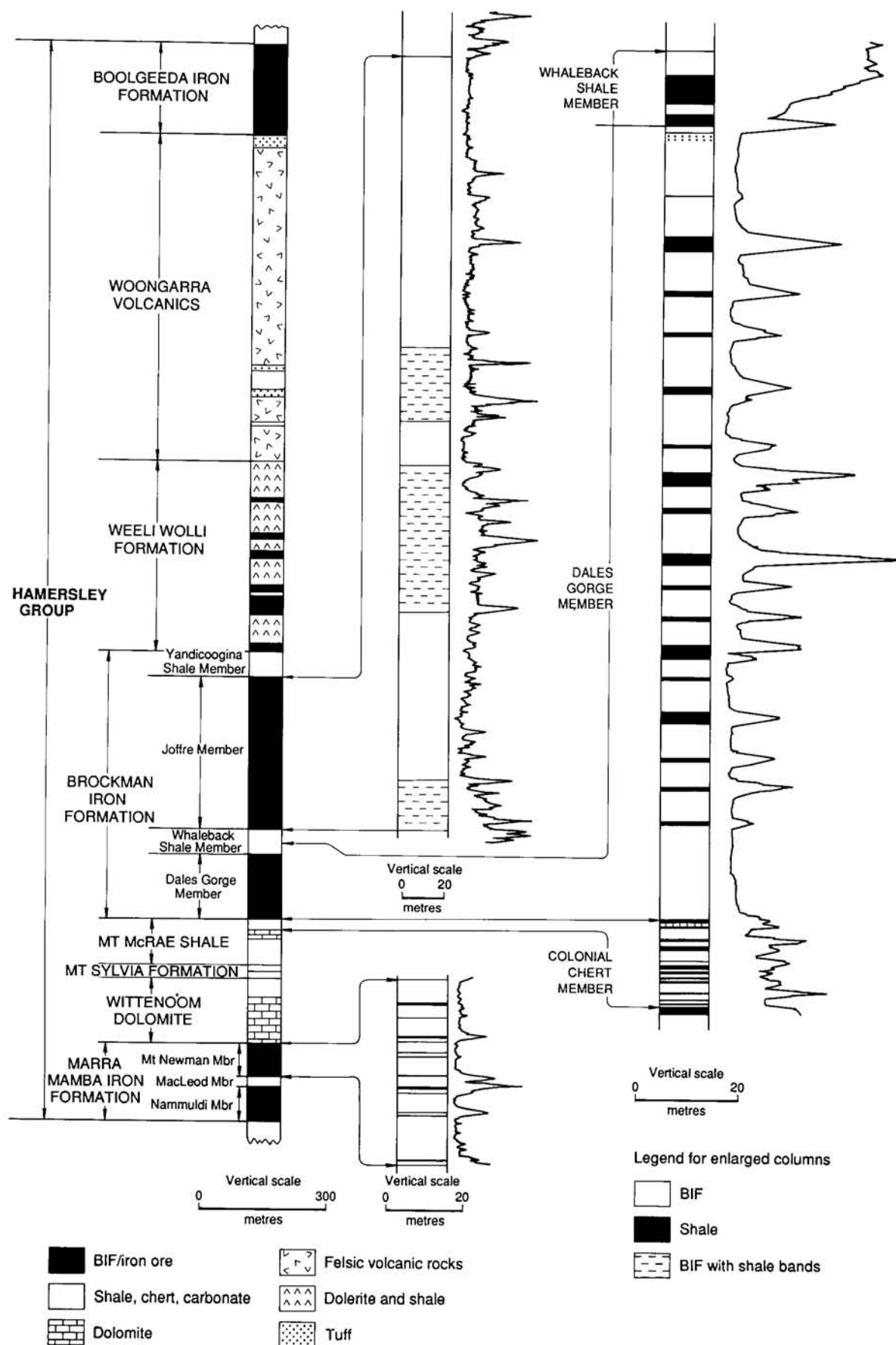


FIGURE 48 Stratigraphic columns of the Hamersley Group with appropriate gamma-ray logs. Geological data from Blockley (1990), detailed stratigraphy of mineralised areas and gamma logs from Harmsworth *et al.* (1990).

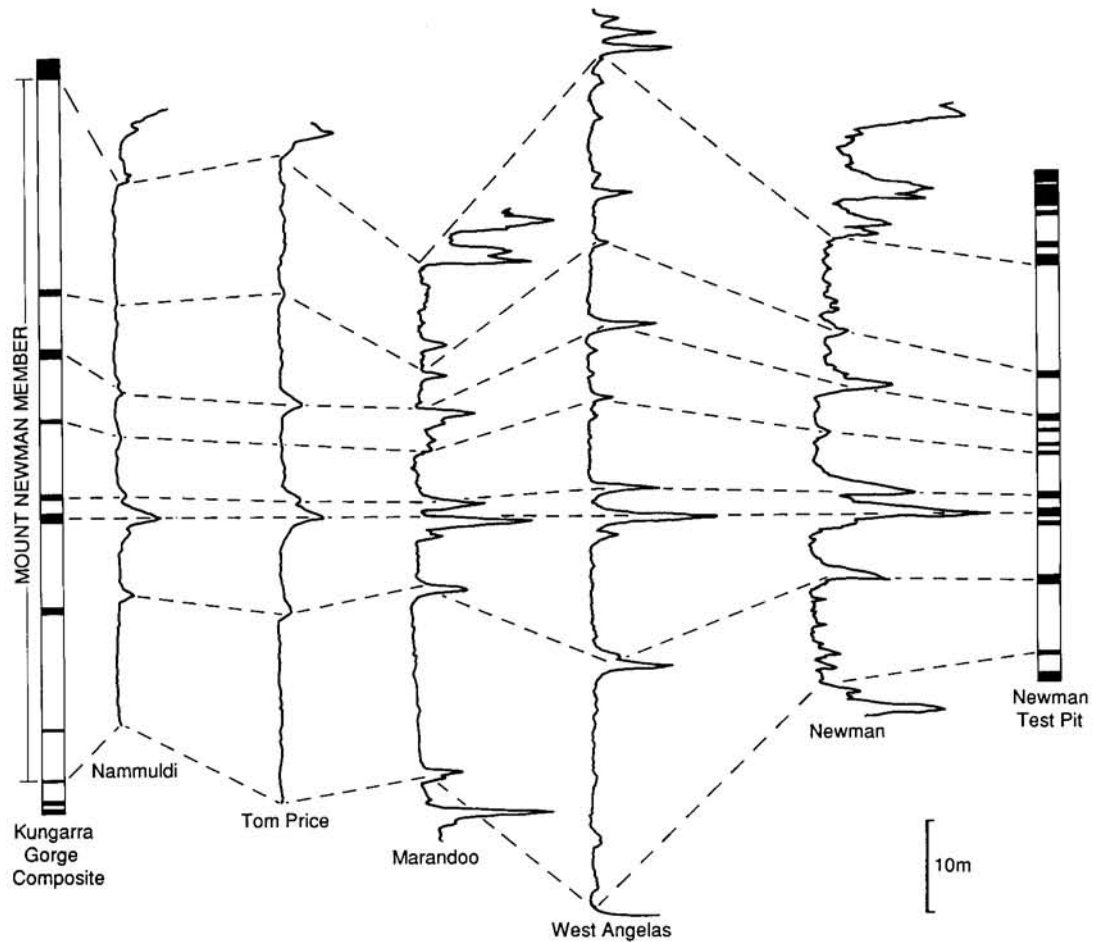


FIGURE 49 Correlation of sections in the Mount Newman Member of the Hamersley Group using gamma logs. See Figure 47 for location of sections and logs. Redrawn from Blockley (1979).

shown in Figure 48, this has allowed standard reference sections or responses to be defined for the mineralised parts of the Marra Mamba Iron Formation (Blockley, 1979; Blockley *et al.*, 1993) and the Brockman Iron Formation (Jones *et al.*, 1973). Figure 49 shows gamma logs from five localities within the Mount Newman Member of the Marra Mamba Iron Formation. Not all shales produce strong gamma-ray responses but several are distinct markers. It should be remembered that the sections being correlated extend over about 300 km (Fig. 47). The use of gamma logs in correlating horizons, and hence determining the structure of an area, is illustrated by Jones *et al.* (1973) and Kerr *et al.* (this volume). The gamma response of the stratigraphic succession is commonly sufficiently distinctive that faults can be located and even inverted strata recognised (Fig. 50). Kerr *et al.* (this volume) describe the use of gamma-ray logging in the Archaean Gorge Creek Formation where the stratigraphy is less consistent than the Proterozoic succession, making the use of the logs more difficult.

Summary

Along with the well-established use of downhole

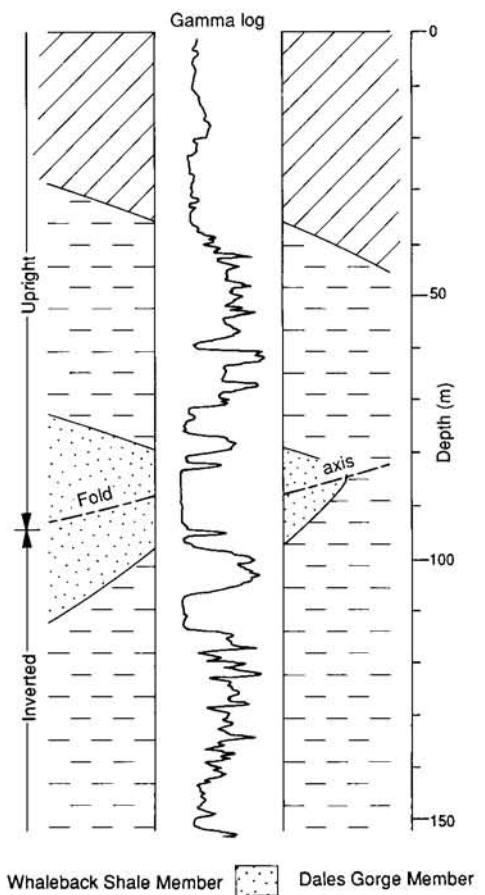


FIGURE 50 Recumbent fold in the Brockman Iron Formation indicated by gamma log. Data from Jones *et al.* (1973).

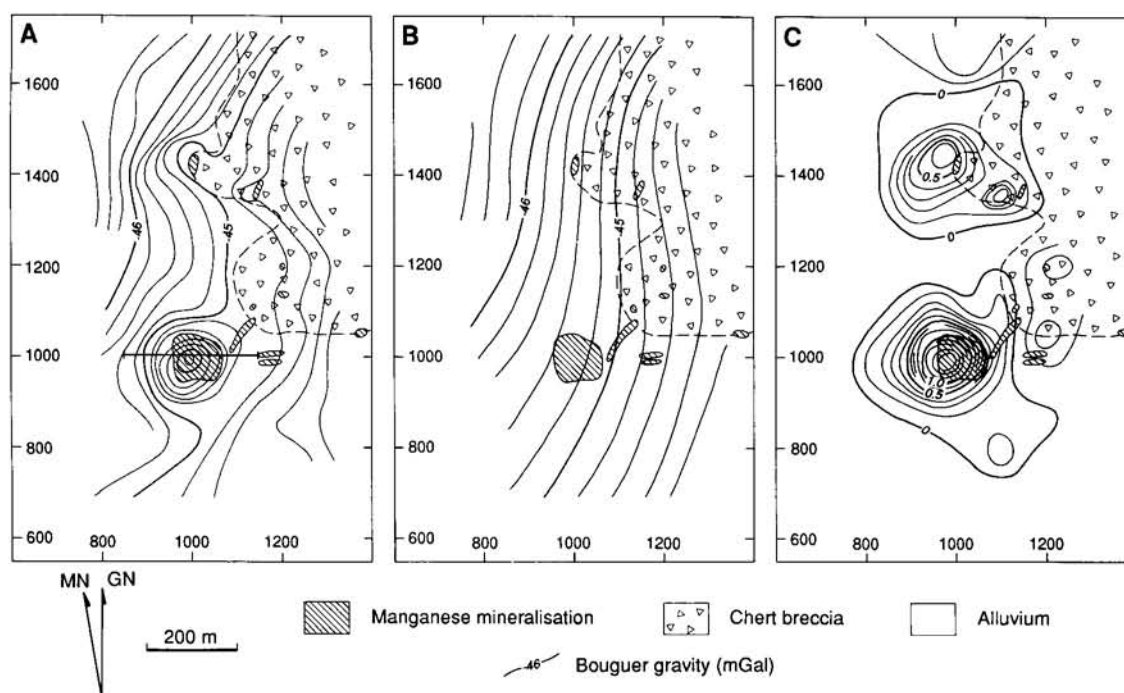


FIGURE 51 Gravity and geological maps of the Lox prospect. A. Observed gravity. The location of the section in Figure 52 is indicated by the horizontal line at 1000NB. Regional gravity. C. Residual gravity.

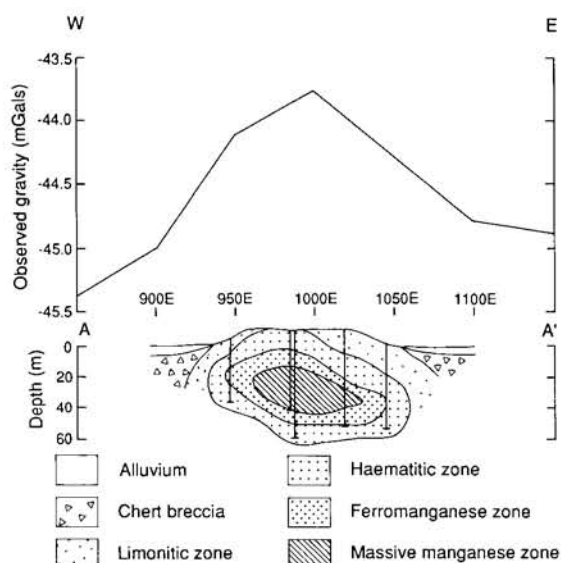


FIGURE 52 Gravity profile and geological cross section across the Lox prospect. See Figure 51 for location.

logging, the iron industry is increasingly using geophysics, especially aeromagnetic and remote sensing data. This trend is likely to continue, especially with respect to exploration for blind orebodies.

MANGANESE

The largest manganese and ferromanganese deposits in Western Australia are in Proterozoic shales in the eastern Pilbara, with the deposits at Woodie Woodie and Ripon Hills being the most important (Fig. 1). These iron-manganese-rich shales overlie chert breccia and dolomite. The ore forms by supergene enrichment of the shales.

TABLE 3 Resistivities of minerals and rocks in the Ripon Hills ferruginous manganese deposits.

Description	Resistivity (ohm m)
Manganese	100-5000
Manganiferous shales	5000-10000
Barren shales	10000-75000
Chert breccia	>75000

Ripon Hill

The deposits at Ripon Hill are preserved within topographic depressions, mainly caused by solution collapse of the underlying dolomites, and are concentrated in the topmost 11 m from the surface (Denholm, 1977). The ore consists of fine-grained pyrolusite intergrown with haematite, and kaolin is the main gangue mineral. The Ripon Hills deposits have been known since the 1950s and it is unlikely that geophysics played any role in their discovery. However, in the early 1970s, the area was reassessed by Longreach Metals NL. In a report submitted to the Western Australian Department of Mines, mention is made of the relatively high electrical conductivity of the manganese ore, specifically that the electrical conductivity of core is directly related to its manganese content. The report also alludes to resistivity soundings carried out over one of the Ripon Hills deposits using an RSP-6 resistivity and SP unit. Table 3 summarises the resistivities of the local rocks as reported by Longreach Metals NL.

The deposits at Ripon Hills were considered to be well suited for resistivity surveys because of their sheet-like form and preliminary tests are described as having demonstrated that orebodies can be delineated in this manner. Nevertheless, it is clear from the report that geophysics played only a very minor role in the delineation of the Ripon Hill deposits.

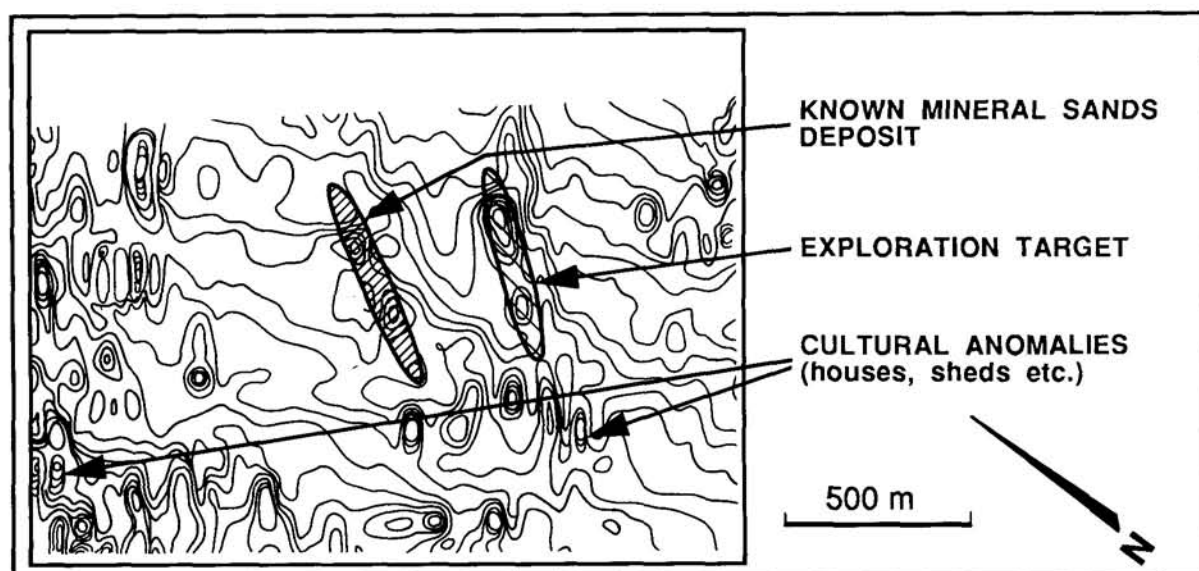


FIGURE 53 Contour map of TMI over a mineral sands prospect in the Capel area. Redrawn from Bullock & Cooke (1990).

Woodie Woodie

In exploring for manganese mineralisation in the Woodie Woodie area, Preussag Australia Pty Ltd made extensive use of gravity surveys. Manganese ore has a density of around 3.8 g/cm^3 whereas the host rocks have densities between 2.0 and 2.7 g/cm^3 (E. Reeves, pers. comm., 1993). Again, this work is described in reports submitted to the Western Australian Department of Mines. Gravity surveys were carried out in areas where outcrops of manganese in dolomites and chert were observed using a La Coste and Romberg gravity meter. Station spacing was 50 m with stations optically levelled. A Bouguer reduction density of 2.3 g/cm^3 was found to be most suitable. Prospects where a positive gravity anomaly was recognised were selected for follow-up drilling. One example of such an area is the Lox prospect, about 8 km south of Woodie Woodie.

Massive ferruginous manganese together with iron-stained chert breccia outcrops at Lox. The exposures of ferruginous manganese coincide with two sub-circular positive gravity anomalies with amplitudes of 0.5 and 1.4 mGal . Excess mass calculations on the southern anomaly indicated a tonnage of 2.0 Mt . However, removal of regional gradients proved a problem in the exploration area, making this figure uncertain. Gravity and geological data from the Lox prospect are summarised in Figure 51. Drilling intersected between 9 and 36 m of massive manganese beneath a haematite cap 10 to 20 m in thickness. The deposit consists of a high-grade core surrounded by shells of mixed iron-manganese oxides, haematite and limonite (Fig. 52). Consequently, of the calculated 2.0 Mt excess mass, only a nucleus estimated at between 0.5 and 0.6 Mt contained commercial-quality manganese oxides. It is important to realise that not all positive gravity anomalies in the area were associated with significant mineralisation. However, the anomalies in the barren areas were of much lower amplitude (0.6 – 1.0 mGal) and had shallower gradients (less than about 5 mGal/km) than at Lox. The sources of these anomalies could be the interface between

dolomite and overlying chert, or they could originate within, or below, the dolomite. Petrological studies of cuttings from the Lox prospect indicated that the main manganese minerals are braunite, psilomelane-cryptomelane and pyrolusite. Significantly, jacobsonite, a magnetic manganese oxide, was not found. However, surveys elsewhere in the area have shown a correlation between gravity and magnetic anomalies in two locations.

Summary

Gravity surveys are an important tool for direct detection of manganese mineralisation. In a few cases there may be magnetic anomalies associated with manganese mineralisation, but the lack of magnetic minerals associated with the majority of mineralisation precludes the use of magnetic surveys. The relatively high conductivity of the manganese ore suggests the use of electrical and EM methods, but the fact that, on a prospect scale, gravity offers a cheaper alternative discourages their use. For more regional-scale exploration, AEM systems may be capable of detecting mineralisation.

MINERAL SANDS

Mineral sand deposits in Western Australia are described by Baxter (1977), Harrison (1990) and Rattigan & Stitt (1990). The deposits consist of quartz sand associated with ilmenite, rutile, leucoxene, zircon, monazite and xenotime. Most mineral sand deposits are associated with palaeo-shorelines and are some distance inland from the present coast. The sources of the heavy minerals are Precambrian igneous and metamorphic rocks, the nature of the source being reflected in the mineralogy of the deposits.

Bullock & Cooke (1990) discuss the use of geophysical surveying in exploration for mineral sands. They point out that ilmenite varies from weakly to strongly magnetic, depending on its composition. However, the magnetic responses of heavy-mineral sand deposits are usually small, although theoretically

TABLE 4 Electrical and magnetic properties of mineral sands from Yoganup central district. Modified from Baxter (1977).

Description	Chargeability (ms)	Resistivity (ohm m)	Magnetic Susceptibility (SI)
Mineralised sand	8.4	280	50×10^{-5}
Mineralised sand	6.0	132	38×10^{-5}
Mineralised sand	6.8	210	No data

detectable using aeromagnetic data. Figure 53 shows aeromagnetic data acquired over heavy-mineral sand deposits in the Capel area (Fig. 1). Note the large number of cultural anomalies in the figure. Mudge (this volume) found that cultural and geological noise was too widespread for aeromagnetic data to be useful in the Eneabba area (Fig. 1). However, high-resolution ground magnetic surveys were useful for locating mineralisation. Rowston (1965) carried out ground magnetic (vertical component) and radiometric surveys over beach deposits near Capel which consisted of ilmenite, monazite and zircon. Two lines 1800 ft (548 m) long were surveyed at a 50 ft (15 m) sampling interval. A correlation was recognised between concentration of heavy minerals in auger samples and maxima on the geophysical data. Concentrations of greater than 6 wt % heavy minerals were detectable in this manner if located less than a few feet below the surface. Subsequent work (Rowston, 1966) was less successful due to noise problems associated with the presence of laterites.

Monazite is strongly radioactive because of the presence of thorium, and zircon is weakly radioactive due to its uranium content. However, radiometric surveys for mineral sands are hindered by masking of the deposits by cover (a few 10s of centimetres is sufficient) and difficulties differentiating their responses from other sources. Baxter (1977) describes the use of radiometrics as effective in the Capel area and around Eneabba, and reports that spectral measurements can be used to discriminate mineralisation from noise such as laterites.

Bullock & Cooke (1990) point out that ilmenite, and to a lesser extent leucocene, can produce substantial IP effects and suggest that this method could be used for exploration and delineation of mineral sand deposits. Baxter (1977) cites a confidential report on IP and vertical electric sounding tests at the Yoganup Central deposit (Fig. 1). It is concluded that ilmenite is a suitable target for IP but the resistivity results were inconclusive. A relationship between chargeability and grade (wt %) was recognised. Petrophysical properties of samples of mineral sands from Yoganup Central are listed in Table 4.

Summary

Although the mineralogy of the mineral sand deposits suggests that modern geophysical surveys ought to be capable of locating such deposits, little use of has been made of such techniques by the mineral sands industry. This is largely a function of the relatively low cost of drilling in mineral sand areas compared to geophysical surveys, plus the difficulty of identifying the weak signatures associated with the mineral sand deposits.

NICKEL

Geophysics is an integral part of nickel exploration in Western Australia, being used from regional-scale exploration (O'Driscoll, 1981) down to that on a prospect-scale (Coggon, 1987). Indeed, the initial discovery of nickel-sulphide mineralisation at Kambalda in 1966 was made when a gossan with a coincident IP anomaly was drilled.

Harrison (1990) identifies six categories of nickel deposit within Western Australia:

- volcanic peridotite-associated deposits,
- intrusive dunite-associated deposits,
- gabbro-associated deposits,
- layered sedimentary-associated deposits,
- vein-type arsenical deposits and
- lateritic nickel deposits.

The first category is by far the most important, followed by deposits in the second category. The other types of deposit are relatively unimportant.

Deposits associated with volcanic peridotites

Deposits of this type occur in Archaean granitoid-greenstone terrains with most within the Eastern Goldfields Province of the Yilgarn Craton. Mineralisation is developed at or near the contact between thick (hangingwall) komatiitic volcanic rocks and underlying (footwall) tholeiitic basalts. In places, there are sulphidic sedimentary rocks at this contact but they are usually absent in areas of mineralisation. Mineralisation occupies troughs within the footwall basalts and consequently appears as elongate zones when projected to the surface. The nickel and associated sulphides are usually massive at their base, grading upwards to disseminated mineralisation. The ore assemblage is typically pyrrhotite, pentlandite, pyrite, chalcocopyrite, magnetite and millerite.

GEOPHYSICAL EXPLORATION

Geophysical exploration for volcanic peridotite-associated nickel deposits in the Kambalda area is reviewed by Pridmore *et al.* (1984) and Trench & Williams (this volume). Mutton & Williams (this volume) describe the Rocky's Reward deposit, located in the northern part of the Eastern Goldfields Province (Fig. 1). Robinson *et al.* (1973), in describing the discovery of the Windarra deposits (Fig. 1), mention some geophysical aspects. Exploration for volcanic peridotite-associated nickel deposits uses all the major types of mineral exploration geophysics with the exception of radiometrics. Although the ores themselves are dense compared to their hosts and also contain magnetic minerals (Mutton & Williams, this volume), direct detection using gravity and magnetic data is generally not possible because of the rela-

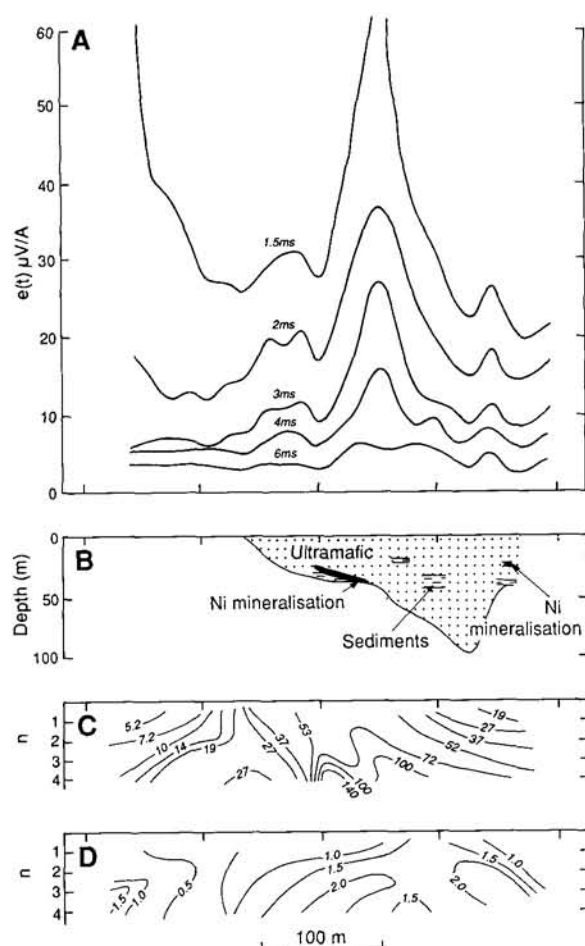


FIGURE 54 Geophysical data from the Edwin shoot, Kambalda. A. TEM. B. Geology. C. Apparent resistivity. D. PFE. Redrawn from Pridmore *et al.* (1984).

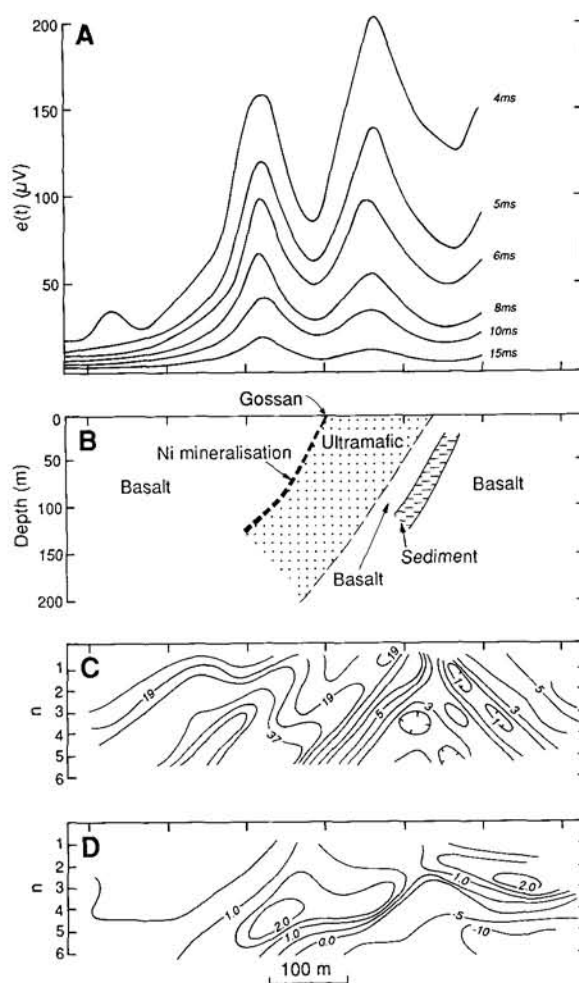


FIGURE 55 Geophysical data from the Carnilya Hill deposit, Kambalda. A. TEM. B. Geology. C. Apparent resistivity. D. PFE. Redrawn from Pridmore *et al.* (1984).

tively small size of the deposits. Hence their signal is swamped by noise originating from the weathered zone and the structurally complex geological environment in which the mineralisation occurs.

The major role of magnetics is in mapping, particularly the mafic-ultramafic contact. At a prospect scale, ultra-high resolution surveys may be used, for example:

- (i) aeromagnetics flown at 50 m flight heights and less than 200 m line spacing, or
- (ii) ground magnetic surveys using caesium-vapour magnetometers and station spacings up to 1 m.

Gravity data can also be used for this purpose but obviously are more costly and have lower resolution. Electrical and electromagnetic methods are the major tools for direct detection of the nickel ores. The relative proportions of massive and disseminated mineralisation, along with its geometry, determine whether EM or IP techniques will give the best response. However, EM is preferred because it can better constrain the geometry of the mineralisation. Unfortunately, graphitic and sulphidic sedimentary rocks can also respond on EM and IP data and are very difficult to discriminate from the responses due to mineralisation. The problem is exacerbated because the sedimentary rocks are commonly in stratigraphic positions where mineralisation would be expected.

KAMBALDA

Pridmore *et al.* (1984) describe geophysical data from the Edwin and Carnilya Hill deposits near Kambalda. Figure 54 shows the dipole-dipole IP [100 ft (30 m) dipole] and TEM data from the Edwin shoot. This shoot consists of relatively shallow-plunging (25–30°) matrix and massive mineralisation just above the contact between footwall mafic and hangingwall ultramafic rocks. There are sedimentary rocks both within the ultramafic succession and at its base. The depth of oxidation is about 30 m, with supergene alteration extending to a depth of around 80 m. The TEM data, collected using a 60 m loop and MPPO equipment, show the mineralisation produces anomalies to about 4 ms, somewhat longer than those due to the weathered layer. The single peak demonstrates the conductor to be flat-lying. Any response from the mineralisation is masked on the IP apparent-resistivity pseudosection by variations in the conductivity of the overburden and the response of hangingwall sedimentary rocks. However, the PFE data, acquired at frequencies of 0.3 and 3 Hz, do show a response from the mineralisation. The Carnilya Hill deposit (Fig. 55) contrasts with the Edwin area in that the mineralisation is steeply dipping and overturned. Again the mineralisation is at the contact between the mafic and ultramafic

sequences. There is a carbonaceous sulphidic sedimentary rock within the footwall sequence. Weathering reaches a depth of about 30 m with supergene effects reaching about 120 m depth. The TEM data, this time with 120 m loops, have anomalies due to both mineralisation and the footwall sedimentary unit. At early times the response from the sedimentary rocks is greatest, but at later times that due to the mineralisation is slightly larger and is clearly decaying more slowly. The resistivity pseudosection obtained from the dipole-dipole IP data (50 m dipole) is dominated by the low resulting from the footwall sedimentary rocks. No response from the mineralisation is evident, even where there are outcrops of gossanous material. The PFE pseudosection (frequencies 0.3 and 3 Hz) shows a small positive anomaly which coincides with the mineralisation. However, as in the apparent resistivity data, the effects of the footwall sedimentary rocks are more obvious, with the diffuse negative anomaly being caused by electromagnetic coupling.

WINDARRA

During initial exploration in the Windarra area, AGSO regional aeromagnetic data were used to identify enclaves of ultramafic rocks and hence direct gossan search (Robinson *et al.*, 1973). Prospective areas were followed up using a combination of geological mapping and ground magnetic and IP surveys. At Mount Windarra, mineralisation occurs as concordant bodies within ultramafic rocks and is associated with a BIF unit. The BIF unit is rich in magnetite and sulphide, and produces strong magnetic and IP anomalies. These anomalies are generally sufficient to obscure any anomalies caused by the mineralisation, but were used to define drilling targets during exploration.

ROCKY'S REWARD

In addition to the methods described above, Mutton describes the use of CR, CSAMT and mise-a-la-masse surveys at the Rocky's Reward deposit. The first two defined very weak anomalies possibly related to the mineralisation. However, the mise-a-la-masse survey, although of limited extent, was able to define the basic geometry of the orebody. Finally, Howland-Rose *et al.* (1980) argue the benefits of MIP in exploration for volcanic peridotite-associated nickel deposits in areas of highly conductive overburden.

BOREHOLE GEOPHYSICS

One area of geophysics that has seen increasing use in nickel exploration in the last few years is borehole geophysics. Coggon (1987) and Coggon & Clarke (1987) describe conventional and hole-to-hole mise-a-la-masse surveys and conventional downhole and fixed receiver EM surveys to define the geometry of mineralisation. DHEM methods are now an integral part of prospect-scale exploration (Mutton, 1987; Trench & Williams, this volume). Mutton (1987) describes examples of DHEM surveys around the Rocky's Reward deposit. Examples are used to illustrate the use of DHEM to:

- (i) search for sub-surface conductors that may give no surface EM anomaly,
- (ii) follow-up drilling by confirming possible conduc-

tive zones as the source of surface anomalies and

- (iii) locate "near-miss" conductors in the vicinity of the drillhole.

Data acquired in several drillholes may be quantitatively modelled, or simply interpreted in terms of in-hole and off-hole responses. Careful integration of all available data of this type, together with geological information, is critical in the evaluation of the prospect and siting of subsequent drilling. However, as with surface geophysics, the discrimination of responses due to mineralisation from those caused by sedimentary rocks is a problem.

Intrusive dunite-associated deposits

Intrusive dunite-associated nickel deposits occur in the Archaean granitoid-greenstone rocks of the Eastern Goldfields and Southern Cross Provinces of the Yilgarn Craton (Harrison, 1990). The nickel-sulphide mineralisation can form massive lenses with associated disseminated and matrix mineralisation or, more commonly, can be entirely disseminated, giving rise to large volumes (up to 2 km long by 300 m thick) of low-grade mineralisation (0.4-1 wt % Ni). Mineralisation is usually contained within subconcordant intrusive dunite lenses consisting of komatiitic dunite with peripheral peridotite. In the Eastern Goldfields Province, many of the dunite lenses are near, or on, the contact between a felsic volcanic-clastic rock sequence and underlying mafic and ultramafic lavas. In the Southern Cross Province, the lenses are overlain by komatiitic volcanic rocks. The massive mineralisation has similar constituents to the volcanic peridotite-associated mineralisation described above. However, the lower-grade disseminated mineralisation can contain a number of additional or alternative phases (see Harrison, 1990).

There is currently much interest in exploring for intrusive dunite-associated nickel deposits in the Eastern Goldfields Province area and geophysical aspects of this exploration are confidential. However, there is some published information on the TEM responses of mineralisation of this type (Staples, 1984; Elliot & Staltari, 1985). Staples (1984) describes EM-37 surveys over the Flying Fox deposit (Fig. 1). The data were dominated by overburden response but, after removal of these effects, a response consistent with a confined conductor coincident with known massive mineralisation was defined. Elliot & Staltari (1985) compared the results of SIROTEM, EM-37 and UTEM surveys, with various loop configurations, over massive nickel-sulphide mineralisation at Mount Keith. All the systems successfully detected the mineralisation.

Gabbro-associated deposits

Gabbro-associated nickel sulphide deposits in Western Australia occur in intrusions of varying age and geological setting. The intrusions are usually layered, consisting mainly of norite and gabbro. Mineralisation is stratabound and low grade, with disseminated or blebby nickel sulphides. Matrix, massive and breccia sulphides are developed in places. Two significant occurrences of nickel mineralisation of this type are at Sally Malay and Radio Hill (Fig. 1).

SALLY MALAY

The Sally Malay deposit is described by Frankcombe *et al.* (this volume). The Sally Malay intrusion is Proterozoic and occurs within high-grade gneisses of the Lamboo Complex within the Halls Creek Mobile Zone. The intrusion consists of subvertical mafic and ultramafic rocks with nickel, copper and cobalt mineralisation in the basal chilled margin. The mineralisation gives rise to magnetic, EM and IP responses, although the steep local topography and small size of the deposit hinder detection using airborne methods.

RADIO HILL

Peters & de Angelis (1987) describe an extensive geophysical exploration program leading to the discovery of the Radio Hill nickel-copper deposit. The Radio Hill mafic-ultramafic complex intrudes intermediate and mafic metavolcanic rocks along its northern margins (Hoatson *et al.*, 1992). The intrusion is interpreted as being a shallow-dipping basinal structure with a basal ultramafic zone overlain by layered gabbroic rocks. The deposit is blind, being overlain by basement volcanic rocks, and consists of disseminated mineralisation in peridotite and dunite units and stringer to massive mineralisation in gabbro and pyroxenite units at the basement contact. The major sulphide minerals are pyrrhotite, chalcopyrite and pentlandite. Magnetite is also present.

Regional aeromagnetic data (400 m line spacing) successfully defined the layered intrusion. Individual units within the complex were defined by higher-resolution surveys, such as aeromagnetism at a 50 m flight height and ground surveys on a 30 m by 120 m grid. Susceptibility measurements showed the source of these anomalies is peridotitic units overlying mineralisation, rather than the mineralisation itself which contains mainly hexagonal pyrrhotite. Various ground EM and electrical techniques were used to directly detect mineralisation and are summarised in Figure 56. Early work consisted of Turam and Crone PEM surveys. The Turam survey did not detect the main mineralisation although the PEM survey did, but was not followed-up. SIROTEM data, collected using 100 m offset loops, defined two clear conductors, drilling of which discovered marginal mineralisation. Mise-a-la-masse surveys delineated two distinct anomalies showing the two areas of mineralisation were not connected. Drilling of one of these areas led to discovery of high-grade mineralisation. Subsequently, an EM-37 fixed transmitter loop survey (800 m by 600 m loops) also detected the mineralisation. The geometry of the mineralisation obtained from modelling of these data was confirmed by drilling. The success of the EM techniques was not matched by gravity data which show no response from mineralisation and provided no useful structural information.

Other types of deposit

Nickeliferous laterites account for almost half of Western Australia's identified nickel resources (Harrison, 1990), but they have only been mined in one location at Bulong (Fig. 1), about 30 km east of Kalgoorlie (Elias *et al.*, 1981). Examples of the application of geophysics in exploration for this type of mineralisation in Western Australia include attempts to use remote sensing to map the ore based on its

spectral signature, and downhole logging for correlation purposes.

The Sherlock Bay copper-nickel deposit (Fig. 1) occurs in the Archaean granitoid-greenstone rocks of the Pilbara Craton. Mineralisation is developed in mafic to felsic volcanic rocks. Sulphides and magnetite are concentrated in amphibole-rich beds. The major sulphide is pyrrhotite, with lesser amounts of pyrite and minor pentlandite and chalcopyrite. Marston (1984) reports the mapping of the mineralised horizon using magnetic data. Howland-Rose *et al.* (1980) use the deposit to demonstrate the ability of MIP to detect mineralisation beneath conductive overburden, the deposit being covered by tidal flats about 10 m thick.

There is also nickel mineralisation at Mount Martin (Fig. 1) in association with gold mineralisation. Keele (this volume) describes aspects of variations in magnetic susceptibility in this area.

Summary

Nickel exploration in Western Australia relies heavily on geophysics. Magnetic data play a major role in delineating prospective areas while IP and surface and downhole TEM data are used to detect the ore itself. However, the discrimination between conductive ore and conductive sedimentary rocks remains a problem, with close integration of geophysical, geochemical and geological data required for success.

RARE EARTH ELEMENTS

The Mount Weld carbonatite (Fig. 1) is associated with significant phosphate and rare-earth-element mineralisation (Duncan 1988, Willett *et al.*, 1989). The carbonatite is a pipe, with a diameter of 3 to 4 km, which intrudes Archaean greenstone rocks of the Eastern Goldfields Province (Fig. 57). The carbonatite consists mainly of sovite with subordinate beforite, calcitic beforite and dolomitic sovite. Magnetite and/or maghemite can comprise up to 15 vol. % of samples from the intrusion. An annulus of altered country rock about 500 m wide surrounds the intrusion, the alteration being regarded as a form of fentisation. The regolith above the carbonatite is up to 90 m thick (Fig. 57C) and hosts all the known potentially economic mineral resources associated with the intrusion, these being lanthanides, niobium, tantalum and yttrium as well as phosphate. There is no surface expression of the Mount Weld carbonatite because it is covered by Quaternary alluvium and Tertiary lacustrine sediments. A Proterozoic dolerite dyke cuts the area and trends northwest-southeast.

The carbonatite was discovered as a result of its magnetic anomaly. On the AGSO regional magnetic data this anomaly has an amplitude of 8150 nT on a flight-line that approximately bisects the pipe. The results of a more detailed aeromagnetic survey are shown in Figure 57A. The data were acquired at a height of 100 m along east-west lines spaced at 400 m. The data delineated the extent of the pipe but the anomaly itself is complex, as is typical of carbonatites, reflecting the polyphase nature of the intrusion. Variations in the magnetic signal reflect the heterogeneous distribution of magnetic minerals within both the primary intrusion and the overlying regolith.

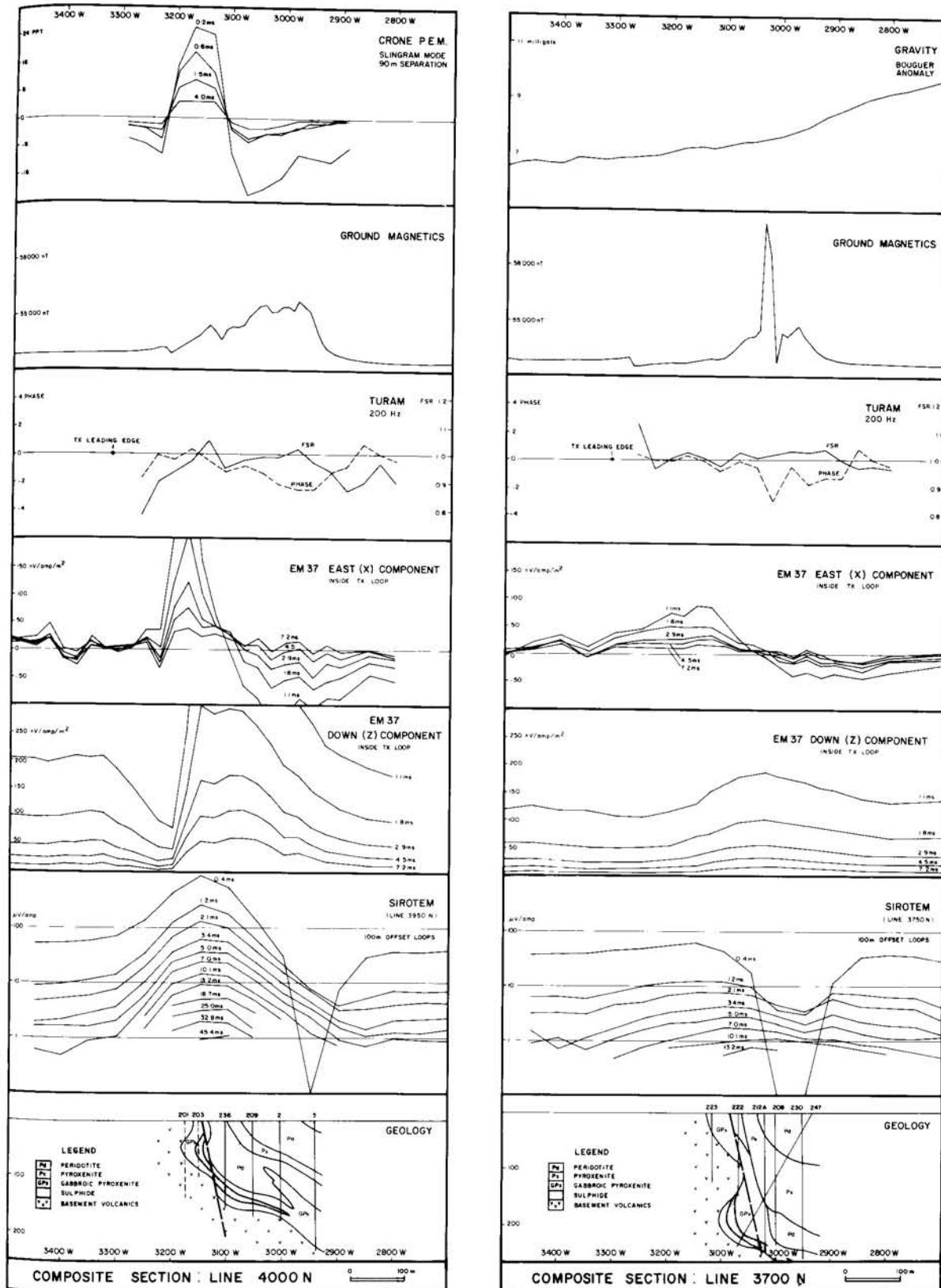


FIGURE 56 Geophysical surveys across the Radio Hill deposit. From Peters & de Angelis (1987).

Aeromagnetic data covering the Mount Weld carbonatite are also shown in Figure 4 of Bullock & Isles (this volume). Gravity data collected on a 100 m by 250 m grid over the carbonatite and surrounds (reduction density 2.2 g/cm³) show the intrusion is associated with a positive anomaly of about 6 mGal (Fig.

57B). The surrounding annulus of altered country rock gives rise to negative anomalies. Other zones of reduced gravity correlate with increased thicknesses of the sediments overlying the intrusion. Radiometric data do not detect the carbonatite due to the thickness of the cover. Electrical soundings were also

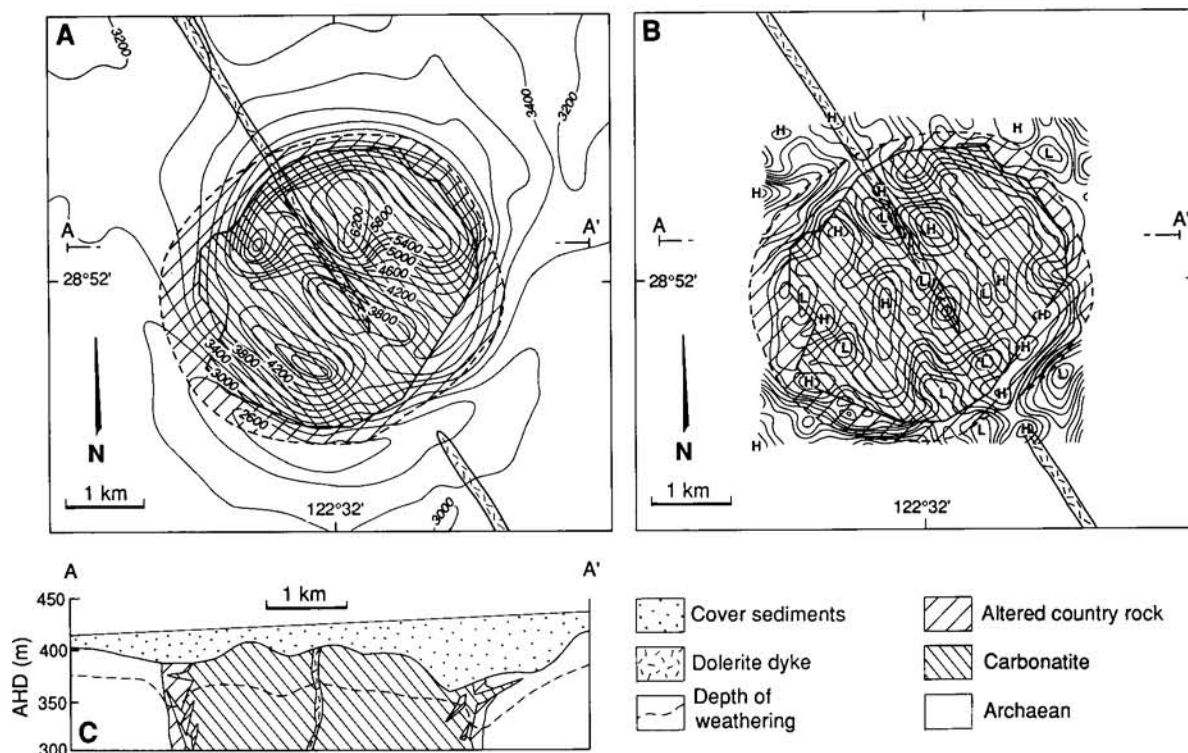


FIGURE 57 Geological and geophysical data from the Mount Weld carbonatite. A. Aeromagnetic data. B. Gravity data. C. Cross section. Redrawn from Willett *et al.* (1989). H = high, L = low.

used at Mount Weld, with the intention of mapping the regolith and the water table. However, these surveys were only partially successful (R. Duncan, pers. comm., 1993).

Rare-earth-element mineralisation is also associated with the Cummins Range carbonatite (Andrew, 1990) which intrudes a sequence of metasedimentary rocks of probable Archaean age within the Halls Creek Province (Fig. 1). The carbonatite was discovered by drilling a sub-circular aeromagnetic anomaly with a maximum amplitude of about 4800 nT and diameter of about 1.5 km (see Andrew, 1990). Subsequent ground magnetic surveys defined curvilinear zones within the intrusion which drilling showed to be due to lithological zoning. Modelling of the aeromagnetic and ground magnetic data show the intrusion to have steep, well-defined margins. The pipe consists mainly of a central plug of sovite and befsorite surrounded by pyroxenite. Magnetite occurs as coarse grains within the carbonatite and as finer grains within the pyroxenite. The pipe is also associated with a radiometric anomaly. As at Mount Weld, there is rare-earth-element mineralisation in the weathered zone. Uranium is also enriched (Lewis, 1990), and presumably is the source of the radiometric anomaly.

Summary

It is clear that aeromagnetic surveys are the most suitable way to locate carbonatites. The AGSO aeromagnetic data are likely to have detected the major intrusions of this type but smaller intrusions (less than about 2 km in diameter) could easily have gone undetected. However, as more of Western Australia is covered by high-resolution aeromagnetic surveys at least some of these carbonatites are likely to be located.

URANIUM

Keats (1990) summarises the nature of uranium mineralisation in Western Australia. Although eight styles of mineralisation are recognised, deposits that fall within the "sandstone-hosted", "unconformity-related" and "calcrete-related" categories are the most important. The Oobagooma and Manyingee deposits fall within the first category, the Kintyre deposit in the second, and the Yeelirrie deposit in the last category. These deposits are located on Figure 1.

Kintyre

The nature and geophysical signature of the Kintyre deposit are described by Jackson & Andrew (1990) and Root & Robertson (this volume), and are not discussed in detail here. To summarise, Kintyre is an unconformity-related vein-style deposit. Mineralisation is in the form of massive pitchblende veins with minor disseminated pitchblende. The host sequence consists of metacarbonate rocks, metacherts and schists within a succession comprising mainly psammities and schists. Root & Robertson (this volume) distinguish between geophysical responses due to mineralisation and those due to the host sequence. The deposit is associated with anomalous radioactivity on the uranium and potassium channels. The former is due to mineralisation and the latter is due to the schists in the host sequence. The host sequence also gives rise to magnetic and gravity anomalies. From an electrical perspective, the deposit is associated with positive apparent resistivity and chargeability anomalies, again due to the host sequence. However, there is no response on INPUT or SIROTEM surveys.

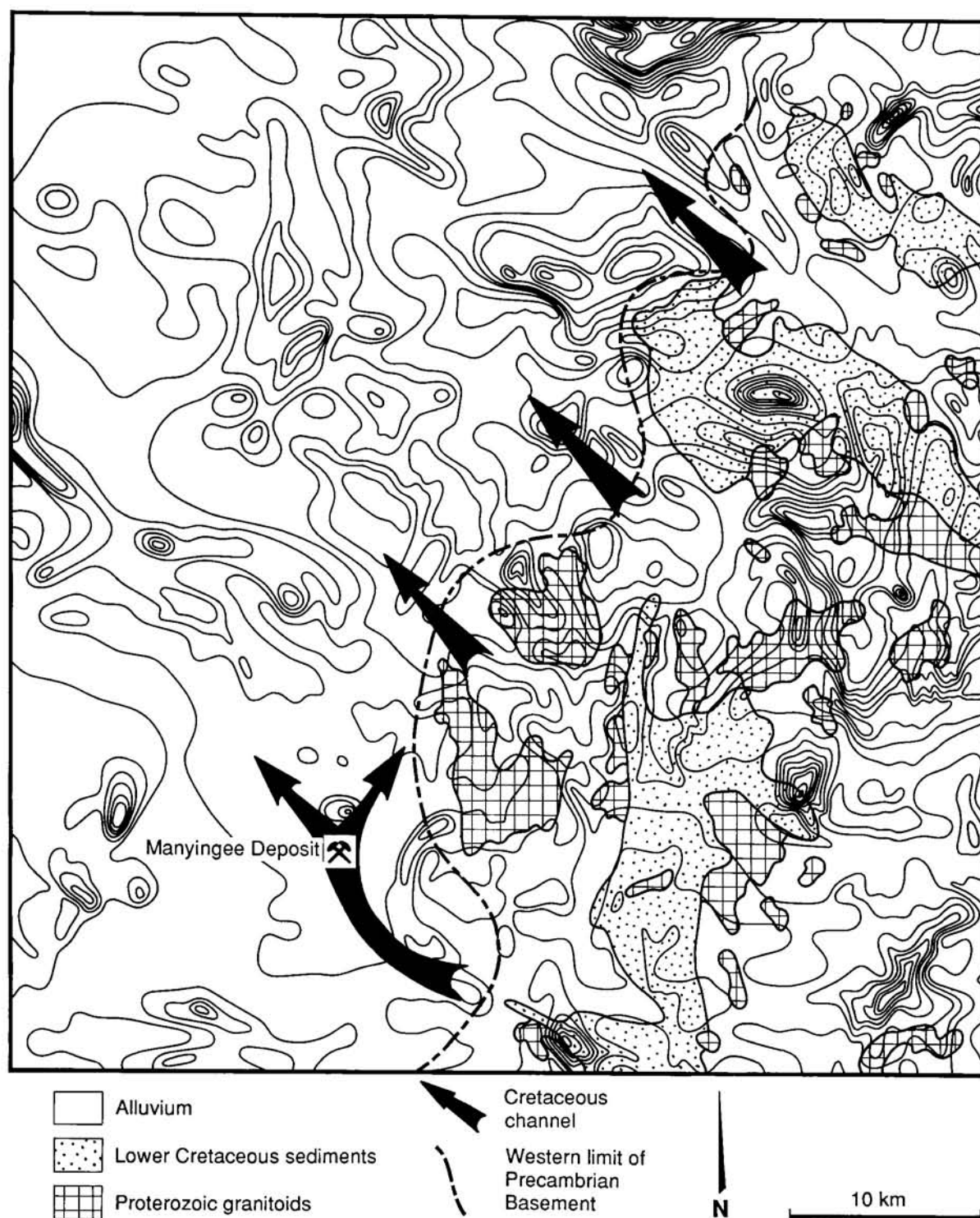


FIGURE 58 AGSO aeromagnetic data, basement geology and Mesozoic channels in the vicinity of the Manyingee uranium deposit. Geology from Valsardieu *et al.* (1981).

Oobagooma and Manyingee

Sandstone-hosted deposits are epigenetic-supergene deposits whose formation is related to redox-boundary reactions. The Oobagooma deposit lies within Lower Carboniferous fluviodeltaic sandstones. Uranium is present in the form of uraninite and pitchblende and is associated with pyrite and organic material. The distribution of uranium is controlled by local facies which, in turn, are a function of local faulting. Botten (1984) describes some aspects of the discovery of this deposit. Geophysics seems to have played a subsidiary role although Landsat, gravity, and air-

borne magnetic and radiometric data were used. The Manyingee deposit lies within Cretaceous fluvio-deltaic sandstones in palaeochannels (Valsardieu *et al.*, 1981). Uranium occurs as coffinite and uraninite and is associated with pyrite. Total-count radiometric surveys over the Manyingee region detected no anomalous radioactivity. However, it was possible to determine the position of palaeochannels using AGSO regional magnetic data (Fig. 58), and their presence was confirmed using gravity surveys, AEM (Butt, 1985) and drilling (Fig. 59). Downhole logging (gamma-ray, resistivity, laterolog, SP) was used to

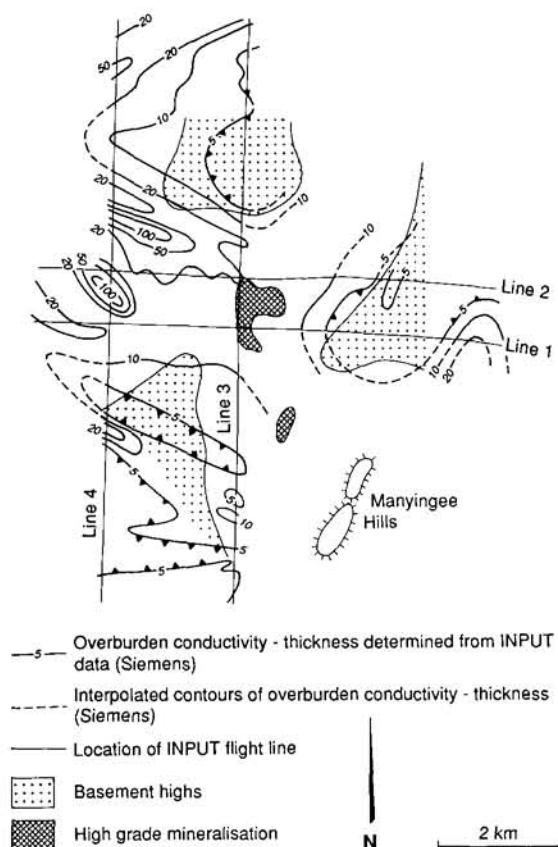


FIGURE 59 Contours of overburden conductivity-thickness determined from INPUT AEM data in relation to channels, basements highs and mineralisation defined by drilling, Manyingee uranium deposit. Redrawn from Butt (1985) with the distribution of mineralisation from Valsardieu *et al.* (1981).

define the stratigraphy within the channels and locate anomalous radioactivity.

Yeelirrie

The most important calcrete-related uranium deposit within Western Australia is the Yeelirrie deposit (Cameron, 1983). The calcrete occurs within a palaeochannel incised into granitic bedrock of above-average radioactivity. Uranium is in the form of secondary oxidised minerals, especially carnotite. Smyth & Barrett (this volume) summarise the geophysical characteristics of the palaeochannels in the Yilgarn Craton. The Yeelirrie deposit occurs within a calcrete sheet that is over 50 km long, up to 6.5 km wide and reaches 20 m in thickness. There is ore-grade uranium within an area about 9 km long, 0.5 to 1.5 km wide and up to 14 m thick. Carnotite is present as a thin film covering cavities, fracture planes and mineral grains, or is disseminated through the host sediments.

Attention was drawn to the Yeelirrie area when regional AGSO total-count radiometric data (see below) detected a prominent anomaly (Fig. 60B). A reconnaissance ground survey confirmed that the anomaly was due to uranium (Haycraft, 1977). Figure 60A shows the results of a more detailed follow-up

ground survey (Cameron, 1983). A McPhar TV5 integrating spectrometer was used on a 500 m by 60 m grid. Readings on the >1.63 MeV channel outlined the mineralisation with the two-times-background contour, which corresponds to about 400 cpm, defining the limits of the orebody. The survey also indicated a low thorium content. Subsequent grade estimation was undertaken using downhole gamma logging. Limited orientation surveys to detect Rn^{222} gas using either scintillation detectors or alpha-sensitive films were also undertaken (Severne, 1978). This work detected high (about eight times background) surface radon flux over the shallow ore-grade mineralisation. However, the strength of the anomaly could not always be correlated to the grade or depth of mineralisation. It was concluded that the response was a function of the local concentration of uranium in the soil immediately surrounding the sampling point. Because of the strong and definitive radiometric signature of the Yeelirrie orebody, and since such surveys were cheaper and faster, radon measurements were not pursued.

Summary

Uranium mineralisation is well suited to discovery using geophysical methods. Radiometrics is obviously the most commonly used exploration technique and, since much of Western Australia is covered by AGSO regional data (mainly 1.6 km flight line spacing, mean terrain clearance 150 m, crystal volume 3700 cm^3) of this type, use of geophysical data is further encouraged. However, as indicated by Dunn *et al.* (1990), the relatively coarse line-spacing of this dataset means that deposits could easily be missed by these surveys. Also, not all deposits give rise to a radiometric anomaly (e.g., the Manyingee deposit described above).

CONCLUSIONS

Western Australia contains deposits of many commodities. Geophysical methods have been used in the exploration programmes for many of these deposits and/or their delineation after discovery. Geophysics have proven invaluable as a mapping tool in many areas. The difficulties imposed by deep and extensive weathering can limit the usefulness of some methods, but have also led to the improvement of existing geophysical techniques and the development of new approaches.

ACKNOWLEDGEMENTS

Nigel Hungerford and Paul Askins of Billiton Australia are thanked for permission to publish and assistance with the Wagon Pass data. Peter Elliot of Peter Elliot & Associates clarified aspects of the mise-a-la-masse survey at the same deposit. Vic Williams of CRA Exploration Pty Ltd provided the data from Admiral Bay and permission to publish them. He and Stuart McCracken (The University of Western Australia) are thanked for helpful discussions. Rob Duncan is thanked for data and discussions regarding the Mount Weld carbonatite. Ed Reeves of Tesla-10 kindly shared his experience in geophysical exploration for Pilbara manganese deposits and the Pilbara

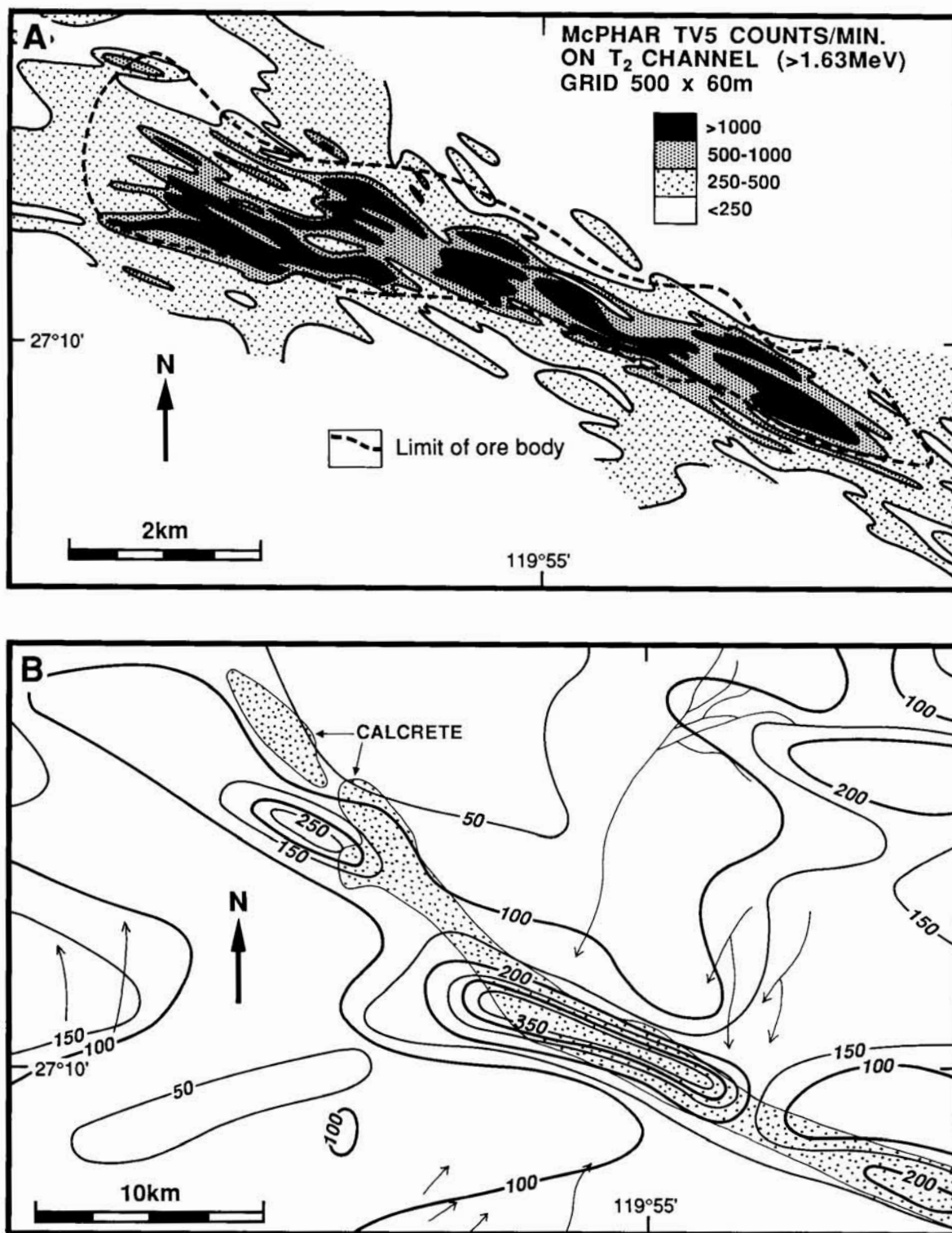


FIGURE 60 A. Ground radiometric from the Yeelirrie uranium deposit. Redrawn from Cameron (1983). B. AGSO airborne radiometric data. Contours in counts per second.

Manganese JV (comprising Portman Mining Ltd, Alsace Pty Ltd and Gayna Park Pty Ltd) gave permission for publication of data from the Woodie Woodie area. Duncan Cowan of Cowan Geodata Services is thanked for his helpful comments on an initial version of the manuscript. Peter Williams of Western Mining Corporation Ltd is thanked for supplying information on Yeelirrie. Vern Wilson of Curtin University kindly

allowed access to B.Sc. (Honours) theses written by students under his supervision. Plutonic Operations Ltd are thanked for permission to describe the regolith EM data. Billiton Australia and Anglo Australian Resources are thanked for allowing publication of the data from Onedin. John Blockley of the GSWA and Peter Ness of Hamersley Iron are acknowledged for discussions on iron ore exploration in the Pilbara.

Sam Bullock of World Geoscience Corporation is thanked for discussions on exploration for mineral sands. Dave Robinson, Carl Knox-Robinson and Cecilia D'Ercole are thanked for their patience and assistance in the production of Figures 1, 8 and 26 using the facilities in the GIS laboratory in the Key Centre for Strategic Mineral Deposits, The University of Western Australia. Figures 16 and 56 are reproduced with permission from the Australasian Institute of Mining and Metallurgy and *Exploration Geophysics*, respectively. Colin Steel drafted most of the remaining figures. The assistance of Leanne Morton (now BHP Minerals) and Henry Wurm of the Geology Library at The University of Western Australia was invaluable while researching this paper.

REFERENCES

- ANDREW R.L., 1990. Cummins Range carbonatite. In Hughes F.E. (ed.), *Geology of the Mineral Deposits of Australia and Papua New Guinea*, pp. 711-713. Australasian Institute of Mining and Metallurgy, Melbourne.
- ANNAN A.P. & LOCKWOOD R., 1991. An application of airborne GEOTEM in Australian conditions. *Exploration Geophysics* **22**, 5-12.
- BARLEY M.E., 1992. A review of Archean volcanic-hosted massive sulfide and sulfate mineralization in Western Australia. *Economic Geology* **87**, 855-872.
- BAXTER J.L., 1977. Heavy Mineral Sand Deposits of Western Australia. *Geological Survey of Western Australia, Mineral Resources Bulletin* **10**, 148 pp.
- BECKER A. & TELFORD W.M., 1965. Spontaneous polarization studies. *Geophysical Prospecting* **13**, 173-188.
- BISHOP J.R. & LEWIS R.J.G., 1992. Geophysical signatures of Australian volcanic-hosted massive sulfide deposits. *Economic Geology* **87**, 913-930.
- BLOCKLEY J.G., 1979. A contribution to the stratigraphy of the Marra Mamba Iron Formation. *Geological Survey of Western Australia, Annual Report* **1978**, 71-73.
- BLOCKLEY J.G., 1990. Iron ore. In *Geology and Mineral Resources of Western Australia. Geological Survey of Western Australia, Memoir* **3**, 679-692.
- BLOCKLEY J.G. & MYERS J.S., 1990. Proterozoic rocks of the Western Australian shield - geology and mineralisation. In Hughes F.E. (ed.), *Geology of the Mineral Deposits of Australia and Papua New Guinea*, pp. 607-616. Australasian Institute of Mining and Metallurgy, Melbourne.
- BLOCKLEY J.G., REID I.W. & TRENDALL A.F., 1990. Geological aspects of Australian iron ore discovery and development. In Glasson K.R. & Rattigan J.H. (eds), *Geological Aspects of the Discovery of Some Important Mineral Deposits in Australia. Australasian Institute of Mining and Metallurgy, Monograph* **17**, 263-285.
- BLOCKLEY J.G., TEHNAS I.J., MANDYCZEWSKY A. & MORRIS R.C., 1993. Proposed stratigraphic subdivisions of the Marra Mamba Iron Formation and the lower Wittenoom Dolomite, Hamersley Group, Western Australia. *Geological Survey of Western Australia, Professional Papers, Report* **34**, 47-64.
- BODDINGTON T.D.M., 1990. Abra lead-silver-copper-gold deposit. In Hughes F.E. (ed.), *Geology of the Mineral Deposits of Australia and Papua New Guinea*, pp. 659-664. Australasian Institute of Mining and Metallurgy, Melbourne.
- BOTTEN P., 1984. Uranium exploration in the Canning Basin: a case study. In Purcell P.G. (ed.), *The Canning Basin, W.A. Proceedings of Geological Society of Australia/Petroleum Exploration Society of Australia Symposium, Perth, 1984*, pp. 485-502. Geological Society of Australia, Perth.
- BUCHHORN I.J., 1986. Geology and mineralization of the Wagon Pass prospect, Napier Range, Lennard Shelf, Western Australia. In Glasson K.R. & Rattigan J.H. (eds), *Geological Aspects of the Discovery of Some Important Mineral Deposits in Australia. Australian Institute of Mining and Metallurgy, Monograph* **17**, 163-172.
- BULLOCK S.J. & COOKE A., 1990. Geophysical methods for mineral sands exploration. In Maiden K.J. (ed.), *Placer Deposits: A Symposium*, pp. 150-162. Australian Institute of Mining & Metallurgy, Geological Society of Australia, and Key Centre for Mines (University of New South Wales), Sydney.
- BUSELLI G., MCCracken K.G. & THORBURN M., 1986. Transient electromagnetic response of the Teutonic Bore orebody. *Geophysics* **51**, 957-963.
- BUTT G.R., 1985. Case histories showing various applications of a combined INPUT-magnetometer-spectrometer airborne geophysical system in Australia. *Exploration Geophysics* **16**, 180-183.
- CAMERON E., 1983. The Yeelirrie uranium deposit, Western Australia. Company report, Western Mining Corporation Ltd, 7 pp. (unpublished).
- CHAN R.A., 1988. Regolith mapping for mineral exploration in Western Australia. *Zeitschrift für Geomorphologie, Supplementband* **86**, 205-221.
- CLARK D.A. & EMERSON D.W., 1991. Notes on magnetisation characteristics in applied geophysical studies. *Exploration Geophysics* **22**, 547-555.
- COGGON J.H., 1984. Geophysics as an aid to gold exploration in the Yilgarn Block. In Doyle H.A. (ed.), *Geophysical Exploration for Precambrian Gold Deposits. Geology Department & University Extension, The University of Western Australia, Publication* **10**, 113-138.
- COGGON J.H., 1987. Variety and applications in drill hole electrical surveys. *Exploration Geophysics* **18**, 16-19.
- COGGON J.H. & CLARKE E.H., 1987. The fixed receiver electromagnetic (FREM) method for drill hole surveys. *Exploration Geophysics* **18**, 305-311.
- COLE A.G., 1991. The effectiveness of geophysics in delineating the geology of the Onedin VMS base metal deposit, Koongie Park, W.A.. B.Sc. (Honours) thesis, Curtin University of Technology, Perth, 66 pp. (unpublished).
- CONNOR A.G., 1990. Admiral Bay zinc-lead deposit. In Hughes F.E. (ed.), *Geology of the Mineral Deposits of Australia and Papua New Guinea*, pp. 1111-1114. Australasian Institute of Mining and Metallurgy, Melbourne.

- COWAN D.R., 1977. An integrated geo-electrical survey on the Nangaroo copper-zinc prospect, near Leonora, Western Australia - A reply. *Geoexploration* **15**, 198-199.
- COWAN D.R., ALLCHURCH P.D. & OMNES G., 1975. An integrated geo-electrical survey on the Nangaroo copper-zinc prospect, near Leonora, Western Australia. *Geoexploration* **13**, 77-98.
- CRAVEN B.L., HAYDEN W.B. & SMITH M.J., 1985. A comparison of electromagnetic prospecting results at the Scuddles Cu-Zn massive sulphide deposit, Golden Grove area, Western Australia. *Exploration Geophysics* **16**, 194-197.
- DAVIES B.M. & BLOCKLEY J.G., 1990. Copper, lead, and zinc. In *Geology and Mineral Resources of Western Australia. Geological Survey of Western Australia, Memoir* **3**, 631-639.
- DENHOLM L.S., 1977. Investigation of the ferruginous manganese deposits at Ripon Hills, Pilbara manganese province, Western Australia. *Proceedings of the Australasian Institute of Mining and Metallurgy* **264**, 9-17.
- DENTITH M.C., EVANS B.J., PAISH K.F. & TRENCH A., 1992a. Mapping the regolith using seismic refraction and magnetic data: results from the Southern Cross greenstone belt, Western Australia. *Exploration Geophysics* **23**, 97-104.
- DENTITH M.C., JONES M.L. & TRENCH A., 1992b. Exploration for gold-bearing iron formation in the Burbidge area of the Southern Cross Greenstone Belt, W.A. *Exploration Geophysics* **23**, 111-116.
- DOCKERY B.A., 1984. Geophysical case history of the Lady Susan gold prospect. In Doyle H.A. (ed.), *Geophysical Exploration for Precambrian Gold Deposits. Geology Department & University Extension, The University of Western Australia, Publication* **10**, 165-182.
- DOYLE H.A., GLOVER J.E. & GROVES D.I., 1981. Geophysical Exploration in Deeply Weathered Terrains. *Geology Department & University Extension, The University of Western Australia, Publication* **6**, 179 pp.
- DOYLE H.A. & LINDEMAN F.W., 1985. The effect of deep weathering on geophysical exploration in Australia — a review. *Australian Journal of Earth Sciences* **32**, 125-135.
- DREW G.J., 1986. A geophysical case history of the AK1 lamproite pipe. Fourth International Kimberlite Conference Extended Abstracts. In *Fourth International Kimberlite Conference, Perth, 1986. Geological Society of Australia, Abstracts* **16**, 454-456.
- DUNCAN R.K., 1988. Discovery of the Mount Weld Carbonatite. In *Western Australian School of Mines Conference '88: R & D for the Minerals Industry*, pp. 86-93. Western Australian School of Mines, Kalgoorlie.
- DUNN P.R., BATTEY G.C., MIEZITIS Y. & MCKAY A.D. 1990. Uranium in Western Australia. In *Glasson K.R. & Rattigan J.H. (eds), Geological Aspects of the Discovery of Some Important Mineral Deposits in Australia. Australasian Institute of Mining and Metallurgy, Monograph* **17**, 477-486.
- EISLER P.L., MATTHEW P.J., YOUL S.F. & WYLIE A.W., 1979. Nuclear activation logging for aluminium in iron ores and coal. *Geoexploration* **17**, 43-53.
- ELIAS M., 1990. Kambalda gold deposits — history of exploration. In *Glasson K.R. & Rattigan J.H. (eds), Geological Aspects of the Discovery of Some Important Mineral Deposits in Australia. Australasian Institute of Mining and Metallurgy, Monograph* **17**, 43-47.
- ELIAS M., DONALDSON M.J. & GIORETTA N., 1981. Geology, mineralogy, and chemistry of laterite nickel-cobalt deposits near Kalgoorlie. *Economic Geology* **76**, 1775-1783.
- ELLIOT P.J. & STALTARI G., 1985. The Mount Keith nickel sulphide deposit — a TEM case study. *Exploration Geophysics* **16**, 210-216.
- FRITZ F.P. & SHEEHAN G.M., 1984. The geophysical signature of the Teutonic Bore Cu-Zn-Ag massive sulphide deposit, Western Australia. *Exploration Geophysics* **15**, 127-142.
- GREGORY G.P., 1984. Exploration for primary diamond deposits with special emphasis on the Lennard Shelf, Western Australia. In *Purcell P.G. (ed.), The Canning Basin, W.A. Proceedings of the Geological Society of Australia/Petroleum Exploration Society of Australia Symposium, Perth 1984*, pp. 475-484. Geological Society of Australia, Perth.
- GREIG D.D., 1984. Geology of the Teutonic Bore massive sulphide deposit, Western Australia. *Proceedings of the Australian Institute of Mining and Metallurgy* **289**, 147-156.
- GRIFFIN T.J., 1990. North Pilbara granite-greenstone terrane. In *Geology and Mineral Resources of Western Australia. Geological Survey of Western Australia, Memoir* **3**, 128-158.
- GROVES D.I., HO S.E., McNAUGHTON N.J., MUELLER A.G., PERRING C.S., ROCK N.M.S. & SKWARNECKI M.S., 1988. Genetic models for Archaean lode-gold deposits in Western Australia. In *Ho S.E. & Groves D.I. (eds), Advances in Understanding Precambrian Gold Deposits, Volume II. Geology Department & University Extension, The University of Western Australia, Publication* **12**, 1-22.
- GROVES D.I., KNOX-ROBINSON C.M., HO S.E. & ROCK N.M.S., 1990. An overview of Archaean lode-gold deposits. In *Ho S.E., Groves D.I. & Bennett J.M. (eds), Gold Deposits of the Yilgarn Craton, Western Australia: Nature, Genesis and Exploration Guides. Geology Department (Key Centre) & University Extension, The University of Western Australia, Publication* **20**, 2-18.
- GUNN P.J. & CHISHOLM J., 1984. Non-conductive volcanogenic massive sulphide mineralisation in the Pilbara area of Western Australia. *Exploration Geophysics* **15**, 143-153.
- HANNA J.P. and IVEY M.E., 1990. Labouchere and Deep South gold deposits. In *Hughes F.E. (ed.), Geology of the Mineral Deposits of Australia and Papua New Guinea*, pp. 667-670. Australasian Institute of Mining and Metallurgy, Melbourne.

- HARMSWORTH R.A., KNEESHAW M., MORRIS R.C., ROBINSON C.J. & SHRIVASTAVA P.K., 1990. BIF-derived iron ores of the Hamersley Province. In Hughes F.E. (ed.), *Geology of the Mineral Deposits of Australia and Papua New Guinea*, pp. 617-642. Australasian Institute of Mining and Metallurgy, Melbourne.
- HARRISON P.H., 1990. Mineral sands. In *Geology and Mineral Resources of Western Australia. Geological Survey of Western Australia, Memoir 3*, 694-701.
- HARRISON P.H., 1990. Nickel. In *Geology and Mineral Resources of Western Australia. Geological Survey of Western Australia, Memoir 3*, 702-709.
- HAYCRAFT J.A., 1977. Sampling of the Yeelirrie uranium deposit, Western Australia. In *Proceedings of the Uranium Exploration Workshop, Perth*, unpaginated. Australasian Institute of Mining and Metallurgy, Melbourne.
- HENDERSON F.B., PENFIELD G.T. & GRUBBS D.K., 1984. Bauxite exploration by satellite. In Jacob L. (ed.), *Bauxite: Proceedings of the 1984 Bauxite Symposium, Los Angeles, California*, pp. 200-242. Society of Mining Engineers of the American Institute of Mining, Metallurgical and Petroleum Engineers Inc., New York.
- HILL A.D. & CRANNEY P.J., 1990. Fortnum gold deposit. In Hughes F.E. (ed.), *Geology of the Mineral Deposits of Australia and Papua New Guinea*, pp. 665-666. Australasian Institute of Mining and Metallurgy, Melbourne.
- HOATSON D.M., WALLACE D.A., SUN S.S., MACIAS L.F., SIMPSON C.J. & KEAYS R.R., 1992. Petrology and Platinum-Group-Element Geochemistry of Archaean Layered Mafic-Ultramafic Intrusions, West Pilbara Block, Western Australia. *Australian Geological Survey Organisation, Bulletin 242*, 319 pp.
- HOWLAND-ROSE A.W., 1984. The use of RRMIP as a regional mapping tool with examples from the Eastern Goldfields of W.A. In Doyle H.A. (ed.), *Geophysical Exploration for Precambrian Gold Deposits. Geology Department & University Extension, The University of Western Australia, Publication 10*, 139-164.
- HOWLAND-ROSE A.W., LINFORD G., PITCHER D.H. & SEIGEL H.O., 1980. Some recent magnetic induced-polarization developments - Part II: survey results. *Geophysics* **45**, 55-74.
- ISLES D., WATT M., HARMAN P. & LEBEL A., 1987. Geophysical experience from the Blendevalle deposit, W.A. *Exploration Geophysics* **18**, 108-110.
- ISLES D., HARMAN P.G. & CUNNEEN J.P., 1989. The contribution of high resolution aeromagnetics to Archean gold exploration in the Kalgoorlie region, Western Australia. In Keays R.R., Ramsay W.R.H. & Groves D.I. (eds), *The Geology of Gold Deposits: The Perspective in 1988. Economic Geology Monograph 6*, 389-397.
- ISLES D.J., COOKE A.C. & HALBERG J.A., 1990. Aeromagnetic evaluation. In Ho S.E., Groves D.I. & Bennett J.M. (eds), *Gold Deposits of the Yilgarn Craton, Western Australia: Nature, Genesis and Exploration Guides. Geology Department (Key Centre) & University Extension, The University of Western Australia, Publication 20*, 342-347.
- JACKSON D.G. & ANDREW R.L., 1990. Kintyre uranium deposit. In Hughes F.E. (ed.), *Geology of the Mineral Deposits of Australia and Papua New Guinea*, pp. 653-658. Australasian Institute of Mining and Metallurgy, Melbourne.
- JENKE G., 1983. The role of geophysics in the discovery of the Ellendale and Fitzroy kimberlites. In *The Third Biennial Conference of the Australian Society of Exploration Geophysicists, Brisbane, Abstracts* pp.66-72. Australian Society of Exploration Geophysicists, Brisbane.
- JONES H., WALRAVEN F. & KNOTT G.G., 1973. Natural gamma logging as an aid to iron ore exploration in the Pilbara region of Western Australia. In *Western Australian Conference, 1973*, pp. 53-60. Australasian Institute of Mining and Metallurgy, Melbourne.
- JORGENSEN G.C., DENDLE P.K., ROWLEY M.R. & LEE R.J., 1990. Sorby lead-zinc-silver deposit. In Hughes F.E. (ed.), *Geology of the Mineral Deposits of Australia and Papua New Guinea*, pp. 1097-1101. The Australasian Institute of Mining and Metallurgy, Melbourne.
- KEATS W., 1990. Uranium. In *Geology and Mineral Resources of Western Australia. Geological Survey of Western Australia, Memoir 3*, 728-731.
- LAWRANCE L.M., 1990. Supergene gold mineralization. In Ho S.E., Groves D.I. & Bennett J.M. (eds), *Gold Deposits of the Yilgarn Craton, Western Australia: Nature, Genesis and Exploration Guides. Geology Department (Key Centre) University Extension, The University of Western Australia, Publication 20*, 300-313.
- LEE R.J. and ROWLEY M., 1990. Sorby Hills (W.A.) lead-silver-zinc. In Glasson, K.R. & Rattigan, J.H. (eds), *Geological Aspects of the Discovery of Some Important Mineral Deposits in Australia. Australasian Institute of Mining and Metallurgy, Monograph 17*, 197-202.
- LEWIS J.D., 1990. Diatremes. In *Geology and Mineral Resources of Western Australia. Geological Survey of Western Australia, Memoir 3*, 565-589.
- LINDEMAN F.W., 1984. Geophysical case history of Water Tank Hill-Mount Magnet, W.A. In Doyle H.A. (ed.), *Geophysical Exploration for Precambrian Gold Deposits. Geology Department & University Extension, The University of Western Australia, Publication 10*, 92-112.
- LORD J.H. & TRENDALL A.F., 1976. Iron ore deposits of Western Australia: geology and development. In Halbouty M.T., Maher J.C. & Lian H.M. (eds), *Circum-Pacific Energy and Mineral Resources. American Association of Petroleum Geologists, Memoir 25*, 410-417.

- MARSTON R.J., 1979. Copper Mineralisation in Western Australia. *Geological Survey of Western Australia, Mineral Resources Bulletin* 13, 208 pp.
- MARSTON R.J., 1984. Nickel Mineralization in Western Australia. *Geological Survey of Western Australia, Mineral Resources Bulletin* 14, 271 pp.
- MAYES K.A., 1992. Application of Geophysical Electrical and Magnetic Methods to Regolith Mapping at Lawlers. B.Sc. (Honours) thesis, Curtin University of Technology, Perth, 68 pp. (unpublished).
- MUTTON A.J., 1987. Applications of downhole SIROTEM surveys in the Agnew Nickel Belt, W.A. *Exploration Geophysics* 18, 295-303.
- MYERS J.S. & HOCKING R.M. (compilers), 1988. *Geological Map of Western Australia, 1:2500000*. Geological Survey of Western Australia, Perth.
- O'DRISCOLL E.S.T., 1981. A broad-scale structural characteristic of major nickel sulfide deposits of Western Australia. *Economic Geology* 76, 1364-1372.
- PARKER T.W.H. & BROWN T., 1990. Horseshoe gold-copper-silver deposit. In Hughes F.E. (ed.), *Geology of the Mineral Deposits of Australia and Papua New Guinea*, pp. 671-675. Australasian Institute of Mining and Metallurgy, Melbourne.
- PETERS W.S. & de ANGELIS M., 1987. The Radio Hill Ni-Cu massive sulphide deposit: a geophysical case history. *Exploration Geophysics* 18, 160-166.
- PRIDMORE D.F., COGGON J.H., ESDALE D.J. & LINDEMAN F.W., 1984. Geophysical exploration for nickel sulphide deposits in the Yilgarn Block, Western Australia. In Buchanan D.L. & Jones M.J. (eds), *Sulphide Deposits in Mafic and Ultramafic Rocks*, pp. 22-34. Institution of Mining and Metallurgy, London.
- PRIDMORE D.F., ISLES D.J. & CUNNEEN J.P., 1988. Airborne magnetism and radiometrics in Archaean gold exploration: advantages, limitations and new directions. In *Western Australian School of Mines Conference '88: R & D for the Minerals Industry*, pp. 42-47. Western Australian School of Mines, Kalgoorlie.
- RATTIGAN J.H., 1990. Aluminium ores. In Glasson K.R. & Rattigan J.H. (eds), *Geological Aspects of the Discovery of Some Important Mineral Deposits in Australia*. *Australasian Institute of Mining and Metallurgy, Monograph* 17, 379-391.
- RATTIGAN J.H. & STITT P.H., 1990. Heavy Mineral Sands. In Glasson K.R. & Rattigan J.H. (eds), *Geological Aspects of the Discovery of Some Important Mineral Deposits in Australia*. *Australasian Institute of Mining and Metallurgy, Monograph* 17, 369-378.
- RINGROSE C.R., 1989. Studies of Selected Carbonate-Hosted Lead-Zinc Deposits in the Kimberley Region. *Geological Survey of Western Australia, Report* 24, 103 pp.
- ROBINSON W.S., STOCK E.C. & WRIGHT R., 1973. The discovery and evaluation of the Windarra nickel deposits, Western Australia. In *Western Australian Conference, 1973*, pp. 69-90. Australasian Institute of Mining and Metallurgy, Melbourne.
- ROTH J., 1977. An integrated geo-electrical survey on the Nangaroo copper-zinc prospect, near Leonora, Western Australia - A comment. *Geoexploration* 15, 195-198.
- ROWSTON D.L., 1965. Geophysical investigations over beach sand deposits, Capel area, Western Australia. *Geological Survey of Western Australia, Record* 1965/8, 8 pp.
- ROWSTON D.L., 1966. Geophysical investigations for beach sand deposits in the Yoganup area. *Geological Survey of Western Australia, Record* 1966/10, 12 pp.
- SEVERNE B.C., 1978. Evaluation of radon systems at Yeelirrie, Western Australia. *Journal of Geochemical Exploration* 9, pp 1-22.
- SMITH C.B., ATKINSON W.J. & TYLER E.W.J., 1990. Diamond Exploration in Western Australia, Northern Territory, and South Australia. In Glasson K.R. & Rattigan, J.H. (eds), *Geological Aspects of the Discovery of Some Important Mineral Deposits in Australia*. *Australasian Institute of Mining and Metallurgy, Monograph* 17, 429-453.
- SMITH R.J. & PRIDMORE D.F., 1989. Exploration in weathered terrains: 1989 perspective. *Exploration Geophysics* 20, 411-434.
- SPENCER G.A., PRIDMORE D.F. & ISLES D.J., 1989. Data integration of exploration data using colour space on an image processor. *Exploration Geophysics* 20, 31-35.
- STAPLES P., 1984. Detection of massive sulphides beneath conductive overburden using the Geonics EM-37: a case study. *Exploration Geophysics* 15, 33-36.
- THOMPSON M.J., WATCHORN R.B., BONWICK C.M., FREWIN M.O., GOODGAME V.R., PYLE M.J. & MacGEEHAN P.J., 1990. Gold deposits of Hill 50 Gold Mine NL at Mount Magnet. In Hughes F.E. (ed.), *Geology of the Mineral Deposits of Australia and Papua New Guinea*, pp. 221-242. Australasian Institute of Mining and Metallurgy, Melbourne.
- TRENDALL A.F., 1990. Hamersley Basin. In *Geology and Mineral Resources of Western Australia*. *Geological Survey of Western Australia, Memoir* 3, 163-191.
- URQUHART D.F., 1956. The investigation of deep leads by the seismic refraction method. *Bureau of Mineral Resources, Geology and Geophysics, Bulletin* 35, 24 pp.
- VALSARDIEU C.A., HARROP D.W. & MORABITO J., 1981. Discovery of uranium mineralisation in the Manyingee channel, Onslow region of Western Australia. *Proceedings of the Australian Institute of Mining and Metallurgy* 279, 5-17.
- WILLETT G.C., DUNCAN R.K. & RANKIN R.A., 1989. Geology and economic evaluation of the Mount Weld carbonatite, Laverton, Western Australia. In Ross J. (ed.), *Kimberlites and Related Rocks, Volume 2*. *Geological Society of Australia, Special Publication* 14, 1215-1235.
- WOLFGRAH P., JAGGAR S. & SWIFT L., 1992. Geological applications of airborne electromagnetic methods. In *Airborne Geophysics in Australia, Pre-Conference Workshop, 9th ASEG Conference, October 1992, Sydney*, unpaginated. Australian Society of Exploration Geophysicists, Sydney.